UNIVERSITY OF ALBERTA

DEVELOPMENT OF NANOPARTICLE-BASED CANCER VACCINE FORMULATIONS FOR THE GENERATION OF POTENT CELLULAR IMMUNE RESPONSE

BY

SAMAR HAMDY ©

A THESIS

SUBMITTED TO THE FACULTY OF GRADUATE STUDIES AND RESEARCH IN PARTIAL FULFILMENT OF THE REQUIREMENTS FOR THE DEGREE OF

DOCTOR OF PHILOSOPHY

Faculty of Pharmacy and Pharmaceutical Sciences

Edmonton, Alberta

Fall 2008

Library and Archives Canada

Published Heritage Branch

395 Wellington Street
Ottawa ON K1A 0N4
Canada

Bibliothèque et Archives Canada

Direction du Patrimoine de l'édition

395, rue Wellington
Ottawa ON K1A 0N4
Canada

Your file Votre référence
ISBN: 978-0-494-46327-7
Our file Notre référence
ISBN: 978-0-494-46327-7

NOTICE:
The author has granted a non-exclusive license allowing Library and Archives Canada to reproduce, publish, archive, preserve, conserve, communicate to the public by telecommunication or on the Internet, loan, distribute and sell theses worldwide, for commercial or non-commercial purposes, in microform, paper, electronic and/or any other formats.

The author retains copyright ownership and moral rights in this thesis. Neither the thesis nor substantial extracts from it may be printed or otherwise reproduced without the author's permission.

AVIS:
L'auteur a accordé une licence non exclusive permettant à la Bibliothèque et Archives Canada de reproduire, publier, archiver, sauvegarder, conserver, transmettre au public par télécommunication ou par l'Internet, prêter, distribuer et vendre des thèses partout dans le monde, à des fins commerciales ou autres, sur support microforme, papier, électronique et/ou autres formats.

L'auteur conserve la propriété du droit d'auteur et des droits moraux qui protège cette thèse. Ni la thèse ni des extraits substantiels de celle-ci ne doivent être imprimés ou autrement reproduits sans son autorisation.

In compliance with the Canadian Privacy Act some supporting forms may have been removed from this thesis.

While these forms may be included in the document page count, their removal does not represent any loss of content from the thesis.

Conformément à la loi canadienne sur la protection de la vie privée, quelques formulaires secondaires ont été enlevés de cette thèse.

Bien que ces formulaires aient inclus dans la pagination, il n'y aura aucun contenu manquant.

Canada

Dedications

I would like to dedicate this thesis to

My dear husband, Sameh and my lovely children, Mostafa and Karim who joined me during the whole process and helped me in every way with their love, support and patience

My dear parents (I. Hamdy and M. El-Enany) and my dear brother, Asser for all their love, encouragement and support throughout my whole life

Abstract

The objective of this research was to investigate the efficacy of poly(D,L lactic-co-glycolic acid) nanoparticles (PLGA-NPs) as a vaccine delivery system for co-delivery of antigens along with immunostimulatory molecules (adjuvants) in eliciting robust antigen specific T cell responses against cancer associated self antigens in both normal and tumor-bearing mice.

Pathogen-mimicking PLGA-NPs containing ovalbumin (OVA), as a model antigen and an analog of bacterial products (7-acyl lipid A) as an adjuvant were developed. Development of quantitative and functional aspects of T cell responses was then investigated measuring the increase in the percentage of antigen-specific T cells and increase in the expression of activation markers/cytokine secretion, respectively, following immunization with developed PLGA-NPs. Our results showed that particulate delivery of OVA and 7-acyl lipid A to dendritic cells leads to a dramatic increase in the $CD4^+$ and $CD8^+$ T cell proliferative responses. The expanded T cells were capable of interferon (IFN)-γ secretion and expressed an activated/effector surface phenotype. As a rigorous test for this vaccination strategy, a real tumor melanoma-associated antigen, i.e., tyrosinase-related protein 2 (TRP2) was encapsulated in PLGA-NPs along with 7-acyl lipid A. The potential of this formulation in eliciting antigen specific T cell responses leading to therapeutic anti-tumor effects was investigated in murine B16 melanoma tumor model. Our results showed that TRP2/7-acyl lipid A-NPs were capable of breaking self-tolerance against TRP2 and generate robust $CD8^+$ T cell immune responses in both normal and tumor bearing mice. Vaccinating B16 melanoma bearing mice with TRP2/7-

acyl lipid A-NPs resulted in the induction of therapeutic anti-tumor immunity, activation of IFN-γ secretion by $CD8^+$ T cells and; finally, reversal of the immunosuppressive network in the tumor microenvironment. In conclusion, our results support the potential use of PLGA-NPs as competent vaccine delivery system, and further illustrate the superior therapeutic outcome of co-delivery of 7-acyl lipid, a very promising immunestimulatory adjuvant, for future cancer vaccine trials.

ACKNOWLEDGEMENTS

I would like to express my gratitude to the following persons:

- My supervisor, the late Dr. John Samuel, whose expertise and knowledge added considerably to my graduate experience. I doubt that I will ever be able to convey my appreciation fully, but I dedicate to him all the success I had or will have in my future career life.
- My supervisor Dr. Afsaneh Lavasanifar who guided our entire research team after the sad loss of Dr. John Samuel and willingly accepted the responsibility for supervising two large research groups. I am greatly indebted to her assistance and guidance at all stages of my work.
- My co-supervisor Dr. Kevin Kane for his advice and guidance throughout the course of this project.
- My supervisory committee members and examination committee for their advice and constructive feedback.
- Dr. Damayanthi Yalamanti and Dr. Rao Koganti (Oncothyreon Inc., Edmonton) for their incessant co-operation and providing the synthetic lipid A analogues used in this study.
- Dr. Vishwa Somayaji for providing outstanding assistance and advice with the liquid chromatography-mass spectrometry.
- Dr. Praveen Elamanchili who trained me in bench work and gave me help and support throughout the whole program.
- Dr. Azita Haddadi for her sincere help in establishing the LC-MS and ELISPOT protocols.
- Dr. Zengshaun Ma for his indebted helping hands during the animal studies throughout the whole course.
- My dear friends and lab mates (Aws Alshamsan, Leila Molavi, Sara Elhasi and Zahra Ghotbi) for the fruitful discussions, the endless help and support they have given me throughout the whole program.
- My dear husband, Sameh and my lovely children, Mostafa and Karim who joined me during the whole process and helped me in every way with their love, support and patience.

- My dear parents (I. Hamdy and M. El-Enany) and my dear brother, Asser for all their love, encouragement and support throughout my whole life

Finally, I would like to thank the following agencies/institutes for the financial support:

- Canadian Institutes of Health Research.
- Izaak Walton Killam Memorial Scholarship.
- Faculty of Pharmacy and Pharmaceutical Sciences, University of Alberta.

TABLE OF CONTENTS

Chapter 1- Introduction..... 1

1.1 The promises and challenges of cancer immunotherapy: an overview.....2

1.2 DCs are the most professional APCs.....9

1.2.1 Intrinsic migratory capability of DCs.....11

1.2.2 Unique distribution of DCs in lymph nodes.....11

1.2.3 DCs have unique ability to activate naïve T cells.....12

1.3 Antigen processing and presentation by DCs.....13

1.3.1 Classical MHC class I pathway.....13

1.3.2 Classical MHC class II pathway.....15

1.3.3 Cross-presentation of exogenous antigens.....17

1.4 Delivering TLR ligands to DCs.....21

1.4.1 TLRs structure and function.....21

1.4.2 Role of TLR ligands in augmenting vaccine-induced immune responses...23

1.4.3 LPS-induced immune activation.....23

1.4.4 Lipid A recognition.....25

1.4.5 Lipid A-initiated signaling cascades.....27

1.4.6 Non-toxic version of lipid A: MPLA.....31

1.5 Targeting DCs with vaccine delivery systems: *ex-vivo* loading versus *in vivo* targeting.....35

1.6 PLGA-based vaccine delivery system.....39

1.6.1 PLGA composition and applications.....39

1.6.2 Manipulating the physicochemical properties of PLGA.....41

1.6.3 Uptake of PLGA-NPs by DCs.....43

1.6.4 Intracellular trafficking of PLGA-NPs.....46

1.7 Thesis proposal.....51

1.7.1 Rationale.....51

1.7.2 Objective.....53

1.7.3 Research outline.....53

1.7.4 Hypotheses.....54

1.7.5 Specific aims.....55

1.8 References.....56

Chapter 2- Development of liquid chromatography-mass spectrometry (LC-MS)-based method for quantification of synthetic lipid A analogues in PLGA-NP...74

2.1 Introduction.....75

2.2 Materials and Methods.....78

2.2.1 Mice.....78

2.2.2 Materials.....78

2.2.3 Preparation of BMDCs.....79

2.2.4 DCs activation/maturation studies.....80

2.2.5 Establishment of LC-MS method for quantification of lipid A analogues...81

2.2.6 Preparation and characterization of lipid A containing PLGA-NPs.....84

2.2.7 Statistical analysis.....86

2.3 Results.....87

2.3.1 Soluble lipid A analogues induce DCs activation/maturation.....87

2.3.2 Validation of the newly developed LC-MS-based method.....91

2.3.3 Particle size analysis of lipid A-containing PLGA-NPs.....97

2.3.4 Extraction and quantification of lipid A content in PLGA-NPs.....98

2.4 Discussion.....99

2.5 References.....103

Chapter 3: Enhanced antigen-specific primary $CD4^+$ and $CD8^+$ T cell responses by co-delivery of ovalbumin (OVA) and 7-acyl lipid A in PLGA-NP.....106

3.1 Introduction.....107

3.2 Materials and Methods.....109

3.2.1 Mice.....109

3.2.2 Reagents.....109

3.2.3 Preparation of murine BMDCs.....110

3.2.4 Preparation and characterization of OVA-containing PLGA-NPs.....110

3.2.5 Flow cytometry.....113

3.2.6 Transgenic $CD4^+$ T cell adoptive transfer and immunization.....113

3.2.7 Transgenic $CD8^+$ T cell activation studies.....114

3.2.8 Wild-type mice studies.....116

3.2.9 Statistical analysis.....119

3.3 Results.....119

3.3.1 Characterization of PLGA-NP formulations.....119

3.3.2 Activation of primary $CD4^+$ T cell responses.....120

3.3.3 Activation of primary $CD8^+$ T cell responses.....127

3.3.4 Simultaneous activation of $CD4^+$ and $CD8^+$ T cell responses.....132

3.4 Discussion.....135

3.5 References.....139

Chapter 4: Co-delivery of cancer associated antigen and Toll-like receptor 4 ligand in PLGA-NP induces potent $CD8^+$ T cell-mediated anti-tumor immunity.....143

4.1 Introduction.....144

4.2 Materials and Methods.....145

4.2.1 Reagents.....145

4.2.2 Preparation of PLGA-NPs encapsulating $TRP2_{180-188}$ with or without 7-acyl lipid A.....146

4.2.3 Quantification of encapsulated $TRP2_{180-188}$ in NPs by LC-MS.....147

4.2.4 Animal studies.....150

4.3 Results.....155

4.3.1 Characterization of PLGA-NPs.....155

4.3.2 Co-delivery of $TRP2_{180-188}$ and 7-acyl lipid A in PLGA-NPs induces IFN-γ secretion by TRP2-specific $CD8^+$ T cells in lymph nodes and spleens of the vaccinated mice.....157

4.3.3 Co-delivery of $TRP2_{180-188}$ and 7-acyl lipid A in PLGA-NPs induced potent therapeutic anti-tumor immunity.....161

4.4 Discussion.....170

4.5 References.....176

Chapter 5: General Discussions, Conclusions and Future Directions.....180

5.1 General discussion.....181

5.2 Conclusions.....187

5.3 Future directions.....188

5.4 References.....197

LIST OF TABLES

Table 1-1	Results of clinical vaccine studies in patients with metastatic cancers…	7
Table 1-2	Mechanisms of action, advantages and disadvantages of various particulate delivery systems used for cancer vaccine……..	38
Table 1-3	FDA-approved drug delivery products using PLGA polymers and under development……	40
Table 2-1	Chromatographic gradient program over LC-MS analysis time (15 min)……	82
Table 2-2	Assay validation data for 7-acyl lipid A……..	95
Table 2-3	Assay validation data for PET lipid A……..	96
Table 2-4	Analysis of 7-acyl lipid A and PET lipid A content in PLGA-NPs……..	98
Table 3-1	List of the different peptides used for stimulation of isolated lymphocytes in the *ex-vivo* ELSPOT assay (described in Figure 3-8)…..	118
Table 4-1	Chromatographic gradient program over LC-MS analysis time (15 min)……	150

LIST OF FIGURES

Figure 1-1	Passive *versus* active immunotherapy	3
Figure 1-2	Major steps in classical MHC class I and MHC class II pathways	14
Figure 1-3	Phagosome-to-cystol pathway of cross-presentation	18
Figure 1-4	Vacuolar pathway of cross-presentation	20
Figure 1-5	Cellular localization of TLRs	22
Figure 1-6	Lipid A receptor complex	26
Figure 1-7	TLR4 signaling	27
Figure 1-8	TLR-mediated MyD88-dependent signaling pathway	29
Figure 1-9	MyD88-independent signaling pathway	30
Figure 1-10	Chemical structure of the main active component of MPLA	31
Figure 1-11	Rules of engagement of lipid A-derived molecules	34
Figure 1-12	Chemical structure and biodegradation of PLGA	39
Figure 1-13	$T_{1/2}$ of various ratios of PLA and PGA	42
Figure 1-14	Schematic representation of particle uptake by macrophages and DCs	45
Figure 1-15	A schematic illustration of intracellular trafficking of PLGA-NPs	49
Figure 2-1	Chemical structure of 7-acyl lipid A and PET lipid A	76
Figure 2-2	Chemical structure of the internal standard; Asp-PET lipid A	82
Figure 2-3	Single emulsification-solvent evaporation technique for preparation of PLGA-NPs containing either 7-acyl lipid A or PET lipid A	85
Figure 2-4	Effect of 7-acyl lipid A and PET lipid A on up-regulation of CD40 and CD86 on BMDCs	88

Figure 2-5 Effect of titrating doses of 7-acyl lipid A and PET lipid A on the secretion of pro-inflammatory cytokines by BMDCs..... 90

Figure 2-6 Mass spectra of 7-acyl lipid A, PET lipid A and Asp-PET lipid A... 91

Figure 2-7 Single ion recorder (SIR) chromatograms of Asp PET lipid A (IS) with either 7-acyl lipid A or PET lipid A..... 92

Figure 2-8 A representative standard curve for 7-acyl lipid A and PET lipid A 92

Figure 2-9 The intensity size distribution of PLGA-NPs containing either 7-acyl lipid A or PET lipid A..... 97

Figure 3-1 Double emulsification solvent evaporation technique for preparation of OVA-containing PLGA-NPs..... 112

Figure 3-2 Flow cytometric analysis of isolated $CD4^+$ T cells from transgenic DO11.10 mice..... 121

Figure 3-3 Clonal expansion and activation of adoptively transferred OVA-specific $CD4^+$ T cells following i.p. vaccination with OVA-containing formulations..... 123

Figure 3-4 Kinetics of *in vivo* clonal expansion of adoptively transferred OVA-specific $CD4^+$ T cells after particulate delivery of OVA and 7-acyl lipid A..... 126

Figure 3-5 Treatment of DCs with particulate OVA dramatically enhances primary antigen specific OT-1 $CD8^+$ T cell proliferation..... 128

Figure 3-6 Expanded antigen specific OT-1 $CD8^+$ T cells express activated effector T cell phenotype..... 130

Figure 3-7 IFN-γ secretion pattern of OT1-$CD8^+$ T cells over 96 h co-culture

period with antigen treated DCs..... 131

Figure 3-8 Wild-type mice s.c vaccinated with OVA/7-acyl lipid A-NP simultaneously develop robust OVA specific $CD4^+$ and $CD8^+$ T cell responses..... 133

Figure 4-1 Liquid chromatography/ mass spectrometry (LC/MS)- based method for $TRP2_{180-188}$ quantification..... 149

Figure 4-2 In vitro release of $TRP2_{180-188}$ from PLGA-NPs..... 156

Figure 4-3 Vaccination of healthy mice with $TRP2_{180-188}$ containing NPs induces IFN-γ secretion by TRP2-specific $CD8^+$ T cells in lymph nodes and spleens of the vaccinated mice..... 159

Figure 4-4 Therapeutic anti-tumor immunity in mice vaccinated with $TRP2_{180-188}$ containing NPs..... 163

Figure 4-5 *Ex-vivo* detection of IFN-γ secretion by $TRP2_{180-188}$ specific $CD8^+$ T cells in lymph nodes and spleen of the tumor-bearing vaccinated mice..... 166

Figure 4-6 Assessment of the level of proinflammatory cytokines and immuno-suppressive factors in tumor microenvironment..... 169

Figure 5-1 Schematic representation of the MTT bitransgenic mouse model and the approximate time line of the tumor progression..... 191

LIST OF ABBREVIATIONS

ADCC	antibodies-dependant cell mediated cytotoxicity
a-GalCer	a-galactosyl-ceramide
ANOVA	one-way analysis of variance
AP-1	activator protein-1
APCs	antigen presenting cells
Asp-PET lipid A	aspartic-pentaerythritol- based lipid A
BCA	bicinchoninic acid
Beta 2 m	β2 microglobulin
BLP25	MUC1 lipopeptide
BMDC	bone marrow derived dendritic cells
C	celsius
CCR	chemokine receptor
CD	cluster of differentiation
CDC	complement-dependant cytotoxicity
CFA	complete Freund adjuvant
CD40L	CD40 ligand
cDNA	complementary DNA
CLIP	class II associated invariant chain peptide
CpG	cytosine-phosphate-guanine
cpm	counts per minute
CTL	cytotoxic T lymphocyte
CTLA-4	CTL antigen-4

CV	coefficient of variation
Cx	calnexin
DCs	dendritic cells
EBV	Epstein-Barr Virus
ELC	EBV-induced molecule 1 ligand chemokine
ELISA	enzyme-linked immunosorbent assay
ER	endoplasmic reticulum
ERK	extracellular signal-regulated kinase
FCS	fetal calf serum
FDA	food and drug administration
FITC	fluorescein isothiocyanate
Flt3-L	fetal liver tyrosine kinase 3-ligand
g	gravitation force
GM-CSF	granulocyte-macrophage colony stimulating factor
GPI	glycosyl phosphatidylinositol
h	hour
HEV	high endothelial venules
HLA	human leukocyte antigen
ICAM	intercellular adhesion molecule
IκB	inhibitory binding protein κB
i.d.	intradermal
IKK	IκB kinase
IFN-γ	interferon gamma

Ii	invariant chain
i.l.	intralymphatic
IL	interleukin
i.p.	intraperitoneal
IP-10	IFN-inducible protein-10
i.t.	intratumoral
IRAK	IL receptor associated kinase
IRF3	IFN regulatory factor 3
IS	internal standard
ISOCOMs	immune-stimulating complexes
JNK	c-jun NH2-terminal kinase
KV	kilovolt
L	liter
LBP	LPS binding protein
LC-MS	liquid chromatography coupled with mass spectrometry
LFA	lymphocyte function-associated antigen
LOD	limit of detection
LOQ	limit of quantification
LPS	lipopolysaccharide
LRR	leucine rich repeats
M	molar
mAbs	monoclonal antibodies
MAL	MyD88- adaptor-like

MAPK	mitogen-activated protein kinase
mg	milligram
MFI	mean florescence intensity
MHC	major histocompatibility complex
MIIC	MHC class II compartment
min	minute
MIP	macrophage inflammatory protein
mL	milliliter
MMT	MUC1-expressing mammary tumor
MPLA	monophosphoryl lipid A
MR	mannose receptors
MUC1	mucin-1
MyD88	myeloid differentiation factor 88
NAP	NF-κB-activating kinase association protein
NEMO	NF-kB essential modulator
ng	nanogram
NFκB	nuclear factor κB
NK	natural killer cells
NKT	NK T cells
nm	nanometer
NPs	nanoparticles
NSCLC	non-small cell lung cancer
OD	optical density

OVA	ovalbumin
o/w	oil-in-water
PAMPs	pathogen-associated molecular patterns
PBS	phosphate buffer saline
PE	phycoerythrin
PET lipid A	pentaerythritol- based lipid A
pg	picogram
PGA	poly glycolic acid
PGE2	prostaglandin E2
PLA	poly lactic acid
PLGA	poly(D,L-lactic-co-glycolic acid)
PVA	polyvinyl alcohol
r^2	correlation coefficient
RANTES	regulated on activation normal T cell expressed and secreted
RIP1	receptor interacting protein 1
RP	reversed phase
s.c.	subcutaneous
SDS	sodium dodecyl sulfate
sec	second
SIR	selected ion recording
SLC	secondary lymphoid tissue chemokine
S/N	signal-to-noise
$T_{1/2}$	half-life

TAB	TAK1 binding proteins
TAK	TGF-β activated kinase-1
TANK	TRAF family member-associated NF- κB activator
TAP	transporter of antigen presentation
TBK	TANK binding kinase
TGF-β	transformation growth factor beta
Th	T helper
THF	tetrahydrofuran
TICAM	TIR-domain-containing molecule
TIR	TLR-IL-1 receptor
TIRAP	TIR-associated protein
TLR	Toll-like receptor
TNF-α	tumor necrosis factor alpha
TRAF	TNF receptor-associated factor 6
TRAM	TRIF-related adaptor molecule
Treg	regulatory T cells
TRIF	TIR-domain-containing adaptor protein-inducing IFN-β
TRP2	tyrosinase related protein-2
UV	ultraviolet
V	volt
VEGF	vascular endothelial growth factor
Vis	visible
VLPs	virus like particles

vol	volume
w/o/w	water-in-oil-in-water
WT	wild-type

AMINO ACIDS

A	alanine
C	cysteine
D	aspartic acid
E	glutamic acid
F	phenylalanine
G	glycine
H	histidine
I	isoleucine
K	lysine
L	leucine
N	asparagine
P	proline
Q	glutamine
R	arganine
S	serine
T	threonine
V	valine
W	tryptophan
Y	tyrosine

Chapter one

Introduction

A version of this chapter has been accepted for publication as a chapter entitled

"Nanotechnology for Vaccine Delivery" in

Nanotechnology in Drug Delivery Text Book

Hamdy S, Alshamsan A and Samuel J, Faculty of Pharmacy & Pharmaceutical Sciences,

University of Alberta, Edmonton, AB, Canada, T6G2N8

1.1 The promises and challenges of cancer immunotherapy: an overview

Cancer still represents one of the leading causes of death, misery and pain. Cancer patients are usually treated by a combination of surgery, radiotherapy, and/or chemotherapy. The primary tumor can be apparently removed by these standard therapies. However, micrometastases of disseminated tumor cells often result in tumor relapse and therapeutic failure. Chemotherapy and radiotherapy are also non-specific, destroying healthy tissues along with cancer cells. As a result, cancer patients usually suffer from devastating side effects and very poor quality of life. To overcome these obstacles, there has been a growing focus on immunotherapy as a new avenue for combating this disease [1].

Immunotherapy refers to therapeutic strategies that utilize the immune system to fight cancer. The main focus of such strategies is not only to target and kill tumor cells in a specific manner, but also to alert the immune system, so that the residual tumor cells are kept in check. The expected outcomes are: prevention of the metastatic spread of the disease and the improvement of the quality of life in the affected individuals. Immunotherapeutics are divided into two general forms; active and passive. Passive immunotherapy refers to strategies that complement the immune system, simply by supplying high amounts of effector molecules, such as tumor-specific monoclonal antibodies (mAbs). In spite of their specificity and lower toxicity, compared to standard therapies, mAb-based therapy is very costly, short-lived and dependant on repeated applications [2].

On the other hand, active immunotherapy refers to strategies that activate patient's immune system to target and destroy cancer cells. Active forms of immunotherapy (also known as cancer vaccines) can result in multi-faceted polyclonal immune responses, i.e. simultaneous activation of antigen presenting cells (APCs), $CD4^+$ T cells, $CD8^+$ T cells, B cells and innate immune cells e.g. granulocytes and natural killer (NK) cells (Figure 1-1, adopted from [1]). This multi-faceted response of cancer vaccines enables them to target and eliminate a wider range of tumor cell phenotypes compared to passive therapy [3]. Cancer vaccines offer distinct advantages over standard therapies, namely: increased specificity, reduced toxicity and long-term effects via immunologic memory [1].

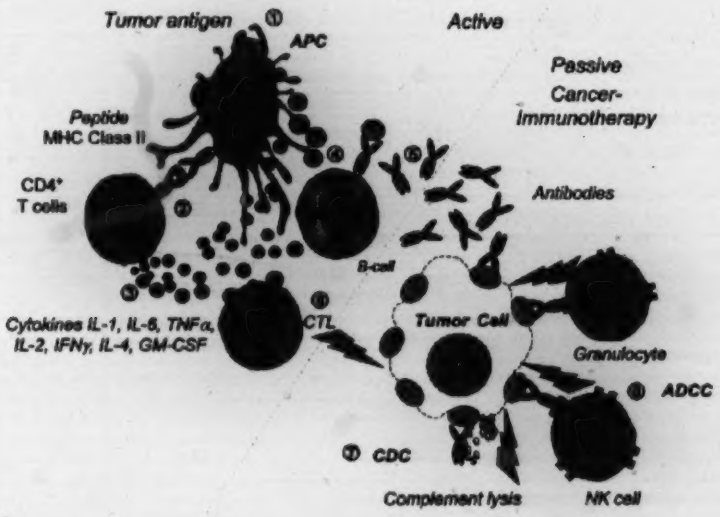

Figure 1-1. Passive *versus* active immunotherapy (adopted from [1])- Active cancer immunotherapy comprises tumor antigen uptake by APCs (1), epitope (peptide) presentation to $CD4^+$ T cells (2), cytokine release (3), B cell activation (4), and antibody production (5), leading to lysis of tumor cells by multiple mechanisms including; antibody-dependent cell-mediated cytotoxicity (ADCC) (6), complement-dependent cytotoxicity (CDC) (7) or attack by cytotoxic T lymphocytes (CTL) (8).

There are five main categories of cancer vaccines. **First** is cell-based vaccine. This category includes various cell types (tumor cells or dendritic cells (DCs)) that have been *ex vivo* activated, or genetically modified to express cytokines, chemokines or growth factors [4-6]. While these strategies show promise, the techniques used are laborious, time consuming and very expensive to carry out in large clinical trials. **Second** category employs the use of antigenic preparations e.g. synthetic peptides, purified antigens, and tumor cell lysates [7-9]. While these alternate approaches bypass many of the production difficulties associated with cellular vaccines, they are poorly immunogenic and often result in less efficient vaccine formulations. **Third** category is plasmid and viral vectors encoding tumor antigens [10,11]. Most of these are powerful activators of immune responses; however, safety concerns have hindered their human application. In addition, repeated administration of most virus vector systems often results in the generation of anti-vector antibodies, which neutralize the effect of subsequent treatments [12,13]. **Fourth** category is heat shock protein (HSP)/tumor peptide complexes (isolated and purified from surgically removed tumor tissues) [14]. HSP are intracellular transporters of peptides. Like normal peptides, tumor associated peptides also transported by HSP. Isolation of such HSP/peptide complexes from tumor tissue captures a wide array of important peptides that can help the immune system to recognize cancer [15]. Administered HSP/peptide complexes are taken up by DCs through specialized receptor (CD91). Engagement of this receptor further lead to enhanced DC maturation. HSP/peptide complexes are thus capable of co-delivering both antigenic material and maturation stimulus to same DC population [15]. However, the applicability of this strategy is limited to the patients with surgically removable tumors. Besides, the process

of production and purification of patient-specific HSP/peptide complexes could be costly and time consuming especially in a large clinical setting. **Fifth** category of cancer vaccines includes non-living nano/micro-sized vaccine delivery systems (also called particulate delivery systems). Particulate delivery systems represent an integrated area of research that combines lipid/polymer technology with molecular immunology, providing specific delivery of vaccine components to the APCs (see section 1.5) [16]. Unlike other cancer vaccination strategies, most of cancer vaccine delivery systems are still under development and have not been extensively studied in clinic yet.

Unfortunately, several factors are hindering the development of effective cancer vaccine formulations for human use. First of all, most cancer antigens are self molecules and are poorly immunogenic or tolerogenic [17]. In addition, cancer cells usually escape from immune responses due to the establishment of an immunosuppressive network [18]. Although the underlying mechanisms have not been fully characterized, these include loss of some MHC class I molecules [19], production of immunosuppressive factors such as vascular endothelial growth factor (VEGF) [20], transforming growth factor-β (TGF-β) [21], and interleukine 10 (IL-10) [22], and up-regulation of antiapoptotic signaling [23]. Cancer induces defects in DC maturation, activation, and generation of myeloid suppressor cells from DC precursors [24]. Tumor microenvironment may facilitate both generation and recruitment of tumor antigen-specific T regulatory (Treg) cells which inhibit effector functions of anti-cancer T cells [25]. Successful cancer vaccine strategies should overcome the aforementioned obstacles and be able to provide sufficient immune activation against "self" cancer antigens, rescue DCs from the tumor

induced-immune suppression, induce robust anti-tumor immune responses that are refractory to Treg- mediated immunosupression and finally reverse immunosuppressant milieu at the tumor microenvironment.

Despite all those challenges, continuous efforts in the field of cancer immunotherapy have led to the development of several cancer vaccine strategies that are now extensively studied in multiple clinical trials for various kinds of cancer (reviewed in [26]). ***At the present time***, only two ***prophylactic cancer vaccines*** have been approved by Food and Drug Administration (FDA); hepatitis B (HB) vaccine and Gardasil™ that prevent the infection with HB virus and human papillomavirus (HPV), respectively [27]. The HB and HPV are believed to be the leading causes of liver cancer [28] and cervical cancer [29], respectively. There is only one ***therapeutic cancer vaccine*** that has been approved by FDA for human use [30]. This vaccine is called Oncophage® and is used for the treatment of renal cell carcinoma patients. Oncophage® is an autologous HSP-peptide complex produced from each patient's own tumor. The approval of oncophage was based on the results from Phase III clinical trials (one of the largest and randomized clinical trials for kidney cancer patients). This study was performed at 118 centers worldwide and enrolled 604 patients that received nephrectomy alone (observation arm) or nephrectomy plus Oncophage® (treatment arm). The results showed that patients in the treatment arm demonstrated remarkable improvement in recurrence-free survival (about 45% over patients in the observation arm). The associated side effects were very mild and mostly related to the injection e.g. edema, pain at the injection site, headache, fatigue and rash [30]. A summary of different vaccination strategies used in clinic and their corresponding objective response is given in Table 1-1 (adopted from [26]).

Table 1-1 Results of clinical vaccine studies in patients with metastatic cancers (adopted from [26]) Overall objective response= 3.8%.

Vaccine type	Cancer type	Vaccine	Total patients	Patients responding
Peptide	Melanoma	Tyrosinase+ GMCSF	16	0
	Melanoma	Peptides in IFA	26	3
	Melanoma	MART-1+ IL-12	28	2
	Prostate	Peptides	10	0
	Melanoma	Peptides on PBMC+ IL-12	20	2
	Breast and prostate	Telomerase	7	0
	Colorectal	Peptides in IFA	10	0
	Multiple	NY-ESO-1	12	0
	Multiple	Ras in DETOX adjuvant	15	0
	Multiple	Peptides in IFA	14	0
Virus	Prostate	Vaccinia-PSA	33	0
	Prostate	Vaccinia-PSA	42	0
	Colorectal	Vaccinia-CEA	20	0
	Colorectal	Vaccinia-CEA and B7-1	18	0
	Multiple	Avipox-CEA (I GMCSF)	60	0
	Multiple	Avipox-CEA	15	0
	Multiple	Vaccinia+avipox-CEA	18	0
Tumor cells	Melanoma	Transduced with GM-CSF	26	1
	Melanoma	Membranes on silicone beads	17	1
	Lung	Transduced with GM-CSF	26	1
	Lung	Transduced with GM-CSF	43	3
	Breast	Transduced with B7-1	30	0
DCs	Melanoma	Pulsed with peptides	17	0
	Melanoma	Pulsed with peptides or lysates	33	3
	Melanoma	Pulsed with peptides or lysates	16	5
	Melanoma	Pulsed with peptides	24	1
	Melanoma	Pulsed with MAGE-3A1	11	0
	Child hood cancers	Pulsed with lysates	15	1
	Kidney	Transfected with RNA	15	0
	Colorectal	Pulsed with CEA peptides	12	1
	Kidney	Pulsed with tumor lysates	35	3
	Multiple	Pulsed with tumor lysates	20	0
HSP	Melanoma	HSP-96	28	2
	Multiple	HSP-96	16	0
		Total	**765**	**29**

The main focus of this chapter will be on the fifth category of cancer vaccine strategies namely, particulate vaccine delivery systems. These systems comprise three main components; first, an antigen against which the immune responses are induced. Second, an adjuvant that acts as danger signals to alert the immune system and activate early as well as long-lasting immune responses. The third component is the delivery system that delivers vaccine antigens and adjuvants to DCs in a targeted and prolonged manner [31]. This chapter will describe the rationale behind the choice of DCs as the target for delivering vaccine components. We will explore the unique features of these cells (DCs) that enable them to be the most professional APCs. Different mechanisms by which the DCs can uptake, process and present vaccine antigens are also described. Next we will highlight the crucial role of Toll-like receptor (TLR) ligands as potent immunostimulatory adjuvants in cancer vaccine formulations. A special emphasis will be put on monophosphoryl lipid A (MPLA), one of the most promising candidates of TLR ligand's family; We will also explore the rational and expected outcomes of simultaneous delivery of antigen and adjuvant to DCs using particulate vaccine delivery systems and provide a brief overview on the application of lipid and polymer based nano-particulate delivery systems for the development of therapeutic vaccines.

1.2 DCs are the most professional APCs

APCs are a group of cells that can process antigens of both endogenous and exogenous origin [32]. Endogenous antigens (such as normal cell proteins, tumor or viral antigens) are processed in the cytosol and presented in the context of major histocompatibility complex (MHC) class I molecules to be recognized by $CD8^+$ T cells [33]. APCs are also capable of internalizing exogenous "extracellular" antigens. Those antigens are processed in specialized compartments called endocytic vesicles or endosome, and presented in the context of MHC class II molecules to be recognized by $CD4^+$ T cells [33]. Whereas MHC class I molecules are constitutively expressed in all nucleated cells, MHC class II molecules are only expressed in APCs. Some APCs have the ability to direct the endocytosed "exogenous" antigens into the MHC class I pathway, leading to the activation of antigen specific $CD8^+$ T cells [32]. This phenomenon is called cross-presentation and will be described in more detail later, in section 1.3.3. Antigen specific $CD4^+$ and $CD8^+$ T cells further differentiate into effector T helper cells (Th) and cytotoxic T lymphocytes (CTL), respectively [33].

APCs include B cells, macrophage and DCs. In addition, other cell types can be induced to express MHC class II/co-stimulatory molecules to present antigens for a short period of time under specific circumstances, such as sustained inflammatory responses. These cells are called non-professional APCs, and they include: fibroblasts, thymic epithelial cells and vascular endothelial cells [33]. Although the general process of antigen presentation is common in all cell types, the efficiency of antigen uptake, processing and presentation differs according to the primary function of each cell type. For example, the

main purpose for antigen presentation by B cells to T cells is to get the help needed for antibody secretion. B cells have moderate capacity for endocytosis, as they are restricted to a single antigenic specificity/B cell [32]. On the other hand, the primary function of macrophages is to clear the tissues from any invading pathogen. Consequently, they have extraordinary ability of endocytosis. However, macrophages are not efficient in antigen presentation, as endocytosed antigens are often subjected to complete degradation by the high levels of proteases in the lysosomes [32]. The inefficient antigen presentation by macrophages could also be explained by their lower expression of surface MHC II and co-stimulatory molecules, compared to B cells and DCs [34]. Unlike B cells or macrophages, the primary function of DCs seems to be antigen presentation [32].

DCs are a heterogeneous population of cells serving as 'sentries' in most peripheral tissues where antigens typically first encounter the immune system [35]. Before antigen encounter, DCs are in the immature state. As they encounter microbial antigens, they engulf them through phagocytosis [36]. This is followed by their activation, maturation and migration to draining lymph node, where they initiate antigen specific T cell immunity. Because of their wide distribution, location at critical sentinel sites (e.g skin and mucosal surfaces), intrinsic migratory capability and ability to activate naïve T cells, DCs are considered the most professional APCs (see details below). Targeting vaccine antigens to DCs would be a valuable strategy to exploit the unique abilities of these cells for antigen acquisition and display, leading to initiation of robust antigen specific T cell responses.

1.2.1 Intrinsic migratory capability of DCs

The intrinsic migratory capability of DCs is mediated by the change of their responsiveness to different chemokines during their development. Immature DCs express a variety of chemokine receptors (CCR) such as CCR1, CCR5 and CCR6. These receptors participate in the localization of DCs in the peripheral tissue and also help in their recruitment to the site of inflammation. For example, CCR6 responds to macrophage inflammatory protein (MIP)-3α that is constitutively expressed in liver and lungs, whereas CCR1 and CCR5 respond to inflammatory mediators in the peripheral tissues, such as MIP-1α and regulated on activation normal T cell expressed and secreted (RANTES) [37]. Upon maturation, DCs down regulate these receptors (so they can leave the inflamed tissue) and up-regulate the expression of CCR7, which directs them into the T cell area of lymph nodes. One ligand for CCR7 is secondary lymphoid tissue chemokine (SLC). SLC is highly expressed in high endothelial venules (HEVs) in lymph nodes and stromal cells in T cell area. The other ligand for CCR7 is Epstein-Barr Virus-(EBV)-induced molecule 1 ligand chemokine (ELC/MIP-3β), which is produced by the resident DC in T cell areas [37-39].

1.2.2 Unique distribution of DCs in lymph nodes

Both SLC and ELC direct antigen loaded DCs into the T cell area of draining lymph node, where continuously moving naïve T cells come to search for their cognate peptide/MHC complexes. In fact, other APCs (B cells and macrophages) are generally excluded from these areas. Antigen bearing DCs are very efficient in seeking out rare antigen specific T cells (1 in 10^5-10^6) [40]. It was estimated that one DC is capable of

scanning 500 different T cells in one hour [41]. The presence of many extensions "dendrites" increases the surface area of DCs and enables them to make contact with multiple T cells simultaneously [42]. Such a competent scanning of the T cell repertoire by DCs helps to guarantee that, even a small number of DCs can initiate an antigen-specific T cell response [41].

1.2.3 DCs have unique ability to activate naïve T cells

Upon activation/maturation, DCs are capable of providing the three signals required for efficient priming of naïve T cells. Mature DCs down regulate their endocytic activity and express high levels of surface MHC class I and MHC class II molecules that present the processed peptides to the naïve $CD8^+$ and $CD4^+$ T cells, respectively (signal 1). Mature DCs also express high levels of accessory molecules, which interact with other receptors in T cells to augment adhesion and co-stimulation (signal 2). Adhesion molecules include: intercellular adhesion molecule (ICAM-1) that interacts with T cell's intercellular adhesion molecule (LFA-1) [33]. Co-stimulatory molecules include: CD40, CD80/CD86 that interact with T cell's CD40 ligand (CD40L) and CD28, respectively. Secretion of large amounts of IL-12 by mature DCs provides the third signal required for the induction of efficient T cell activation [43]. In fact, one of the unique features of DCs is their ability to activate immunologically naïve T cells. This is because DCs are the only APCs that have constitutive expression of MHC class I and class II as well as co-stimulatory molecules. In contrast, B cells and macrophages require activation to express co-stimulatory molecules. Consequently, before they get activated, neither B cells nor macrophage can stimulate naïve T cells [33].

1.3 Antigen processing and presentation by DCs

1.3.1 Classical MHC class I pathway

In the cytoplasm, endogenous proteins are degraded by proteosome into smaller peptides. The peptides are then transported to the endoplasmic reticulum (ER) via transporter associated with antigen presentation (TAP). In the ER, newly synthesized MHC class I molecules bind calnexin (Cx), then β2 microglobulin (β2 m) bind. Binding of β2 m to MHC class I molecules displaces the Cx and allows binding of other chaperone proteins (e.g. calreticulin, tapasin and Erp57) to MHC class I molecules. These proteins bring the MHC class I/ β2 m complex to bind with TAP (via tapasin), where it waits for the arrival of peptides. Peptides then bind the antigenic groove of the MHC class I molecule. This binding stabilize the MHC class I molecule and complete its folding. The loaded MHC class I complex is then released from the TAP and exported to the cell surface via Golgi complex (Figure 1-2, adopted from [33]) [33,44].

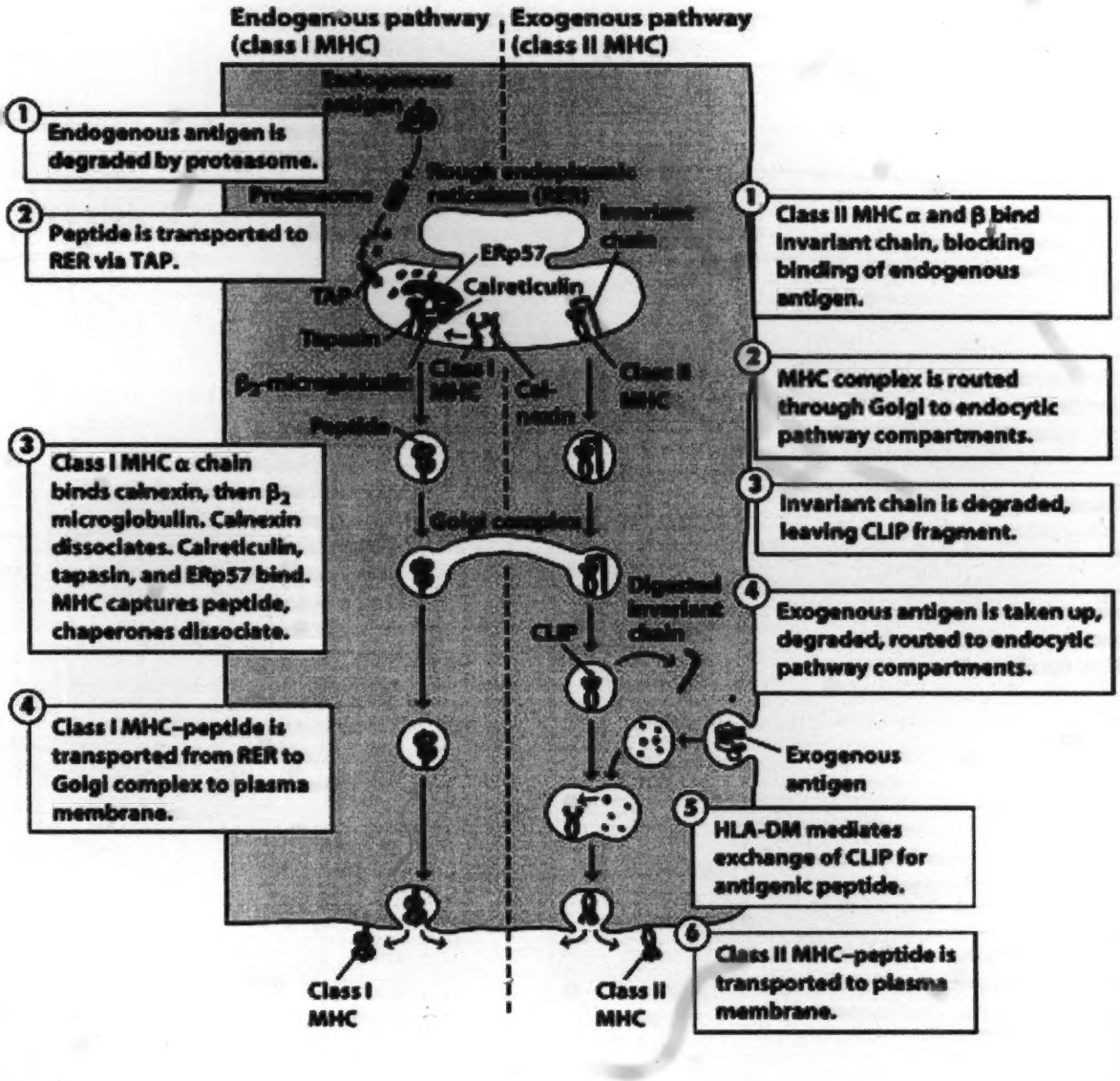
Endogenous pathway (class I MHC)
Exogenous pathway (class II MHC)
1 Endogenous antigen is degraded by proteasome.
2 Peptide is transported to RER via TAP.
3 Class I MHC α chain binds calnexin, then β2 microglobulin. Calnexin dissociates. Calreticulin, tapasin, and ERp57 bind. MHC captures peptide, chaperones dissociate.
4 Class I MHC–peptide is transported from RER to Golgi complex to plasma membrane.
Proteasome
ERp57
Calreticulin
TAP
Tapasin
β2-microglobulin
Class I MHC
Cal-nexin
Class II MHC
Peptide
Golgi complex
Class I MHC
Class II MHC
1 Class II MHC α and β bind invariant chain, blocking binding of endogenous antigen.
2 MHC complex is routed through Golgi to endocytic pathway compartments.
3 Invariant chain is degraded, leaving CLIP fragment.
4 Exogenous antigen is taken up, degraded, routed to endocytic pathway compartments.
Digested invariant chain
CLIP
Exogenous antigen
5 HLA-DM mediates exchange of CLIP for antigenic peptide.
6 Class II MHC–peptide is transported to plasma membrane.

Figure 1-2. Major steps in classical MHC class I and MHC class II pathways (adopted from [33])- Steps are illustrated in the figure and are explained in the text.

1.3.2 Classical MHC class II pathway

The presentation of exogenous antigen is very complex as it involves multiple cellular processes and relies on the ability of DCs to deliver the antigens to the appropriate processing compartment. The first process involved is antigen internalization (endocytosis). Immature DCs can internalize exogenous antigens through several pathways. The nature and size of antigens determine which internalization pathway is utilized. Large particulate antigens are taken up by phagocytosis. Small particulate antigens can be internalized through membrane-bound receptors (receptor-mediated endocytosis). DCs express many cell surface receptors that are involved in this process such as mannose receptors (MR), DEC-205, Fcγ receptors (CD32 and CD64) and the scavenger receptors (αvB5 and CD36). Fluid phase endocytosis (also called micro- or macropinocytosis) involves the uptake of extracellular fluid dissolved antigens. Immature DCs are very efficient at all forms of endocytosis [32,45].

Endocytosed antigens move into the interior of the cells in a specialized route known as, the endocytic pathway. The endocytic pathway comprises 3 increasingly acidic compartments: early endosomes (pH 6.0-6.5); late endosomes or endolysosomes (pH 5-6) and lysosomes (pH 4.5-5) [32]. Both endosomes and lysosomes contain protein degradation enzymes known as acid proteases. These proteases are activated in the acidic pH resulting in the degradation of enclosed antigens into smaller peptides, which bind to class II molecules. The most active members of the acid proteases are the cysteine proteases cathepsins B, D, S and L. The generated peptides are then ready to bind newly synthesized MHC class II molecules for presentation to $CD4^+$ T cells [32].

The question that arises here is how MHC class II molecules gain access to the generated peptides in the endosomes. In the ER, the newly synthesized MHC class II molecules bind to a protein known as the MHC class II-associated invariant (Ii) chain. Li binds to the MHC class II α:β heterodimers with part of its polypeptide chain lying within the peptide binding groove of the MHC molecule. This binding blocks the groove and prevents the loading of any misfolded proteins that are present in the ER [46]. In addition to this role, the invariant chain possesses sorting signals in its cytoplasmic tail, which direct the transportation of newly synthesized MHC class II molecules from the ER into the endocytic pathway (through Golgi complex). Within the endocytic vesicles, the acid proteases cleave the invariant chain, leaving a short peptide fragment called CLIP (class II associated in variant chain peptide) still bound to the peptide binding groove of MHC class II molecule [47,48]. Loading of antigenic peptide to the MHC class II molecules occurs in an endosomal compartment called MHC class II compartment (MIIC), where MHC class II–containing vesicles are fused with the acidified vesicles that contain the fragmented peptides. In these compartments, CLIP is removed with the help of a MHC II-like molecule known as HLA-DM. HLA-DM binds to MHC class II molecules allowing the exchange of CLIP with the antigenic peptide [49]. The resulting peptide/MHC class II complexes are then transported to the cell surface for recognition by the $CD4^+$ T cells. Surface MHC class II molecules are recycled again through the endocytic pathway and get loaded with the newly generated peptide fragments. Summary of the steps involved in MHC class I and class II pathway is illustrated in Figure 1-2 (adopted from [33]).

1.3.3 Cross-presentation of exogenous antigens

Cross-presentation is defined by the ability of certain types of APCs to engulf exogenous antigens and deliver them to the MHC class I molecules for recognition by $CD8^+$ T cells. This process ensures that APCs can develop CTL immunity against tumor cells and viral infected cells (by taking up tumor or virus-derived antigen/cellular debris and cross-present them to $CD8^+$ T cells) [50,51]. Cross-presentation is also highly relevant for anti-tumor vaccines. Development of cancer vaccine formulations capable of delivering tumor antigens intracellulary into the MHC class I processing pathway would facilitate cross-presentation and the subsequent induction of anti-tumor CTL responses. The exact mechanism by which exogenous antigens reach the MHC class I pathways is poorly understood, however, two distinct routes have been proposed; phagosome-to-cytosol pathway and vaculolar pathway.

Phagosome-to- cytosol pathway

In this pathway (Figure 1-3, adopted from [52]), the endocytosed antigens have to be transferred from the phagosome into the cytosol for further processing. The issue that comes up is how these antigens gain access to the cytosol. It was recently found that several ER-resident proteins are present in the phagosome [53-55]. Examples of these proteins are: MHC class I and associated proteins (TAP, Tapasin) as well as SEC61. Interestingly, SEC61 forms a doughnut shape pore in the phagosomal membrane and is thought to be responsible for the export of antigens out of the phagosome [56,57]. Once in the cytosol, the antigen is degraded by proteasomes into smaller peptides, which are then transported via TAP into the ER, where they can be loaded onto MHC class I

molecules. Similar to the conventional MHC class I processing pathway, phagosome-to-cystol pathway requires functional TAP, and can be blocked by proteosome inhibitors (e.g. lactacystin).

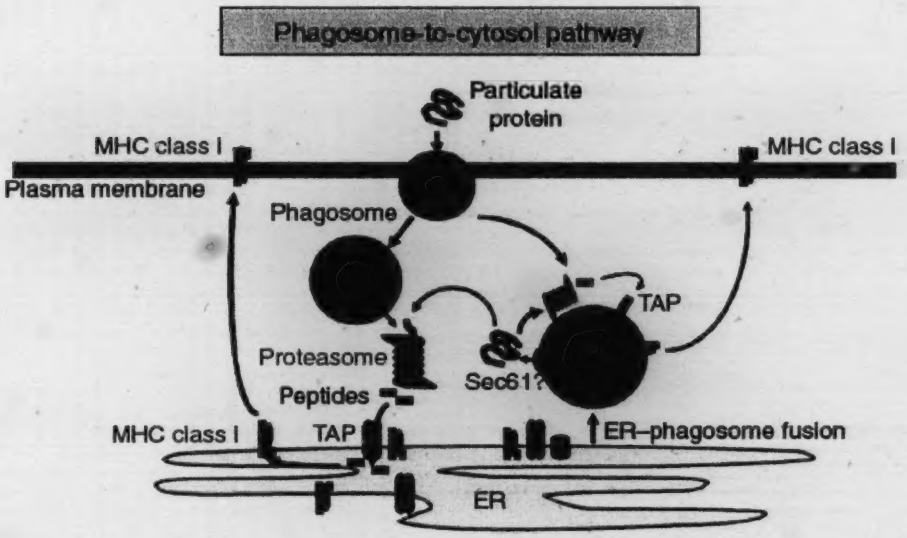

Figure 1-3. Phagosome-to-cystol pathway of cross-presentation (adopted from [52])- In the phagosome-to-cytosol pathway, antigen is internalized into phagosomes or macropinosomes and then transferred into the cytosol. Recently, it was found that a subset of phagosome acquires TAP, MHC class I, Tapasin, and SEC61 from the ER, and it is not presently clear to what extent these vesicles versus standard phagosomes participate in this pathway. The mechanism by which proteins are transferred from phagosomes into the cytosol is not understood, although it has been hypothesized that this export may occur through SEC61. Once in the cytosol, the antigen is hydrolyzed by proteasomes into oligopeptides that are then transported by TAP and loaded onto MHC class I molecules in the ER or the 'ER – phagosome' vesicles.

The discovery of MHC class I machinery inside the phagosome had led to the proposal of an alternative route, in which the degraded peptide are re-imported to the phagosome (through TAP-dependant mechanism), where they can be loaded onto MHC class I molecules and exported to the cell surface. This pathway is thus called phagosome-to-cystol-to-phagosome pathway [53]. The question that arises here is how the ER-resident MHC class I molecules gain access to enter the phagosomes. While the exact answer to this question remains unknown, two routes of entry had been proposed. First possible route is that cell surface MHC class I molecules could be internalized into the phagosomes through membrane invagination during phagocytosis [58]. An alternative route is based on the previously discovered fusion between the ER and phagosomes. This fusion may also account for the presence of other ER-resident proteins inside the phagosomes, such as TAP, Tapasin and Sec61 [59].

Vacuolar pathway

In contrast to the phagosome-to-cystol pathway, cross-presentation by vacuolar pathway doesn't require TAP and is insensitive to proteosome inhibitors [60]. However, vacuolar pathway could be blocked by another protease inhibitor (leupeptin) [61]. It has been found that leupeptin mainly inhibits phagosome-resident proteases, such as cathepsins. These observations imply that in the vacuolar pathway, the antigens don't have to leave the phagosome for degradation in the cytosol. Instead, they are degraded by the acid proteases existing inside the phagosomes. It appears that cathepsin S is the major protease involved in generating peptides for cross-presentation by the vacuolar pathway. In fact, DCs or macrophages that were negative for cathepsin S were unable to cross-present

antigens by the vacuolar pathway [61]. Once degraded, the peptides can be loaded onto the MHC class I molecules inside the phagosome and exported to the cell surface (Figure 1-4, adopted from [52]) .

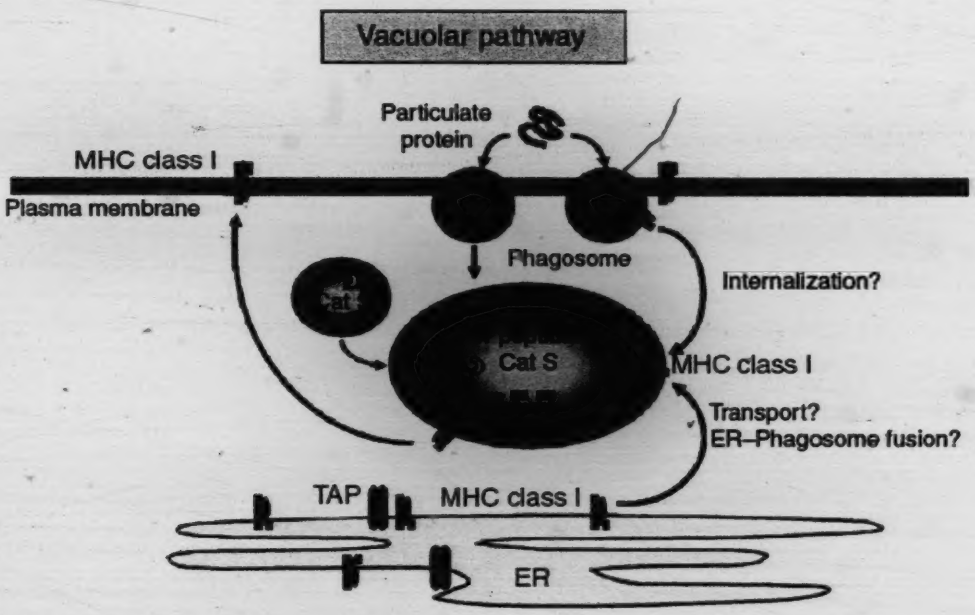

Figure 1-4. Vacuolar pathway of cross-presentation (adopted from [52])- In the vacuolar pathway, antigen is internalized into phagosomes where it is degraded into oligopeptides by cathepsin S and possibly other endosomal proteases. The resulting peptides are probably loaded onto major histocompatibility complex class I molecules that have trafficked into the vesicle from the plasma membrane or from the endoplasmic reticulum (ER), either by internalization, transport or ER–phagosome fusion.

1.4 Delivering TLR ligands to DCs

1.4.1 TLRs structure and function

One of the hallmarks of DCs is their ability to detect the presence of microbial organisms by recognition of evolutionary conserved molecules, known as pathogen-associated molecular patterns (PAMPs). PAMPs binds to specialized family of receptors on DCs called TLRs. TLRs are type I transmembrane proteins that are characterized by the presence of extracellular tandem repeats of leucine-rich region (known as leucine rich repeats, LRR), and intracellular Toll/IL-1 receptor homology (TIR) domain. Until now, 13 members have been identified in the TLR family. The presence of various TLRs with different specificity ensures that the immune system can recognize wide range of microbial-associated molecules. For example, peptidoglycan of gram-positive bacteria, lipopolysaccharides (LPS) of gram-negative bacteria, viral double-stranded RNA and bacterial unmethylated CpG motifs are recognized by TLR2, TLR4, TLR3 and TLR9, respectively (Figure 1-5, adopted from [62]). Interaction of TLRs with their specific PAMPs induces DC maturation/activation and initiates the proper T cell responses to eliminate the invading microbe [62].

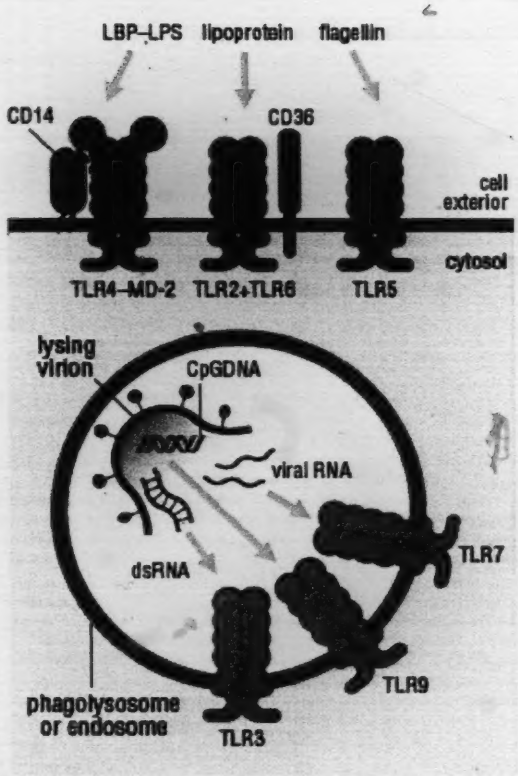

Figure 1-5. Cellular localization of TLRs (adopted from [62])- TLRs that recognize bacterial and fungal cell wall components, such as TLR4-MD2, TLR5 and the heterodimers TLR2+TLR6, are localized to the plasma membrane and can recognize ligands there. In contrast, TLRs recognizing nucleic acids (TLR3, TLR7, TLR8 and TLR9) are primarily or completely contained in intracellular membranes and unavailable for interaction with extracellular ligands.

1.4.2 Role of TLR ligands in augmenting vaccine-induced immune responses

Tumor-induced impairment in DC functions is one of the leading causes of compromised anti-tumor immune responses [63]. Vaccine strategies that co-deliver cancer antigens along with an appropriate TLR ligand to the same DC population, can not only target antigen actively to DCs, but also provide immune activation and rescue impaired DCs from tumor-induced immuosupression [64]. TLR ligands enhance vaccine efficacy through multiple mechanisms: TLR stimulation of DCs results in increase in surface peptide/MHC complexes, co-stimulatory molecules, and cytokine secretion, the three signals required for T cell activation and proliferation [65]. Moreover, enhanced cross-presentation of exogenous vaccine antigens has been demonstrated, when TLR3 or TLR9 ligands were co-administered with the vaccine [66]. Remarkably, TLR activated DCs are also capable of reversing the Treg suppressive effects. In fact, it has been recently shown that IL-6 secreted by TLR4-activated DCs renders antigen specific T cells refractory to the suppressive activity of Treg cells [67]. Other studies have shown that stimulation of DCs with TLR ligands enhances the proliferation of antigen specific T cells, making them resistant to Treg-mediated immunosupression [68,69].

1.4.3 LPS-induced immune activation

LPS (also known as bacterial endotoxin) is a major cell wall constituent of Gram-negative bacteria, and is considered one of the most potent inducers of the immune system. LPS is highly toxic to most mammals and if released in large quantities into the blood stream, it causes a wide spectrum of nonspecific pathophysiological reactions, including: inflammation, fever, intravascular coagulation, endothelial injury, hypotension

and multi-organ failure that may lead to death [70]. LPS exerts its toxicity in an indirect fashion. It activates many host cells (e.g DCs, macrophage, and epithelial cells) to release a wide range of endogenous mediators, such as: cytokines (e.g IL-1, IL-6, IL-8, tumor necrosis factor (TNF-α)), bioactive lipids (thromboxane A2 and platelet activating factor), oxygen radicals and adhesion molecules [70]. The potent immumnostimulatory effects of LPS would be very beneficial in improving the efficacy of poorly immunogenic vaccine formulations. But, unfortunately, it's extreme toxicity and the induction of a sepsis-like systemic inflammatory response syndrome has prohibited its use in clinical settings.

LPS exhibits a great variability among different strains of bacteria. However, it has a common basic structure consisting of a highly variable outer O-antigen segment; core region, and a conserved lipid moiety (known as lipid A). Previous studies have shown that the lipid A component is responsible for both the adjuvant and the toxic effects of LPS [71]. Lipid A is embedded in the bacterial cell membrane, but can be released upon bacterial division and/or lysis. The following two sections will describe how lipid A moiety is delivered to the immune cells and what are the molecular mechanisms responsible for the immunostimulatory properties of lipid A. The last section will be focused on MPLA, a lipid-A derived compound that maintains all the immunostimulatory properties of the parent lipid A molecule, but it is not toxic.

1.4.4 Lipid A recognition

Recognition of LPS (or lipid A) is an indirect process that occurs in multiple steps and utilizes a variety of proteins (Figure 1-6, adopted from [72]). The first protein involved in LPS recognition is called LPS binding protein (LBP). LBP is an acute phase protein that is synthesized in the liver and plays an important role in the transfer of LPS from bacterial membrane to its receptor (LPS receptor complex). LBP binds polymeric LPS aggregates and disrupt them into lipid A monomers. Several hundreds of lipid A monomers per LBP molecule are then transferred to form a ternary complex with the CD14 receptor. CD14 is not transmembrane protein, but it is anchored to the cell membrane through glycosyl phosphatidylinositol (GPI) linkage. Lack of cytoplasmic domain of CD14 limits the ability of CD14 to activate intracellular signaling cascade upon binding with its ligand (lipid A/LBP). To overcome this problem, CD14 has to transfer lipid A into another co-receptor that spans the cell membrane and hence can initiate signaling pathways. This co-receptor is TLR4/MD2. TLR4, as previously mentioned, is a member of TLR family that is specialized for the recognition of lipid A moiety of the Gram negative bacterial LPS. MD2 is an extracellular accessory molecule that binds the extracellular domain of TLR4. In co-operation with TLR4, MD2 controls lipid A recognition and fine discrimination among LPS from different strains of Gram-negative bacteria [72]. In fact, lipid A is not directly bound to TLR4, rather it is sandwiched inside of MD2 protein. Lipid A binding to TLR4/MD2 complex induces homodimerization of the receptor and initiate several signaling pathways (discussed below).

For the sake of simplicity, downstream signaling molecules will be mentioned by their abbreviated names. The full names and their abbreviations are provided at the beginning of the thesis in the list of abbreviations.

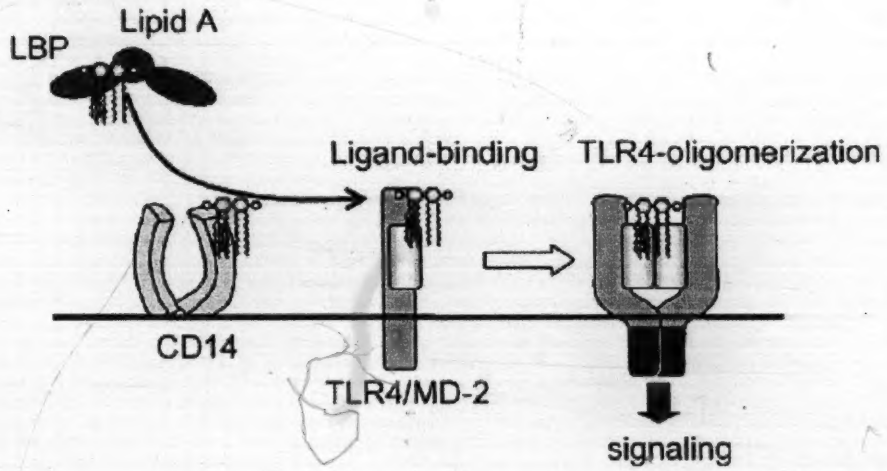

Figure 1-6. Lipid A receptor complex (adopted from [72])- LBP binds polymeric LPS aggregates and disrupts them into lipid A monomers. LBP then transfer lipid A to bind with the CD14 receptor, which further load lipid A onto TLR4/MD2. After lipid A binding, homotypic interaction of TLR4 is induced, leading to dimerization of the cytoplasmic portion and triggering of the signal.

1.4.5 Lipid A-initiated signaling cascades

LPS/lipid A recognition by TLR4/MD2 complex is followed by receptor homodimerization and recruitment of four TIR-containing adoptor molecules to TIR domain of the TLR4, namely: MyD88, MAL (also known as TIRAP), TRIF (also known as TICAM1), TRAM (also known as TICAM2). These four molecules can initiate two different signaling pathways. Based on the utilization of MyD88 or other adoptor molecules (such as TRIF and TRAM), those pathways are named MyD88-dependent, and MyD88-independent pathways, respectively (Figure 1-7, adopted from [73]).

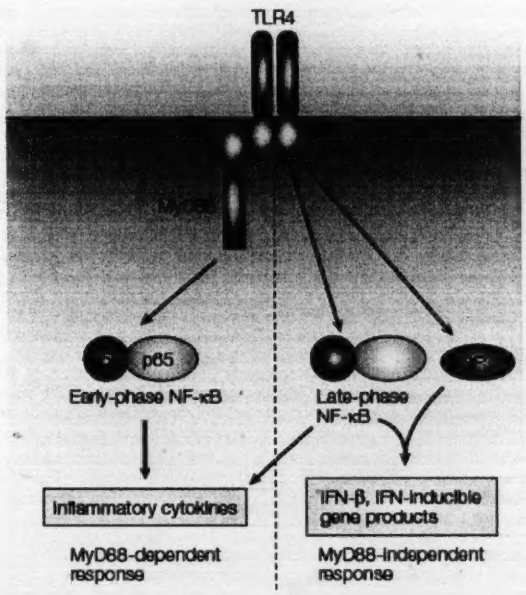

Figure 1-7. TLR4 signaling (adopted from [73])- Stimulation of TLR4 facilitates the activation of two pathways: the MyD88-dependent and MyD88-independent pathways. The MyD88-dependent pathway involves the early phase of NF-κB activation, which leads to the production of inflammatory cytokines. The MyD88-independent pathway activates IRF3 and involves the late phase of NF-κB activation, both of which lead to the production of IFN-β and the expression of IFN-inducible genes.

First pathway occurs early and activates NF-κB, leading to the production of many pro-inflammatory cytokines. The other pathway activates Interferon (IFN)-regulatory factor (IRF3) and involves the late phase of NF-κB activation, leading to the production of IFN-β and the expression of IFN-inducible gene products (Figure 1-7, adopted from [73]). Details of each pathway are explained below.

MyD88 dependant pathway

Schematic diagram of MyD88 dependant pathway is shown in Figure 1-8 (adopted from [74]). Upon stimulation, TIRAP and then MyD88 are recruited to bind the cytoplasmic domain of TLR4. MyD88 then recruits IRAK-4 and IRAK1 through death domain-death domain interactions. IRAK1 then is transphosphorlated by the the IRAK-4 kinase activity. Phosphorylated (activated) IRAK1 then associates with TRAF6 (which is also recruited to the receptor complex upon TLR stimulation) and activates it. The IRAK1/TRAF6 complex then dissociates from the receptor complex and binds to a protein kinase complex composed of TAK1, TAB1, TAB2 and TAB3, at the membrane portion. IRAK1 remains in the membrane and is degraded, while [TRAF6, TAK1, TAB1, TAB2 and TAB3] complex migrates to the cytoplasm, where it binds to other proteins (E2 ligases Ubc13 and Uev1A) forming a larger complex with them. Ubc13 and Uev1A complex promotes the synthesis of lysine 63-linked polyubiquitin chain of TRAF6, and by this means, induces TRAF6-mediated activation of TAK1. TAK1 then activates the IKK complex (composed of IKK-α, IKKβ and IKKγ/NEMO), which catalyses the phosphorylation of IκB proteins. Phosphorylated IκB proteins are ubiquitinated and degraded by the proteosome, with the subsequent release of NF-κB that translocates into

the nucleus. In addition to NF-kB, TAK1 activates several members of the MAPKs, e.g. p38, ERK and JNK, leading to the activation of another transcription factor, AP-1. In the nucleus, NF-kB and AP-1 control the expression of many genes encoding inflammatory cytokines, e.g. TNF-α, IL-6, IL-12 and IL18.

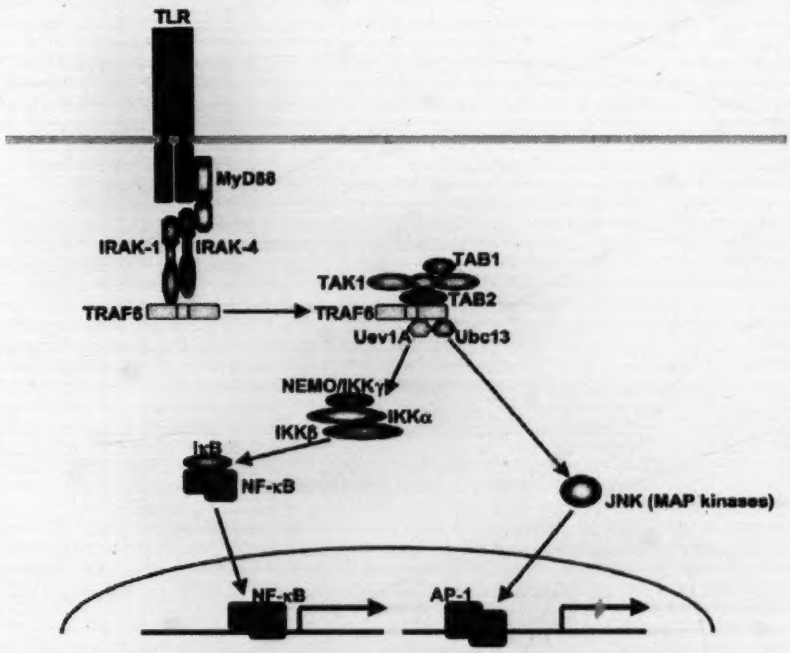

Figure 1-8. TLR-mediated MyD88-dependent signaling pathway (adopted from [74])- MyD88 binds to the cytoplasmic portion of TLRs through interaction between individual TIR domains. Upon stimulation, IRAK-4, IRAK-1, and TRAF6 are recruited to the receptor, which induces association of IRAK-1 and MyD88 via the death domains. IRAK-4 then phosphorylates IRAK-1. Phosphorylated IRAK-1, together with TRAF6, dissociates from the receptor and then TRAF6 interacts with TAK1, TAB1, and TAB2. The complex of TRAF6, TAK1, TAB1, and TAB2 further forms a larger complex with Ubc13 and Uev1A, which induces the activation of TAK1. Activated TAK1 phosphorylates the IKK complex, consisting of IKKα, IKKβ, and NEMO/IKKγ, and MAP kinases, such as JNK, and thereby induces the activation of the transcription factors NF-κB and AP-1, respectively.

MyD88 independent pathway

Schematic diagram of MyD88 independent pathway is shown in Figure 1-9 (adopted from [75]). In this pathway, TRIF and TRAM adoptor proteins are recruited to the receptor complex upon TLR stimulation. TRIF then associate with TRAF6 and RIP1, resulting in the late phase activation of NF-κB. In a parallel pathway, TRIF also recruit and interact with NAP1 and TBK1/IKKi (also known as IKKε) complex. This complex phosphorylates IRF-3, which then dimerizes and translocates to the nucleus. In the nucleus, IRF-3 induces the expression of IFN-β and IFN-inducible genes e.g IP-10.

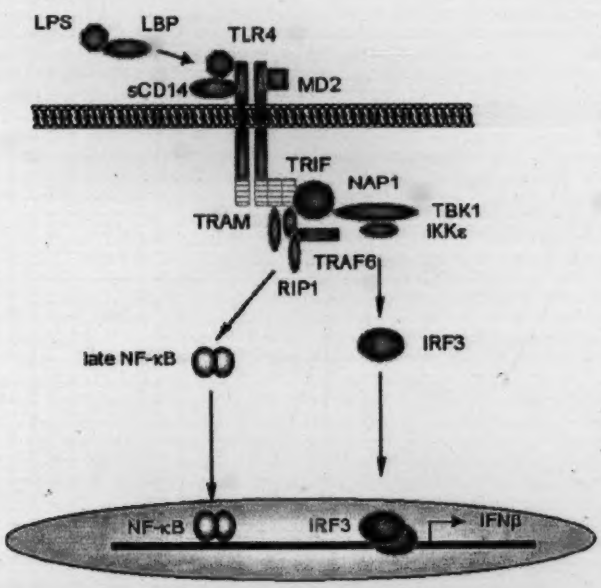

Figure 1-9. MyD88-independent signaling pathway (adopted from [75])- The late-phase activation of NF-kB occurs through the MyD88-independent pathway involving the adaptor molecules, TRIF and TRAM. TRIF associates with TRAF6 and RIP1, as well as NAP1 and TBK1, to lead to the activation of the transcription factors, NF-kB and IRF3, respectively.

1.4.6 Non toxic version of lipid A: MPLA

It has been shown that both toxicity and adjuvant effects of LPS are mediated by lipid A moiety. The chemical structure of lipid A was elucidated, and the structure-activity relationship of the lipid A has been extensively studied with the intension of uncoupling the toxic effects and adjuvant effects [71,76-78]. The toxic effects of lipid A moiety appear to be dependant on a peculiar conformation that is determined by the presence of two phosphate (PO_4) groups and at least one ester linked fatty acid. Removal of one phosphate group from the reducing end 'right handed' sugar of the lipid A disaccharide extracted from *Salmonella minnesota RC595* has dramatically reduced its toxicity 100-1000 fold, without affecting the immunostimulatory effects of the parent LPS molecule [79]. The resulting product was thus named MPLA.

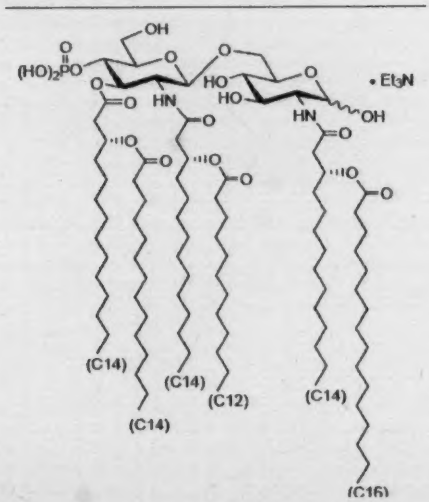

Figure 1-10. Chemical structure of the main active component of MPLA (adopted from [80])- MPLA is extracted from *Salmonella minnesota* as a mixture of tetra-, penta- and hexa-acylated forms. Each congenger has been synthetically reproduced and tested for individual reactivity. Shown here, is the most active congener.

Additional studies have been done to refine MPLA structure and they showed that removal of an ester-linked fatty acid group from the 3-position further reduced the toxic properties of LPS without affecting the adjuvant activity [81]. Structure of MPLA is shown in Figure 1-10 (adopted from [80]).

As described earlier, the main toxicity of LPS is attributed to its potent ability to induce the production of pro-inflammatory cytokines from immune cells (mainly monocytes and mcrophages). In fact, it has recently been found that LPS modulates the expression of almost 1000 genes in macrophages [82]. In order to investigate why MPLA is not as toxic as LPS, several studies have compared the induction of cytokine secretion by equivalent doses of MPLA *versus* LPS. These studies have shown that the low toxicity of MPLA could be explained by: a) its decreased ability (10-fold less than LPS) to induce the production of pro-inflammatory cytokines (mainly IFN-γ, TNF-α and IL-6) [83], and b) its ability to induce higher level of immunoregulatory cytokines (e.g. IL-10) [84]. The exact molecular mechanism for this difference in MPLA and LPS ability to control cytokine secretion was not properly understood. But, it was proposed that the conformational change of MPLA (due to the lack of phosphate group) may lead to unfavorable binding with the receptors, which may result in weak intracellular signaling and less efficient induction of cytokine secretion [84]. However, Mato *et al* [85] have recently demonstrated that interaction of different lipid A ligands with TLR4/MD2 receptor complex can induce different arrangement of the TLR4/MD4 receptor that results in the recruitment of specific adoptor proteins on the expense of others. For example, engagement of MPLA with TLR4/MD2 receptor leads to selective activation of

TRIF or "MyD88 independent pathway", which results in the production of IFN-β, a potent inducer of T cell activation, which explains the efficacy of MPLA as an adjuvant. Lack of toxicity of MPLA is then explained by the failure of MPLA to activate the MyD88 dependent pathway, which controls the expression of pro-inflammatory cytokines, the main mediators of lipid A toxicity. On the other hand, LPS binding to its receptor leads to the recruitment of the 4 adoptor molecules (MyD88, Mal, TRIF and TRAM) and activation of both signaling pathways resulting in combined adjuvant and toxic effects (Figure 1-11, adopted from [86].

MPLA has been evaluated extensively in human clinical trials with infectious diseases (hepatitis B, malaria, herpes simplex virus), cancer (metastatic melanoma, glioma, breast cancer, colorectal cancer and ovarian cancer) and allergy vaccines (for prevention or relief of symptoms that are caused by pollens from certain grasses, trees, and household dust mites). Throughout these trials, more than 33,000 doses of MPLA have been given to over 12,000 patients, demonstrating both safety and efficacy for human use [87-89].

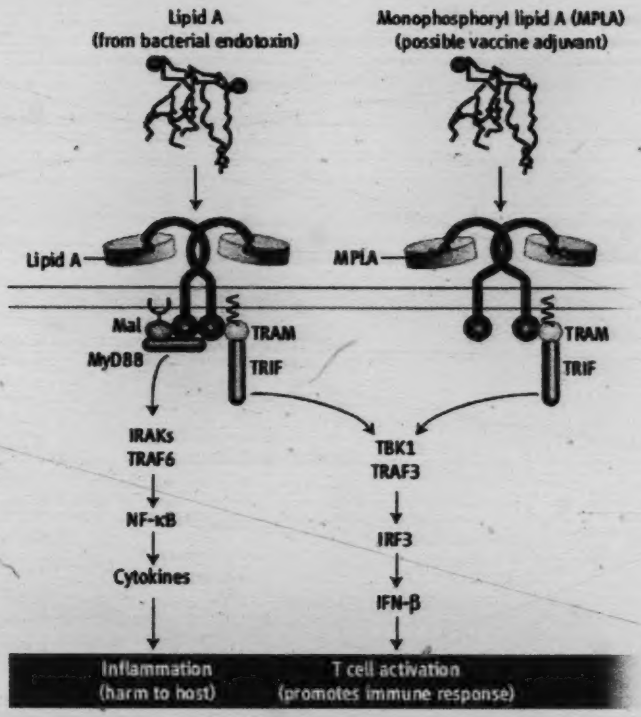

Figure 1-11. Rules of engagement of lipid A-derived molecules (adopted from [86])- The TLR4–MD-2 complex is expressed as dimers on the surface of immune cells (T and B cells, phagocytes). Lipid A and its analog, MPLA, bind to MD-2. There is no direct evidence that these lipids bind TLR4. The specific engagement of each lipid may cause structural changes in MD-2 and TLR4, resulting in new protein binding sites in the cytoplasmic domain of TLR4. The resulting recruitment of specific adapter proteins activates distinct signaling pathways and associated cellular responses.

1.5 Targeting DCs with vaccine delivery systems: *ex vivo* loading *versus in vivo* targeting

The recognition of DC role in initiating T cell immune response, along with the development of protocols for the isolation and culture of large number of DCs *in vitro* have grabbed the attention of many researchers to the use of DCs-based cancer vaccines. In these strategies, monocytes ($CD14^+$) are isolated from peripheral blood and cultured in the presence of granulocyte-macrophage colony stimulating factor (GM-CSF) and IL-4 to generate immature DCs [90]. Alternatively, DCs could also be generated from $CD34^+$ precursors cultured in the presence GM-CSF, fetal liver tyrosine kinase 3-Ligand (Flt3-L) and TNF-α [91-93]. Immature DCs are then loaded with the tumor antigens through the addition of proteins [94], peptides [95-97] or tumor lysates [98] to culture medium or through transfection of complementary DNA (cDNA) encoding tumor antigens [99]. The generation of DC-tumor cell hybrid is also reported [100]. To ensure the co-stimulatory capacity and the ability to induce potent antigen-specific cellular immune responses, loaded DCs are treated with various maturation stimuli such as: CD40L or pro-inflammatory cytokines e.g. IL-6, IL-1 and PGE2 [101]. The final step is the injection of fully loaded and mature DCs back into the patient. Several routes of administration had been examined; intravenous (i.v.), subcutaneous (s.c.), intradermal (i.d.), intratumoral (i.t.) and intralymphatic (i.l.) [102].

Ex-vivo loaded DC-based cancer vaccines have been extensively studied in a variety of experimental models and clinical trials (Reviewed in [103]). These studies have shown that this strategy is safe, well tolerated and capable of inducing cellular immune

responses. However, the overall rate of objective clinical response in patients is only 7% [26]. One major concern is that, the migration of *ex-vivo* generated DCs is inefficient. Only 3-5% of the injected DCs could actually migrate to the lymph node for presenting the loaded antigen to the T cells [104]. This can be improved by pre-conditioning of the vaccine injection site with pro-inflammatory cytokines (e.g TNF-α and/or IL-6). However, administration of these cytokines often leads to non-specific immune stimulation and undesirable side effects. In addition to their poor migratory capacity, there are numerous limitations of the *ex vivo* loaded DCs that truly hinder their development for human use (reviewed in [103]). Ex vivo loaded DCs have to be tailor made for each individual. Therefore, the process of vaccine development is time consuming, requires extensive lab work and is costly. The strategy is restricted to DC subsets that can be isolated in sufficient quantity or cultured *in vitro*. Besides, the excessive physical handling of DCs/precursors may increases the risk of endotoxin contamination. Moreover, standard culture/activation protocols for generation of clinical grade DCs are lacking; therefore, vaccine quality may differ among different clinic centers. The half life of peptide/MHC complexes on the DC surface is relatively short. Furthermore, in addition to added proteins/peptide or tumor lysate, cultured DCs take up all sorts of proteins in the culture medium, decreasing the number of effective peptide/MHC complexes. Finally, lots of variable parameters exist in the process (e.g dose of DCs, route and frequency of administration).

As a next step in the development of DC–based vaccines, it is proposed to load DCs with tumor antigens along with appropriate adjuvants *in vivo* using particulate vaccine

delivery systems. Such vaccines deliver antigens and maturation stimuli to the same cell enabling the usage of the intricate migratory capacity of DCs in their natural environment. Previous studies have shown that timing at which antigen and adjuvant reach DCs is crucial and has profound effect on the immune outcome. If the maturation stimulus is given too late after the antigen reaches the DCs, tolerance may be induced. On the other hand, if the antigens reach already mature DCs, they will not be efficiently presented [105]. Delivering both antigen and adjuvant coincidently to DCs will maximize the immune activation and limits the undesired toxicities that often result from systemic administration of adjuvants. Furthermore, the particulate delivery of antigens to DCs provides continuous supply of peptide to be presented by the newly formed MHC molecules on DC surface [106]. Particulate vaccine delivery systems can circumvent the extensive laboratory work that is needed to generate tailor-made DC vaccines for individual patients. Using such approaches, clinical intervention is limited only to vaccination and there is no need for several cycles of blood withdrawal, cytapheresis, *in vitro* culture and DC administration [103]. Additionally this approach will provide on-shelf products, feasible large scale production with lower costs, equal product quality among different locations and accessibility to a large number of patients. Particulate delivery systems include micro/nanoparticles, liposomes, archaeal lipid liposomes (archaeosomes), immune-stimulating complexes (ISOCOMs) and virus like particles (VLPs) [107]. Table 1-2 (adopted from [107]) summarizes mechanism of action, advantages and limitation of each delivery system.

Table 1-2. Mechanisms of action, advantages and disadvantages of various particulate delivery systems used for cancer vaccines (adopted from [107])

Delivery system	Mechanism of action	Advantages	Limitations
Micro-and Nanoparticles	APC targeting, prolonged release, absorbance onto organs, tissues, mucosal surfaces, possibility of continued stimulation	Biodegradable Polymers available High antigen loading Enhanced antigen protection Enhanced antigen presentation	Size limits use for parental application Use of organic solvents during production process
Liposomes	Modified liposomes can target APC and APC activation	Versatile Non-toxic Biodegradable Biocompatible Enhanced antigen protection	Physical instability Low entrapment rates Scaling –up problems
Archaeosomes	APC targeting and activation	High physicochemical stability Highly immune stimulatory	Experimental Low entrapment rates Biological production
Immune-stimulating complexes	APC activation	Highly immune stimulatory	Toxicity Antigen must contain lipophilic domain
Virus-like particles	APC targeting and activtion	Highly immune stimulatory	Biological production

1.6 PLGA-based vaccine delivery system

1.6.1 PLGA composition and applications

PLGA is an FDA approved biodegradable polymer that had been widely used in the manufacturing of surgical sutures and in several controlled release drug products for human use (including children) [108,109]. PLGA co-polymers are aliphatic polyesters composed of varying proportions of lactic and glycolic acids. Upon encountering aqueous media, PLGA is hydrolysed (degraded) into lactic and glycolic acid monomers (Figure 1-12), which are normal metabolites and well tolerated in the human body [110].

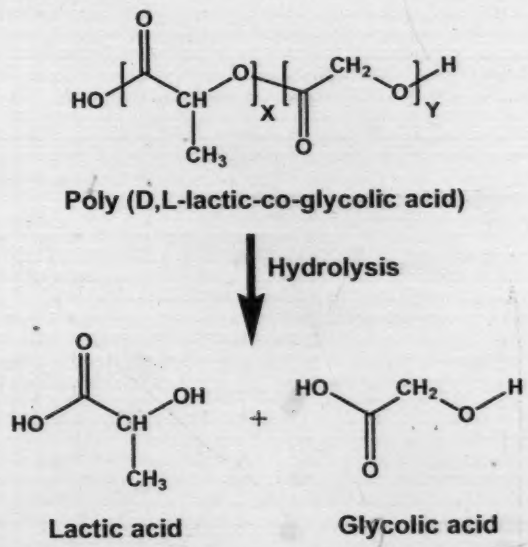

Figure 1-12. Chemical structure and biodegradation products of PLGA- PLGA are aliphatic polyesters composed of varying proportions lactic and glycolic acid. X and Y represent number of units of lactic and glycolic acid, respectively. Degradation of the polymer occurs through non-enzymatic hydrolysis of the backbone ester linkages giving rise to lactic and glycolic acids.

Several studies have employed PLGA co-polymer to fabricate micro/nanoparticles. These nanoparticles can entrap a wide range of biologically active compounds varying in physicochemical properties (e.g hormones, antibiotics, anti-cancer drugs). Many of these products are either marketed or in clinical trials (reviewed in [109]). A list of FDA-approved drug delivery products using PLGA polymers and under development is shown in Table 1-3 (adopted from [109]).

Table 1-3. FDA-approved drug delivery products using PLGA polymers and under development (adopted from [109])

Product	Active ingredient	Indication	Status
Nutropin Depot®	growth hormone	Growth hormone deficiencies	Marketed
Sandostatin LAR®	Octreotide acetate	Acromegaly	Marketed
TrelstarTM Depot	Triptorelin pamoate	Prostate cancer	Marketed
Decapepyl®	Triptorelin pamoate	Prostate cancer	Marketed
Pamorelin	Leuprolide acetate	Prostate cancer	Marketed
Oncogel®	Paclitaxel	Solid tumors	Clinical trial; Phase II
Atridox®	Doxycycline hyclate	Chronic adult periodntitis	Marketed
Sanvar® SR	Vapreotide	Esophageal bleeding varices	Clinical trial; Phase III
Lupron depot	Leupride acetate	Prostate cancer, endometriosis	Marketed
Zoladex	Goserelin acetate	Prostate cancer, endometriosis	Marketed

PLGA nano/micro particles are also well suited for vaccine delivery. Numerous antigens (proteins, peptides, lipopeptides, oligonucleotides, viruses or plasmid DNA) and immunomodulatory molecules have been successfully formulated in PLGA [105,106,111-118]. Hydrophobic compounds (such as lipopeptides, lipid A-based adjuvants or glycolipids) are usually incorporated in a single emulsion (oil/water) solvent evaporation method, whereas hydrophilic compounds (such as proteins, peptides or nucleic acids) are incorporated in a double emulsion (water/oil/water) solvent evaporation method [110]. Detailed explanation of these two methods will be given in the following chapters.

1.6.2 Manipulating the physico-chemical properties of PLGA

A major advantage of PLGA co-polymer is the ability to manipulate its physico-chemical properties in order to tailor its rate of degradation and the subsequent release profile of the encapsulated molecules. Tailoring the release of antigen from the polymeric nanoparticles can avoid the need for booster vaccination and allow the use of less frequent vaccine injections [105].

The rate of PLGA degradation depends mainly on the molecular weight and hydrophilicity of the polymer [119-121]. The smaller molecular weight and the more hydrophilic PLGA polymers, tend to increase the rate of polymer degradation. The hydophilicity of the polymer is mainly influenced by the the monomers' ratio used in its production. Glycolic acid is more hydrophilic than lactic acid. Employing higher proportions of glycolic acid results in increased hydrophilicity and hence increased

degradation rate of the nanoparticle formulation. One exception to this rule is the co-polymer with 50:50 glycolic:lactic acid ratio which has the fastest degradation rate (half-life ($T_{1/2}$) about 2 weeks) among PLGA polymers of different monomer ratios even those with higher glycolic acid content (Figure 1-13, adopted from [120]). This is due to the amorphous nature of PLGA 50:50. The rate of polymer degradtion can also be manipulated by changing the ratio of crystalline:amorphous regiosn, which in turn depends on polymer stereochemistry. Because L-lactic acid is crystalline, nanoparticle formulations employing L-lactic acid have slower rate of degradtion. However, the D, L lactic acid is preferred as it forms an amorphous polymer where in the antigen is homogeneously dispersed within the polymeric matrix [122]. At 50:50 glycolic:lactic acid ratio, PLGA polymer has the least crystalinity in its structure and is therefore more prone to hydrolysis and degradation than other PLGA polymers with lower or higher monomer ratios.

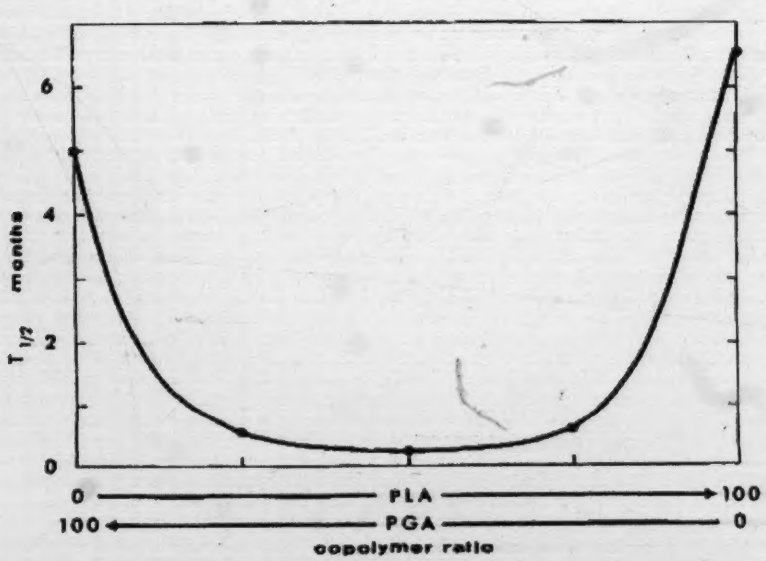

Figure 1-13. $T_{1/2}$ of various ratios of PLA and PGA (adopted from [120])

PLGA is a bulk eroding polymer, where the diffusion of water is faster than the rate of degradation of polymer bonds. In this case, degradation takes place throughout the whole polymer matrix and continues until a critical molecular weight is reached, at which the degradation products become small enough to be solubilized. At this stage, the structure start to become extensively porous and hydrated, and it is possible for encapsulated antigens to be released from the polymer matrix. Therefore, there is a lag phase before the antigen can be released, corresponding to the time needed for the critical molecular weight for release to be reached [123,124].

1.6.3 Uptake of PLGA-NPs by DCs

Uptake mechanism

Several research groups have demonstrated that PLGA nano and microparticles are taken up by human and mouse DCs [125-129]. In our research group, uptake of PLGA-NPs by *in vitro* generated DCs had been investigated using 3 different models, human peripheral blood-monocytes-derived DCs [127], human cord-blood $CD34^+$ stem cells-derived DCs [125] and mouse bone marrow-derived DCs [128]. The results convincingly have shown that more than 90% of DCs were able to internalize PLGA-NPs within a 24h incubation period (for all three systems). The uptake of PLGA-NPs was abolished by cytochalasin B, a reagent that inhibits actin polymerization [128], pointing to the involvement of actin polymerization in the phagocytosis of PLGA-NPs by DCs. This conclusion was further supported by electron microscopy studies, where membrane ruffling around the phagocytosed particle was visualized [125]. Intracellular localization of PLGA-NPs had been further confirmed by confocoal microscopy [128].

Without specific recognition, PLGA-NPs are naturally targeted to DCs through phagocytosis, as their size is comparable to that of pathogens. DCs express cell surface receptors e.g mannose receptor, DEC-205 and DC-SIGN, which facilitate binding and endocytosis of ligands that have a terminal sugar such as mannose, fucose and N-acetyl glucosamine. To increase targeting, such ligands can be used to decorate the surface of PLGA-NPs (e.g. mannose grafted-NPs). PLGA-NPs can also be conjugated with DC-specific antibodies (e.g anti-CD11c and anti-DEC205). Interaction between PLGA-NPs-attached ligand and/or antibody with DC receptors improves the specificity of NPs for DCs and results in enhanced uptake of NPs by DCs through receptor-mediated endocytosis [130,131].

Influence of route of administration

The site of administration was shown to significantly affect the type of cells internalizing the particles in mice. Intra-dermal (i.d) [132] or subcutaneous (s.c.) [133] administration of PLGA-NPs results in their uptake by DCs. Nanoparticles-loaded DCs were located in the draining lymph nodes of the vaccinated mice. This finding provides direct evidence of migration of these DCs from the skin to the draining lymph nodes after they take up PLGA-NPs [132,133]. In contrast, following intra peritoneal administration, macrophages were found to be the predominant cells internalizing PLGA-NPs in the peritoneal cavity [110].

Influence of particle size and charge

DCs and macrophages are highly phagocytic, capable of taking up any particles with similar dimensions to the pathogens (up to 10 μm). It is thus reasonable to expect that both large "micro-" and small "nano-" particles can efficiently be taken up by both types of cells. However, for targeting vaccine antigens to DCs, nanoparticles are more preferred than microparticles due to several reasons. Earlier study had shown that DCs preferentially take up smaller particles in the viral size range, whereas macrophages ingest more of the bigger, bacterial size particles (Figure 1-14, adopted from [134]). In fact, an inverse relationship had been reported between particle size and the efficiency of uptake by DCs [135].

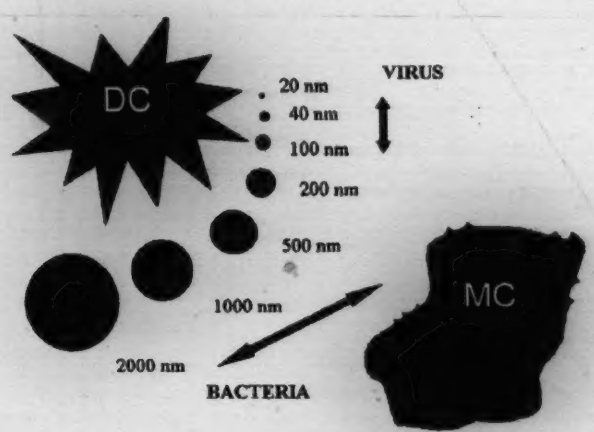

Figure 1-14. Schematic representation of particle uptake by macrophages and DCs (adopted from [134])- DCs preferentially ingest smaller particles in the viral size range, while macrophages take up more of the larger, bacterial size particles.

It is also worth mentioning that PLGA-NPs (<500 nm) were more effective than microparticles (> 2um) in stimulating CTL responses *in vivo* [136]. The large surface area of the nanoparticles allows faster degradation and rapid release of the encapsulated antigens inside the phagosome. Furthermore, this larger surface area allows for increased protein load by adsorption [105,106]. The uptake of PLGA nano/microparticles is also affected by surface charge. Cationic particles are particularly effective for uptake by DCs and macrophages. The ionic attraction between the positively charged particles and the negatively charged cell surface initiates efficient binding and facilitate particle internalization [137].

1.6.4 Intracellular trafficking of PLGA-NPs

Following PLGA-NP uptake by DCs, endocytosed particles can be located in three distinct types of endosomes. Accordingly, PLGA-encapsulated antigens can be processed by three different pathways (summarized in Figure 1-15). As shown in the right panel of Figure 1-15, PLGA-NPs can be hydrolyzed in the endo-lysosomes. Encapsulated proteins are processed by lysosomal protease, resulted peptides will bind MHC II molecules and presented on the cell surface, where they can be identified by $CD4^+$ T cells (right panel of Figure 1-15). Meanwhile, some of the phagocytosed particles can escape the endosome and act as depot that slowly hydrolyze and release its encapsulated proteins in the cytoplasm (left panel of Figure 1-15). Released proteins are degraded by the proteosomes into smaller peptides. Peptides are then transported by TAP into the endoplasmic reticulum, where they bind MHC class I and migrate to the cell surface to be identified by $CD8^+$ T cells (phagosome-to-cytosol cross-presentation pathway) [52].

The exact mechanism by which PLGA-NPs can escape the endosome is not clear. However, two possible mechanisms are proposed. PLGA-NPs are negatively charged in neutral pH. Upon acidification of endosomes, hydronium ions form hydrogen bonds with the carboxyl groups of lactic or glycolic acids, leading to the reversal of the charge on PLGA surface (from negative to positive). Positively charged PLGA-NPs can locally interact with the negatively charged endosomal membrane and extrude through it into the cytoplasm [138]. Alternatively, the influx of hydronium and chloride ions during endosomal acidification can cause increase in the osmotic pressure followed by rupture of the endosomal membrane and release of its content (PLGA-NPs) in the cytoplasm (proton-sponge mechanism) [139].

Endosomal escape of PLGA-NPs and the subsequent cytosolic delivery of the encapsulated antigens are not absolute requirements for cross-presentation of the encapsulated antigen. An elegant study by Shen *et al* [61] had demonstrated that PLGA-encapsulated antigens can be cross-presented by both phagosome-to-cytosol pathway (left panel of Figure 1-15) and vacuolar pathway (middle panel of Figure 1-15). It seems that some particles can localize in endocytic compartments where the vacuolar pathway is present (containing cathepsin S), while other particles may localize in different endosomes (containing lower level or less active cathepsin S) where transfer to the cytosol and degradation by proteosome occurs. In contrast to PLGA-encapsulated antigens, other particulate antigens (e.g. OVA covalently linked to iron particles) were exclusively presented by the proteosome/TAP-dependant phagosome-to-cytosol pathway [61]. Both *in vitro* and *in vivo* studies have shown that PLGA-encapsulated OVA can be

efficiently cross-presented to OVA specific T cells by either $TAP^{-/-}$ or cathepsin $S^{-/-}$ DCs. The observed T cell activation in either $TAP^{-/-}$ or cathepsin $S^{-/-}$ mice was slightly less compared to wild-type mice, indicating that both pathways are operating simultaneously and both are equally important for the cross-presentation process [61]. These results are of great interest for designing PLGA-based cancer vaccines. First, having two distinct pathways involved in generating peptide fragments could help in increasing the total number and the diversity of peptides that are effectively presented on MHC class I molecules and thereby broaden the resulting immune responses [61]. Furthermore, TAP loss and/or down regulation are well known mechanisms by which most of the tumors escape from immune recognition [140-142]. TAP deficiency will limit the efficacy of vaccine formulations that are exclusively dependant on TAP. PLGA-encapsulated antigens circumvent this problem as they could be efficiently cross-presented in the absence of TAP (by the vacuolar pathway).

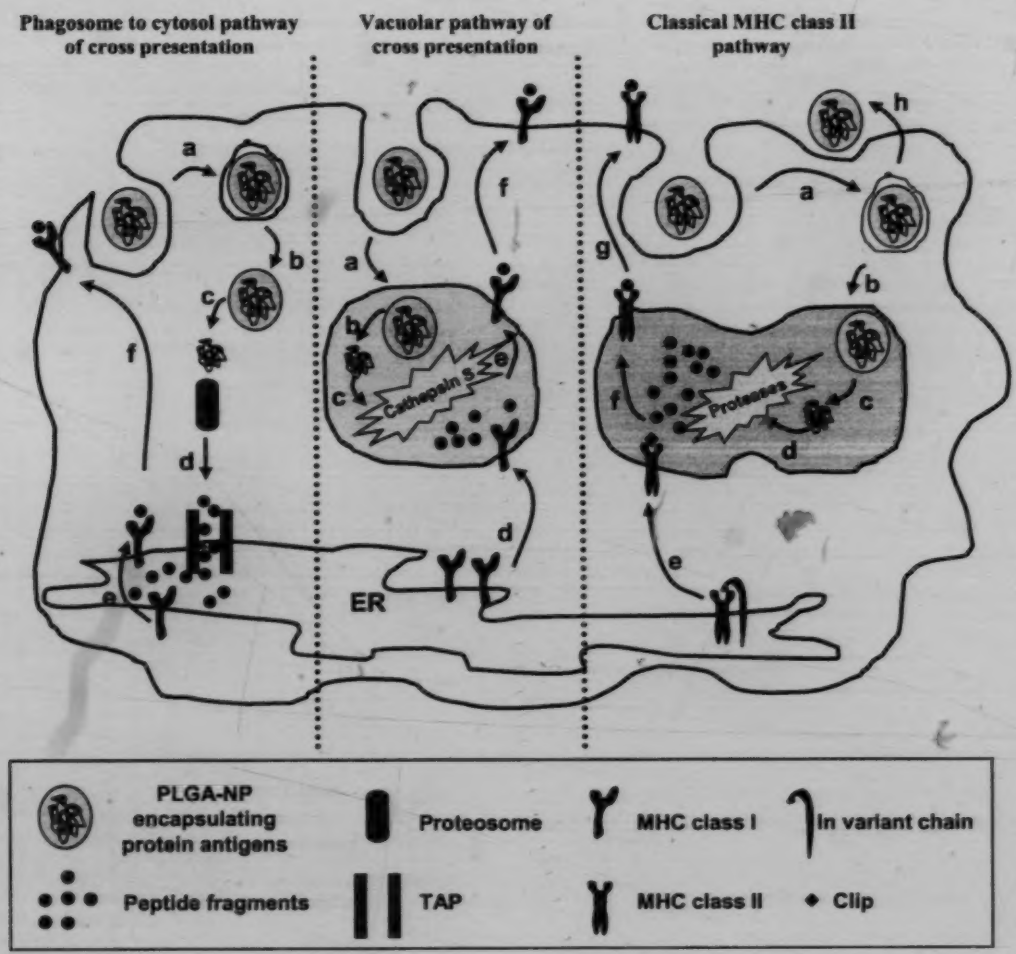

Figure 1-15. A schematic illustration of intracellular trafficking of PLGA-NPs- Following PLGA-NPs upake by DCs, endocytosed particles can be located in three distinct types of endosomes. Accordingly, PLGA-encapsulated antigens can be processed by three different pathways. **First pathway** is illustrated in the left panel of the figure (phagosome to cytosol pathway of cross-presentation); where phagocytosed particles (a) can escape from the endosome (b) and slowly hydrolyze in the cytoplasm, releasing the encapsulated proteins (c). Released proteins are degraded by the proteosomes into smaller peptides. Peptides are then transported by TAP into the endoplasmic reticulum (d), where they bind MHC class I (e) and migrate to the cell surface (f). **Second pathway** is the vacuolar pathway of cross-presentation (middle panel), in which particles are localized in endocytic compartments containing high level of active cathepsin S (a). Inside this endosome, PLGA-NPs hydrolyze and release the encapsulated proteins (b), which then degraded by the cathepsin S into smaller peptide fragments (c). MHC class I molecules

can also be found in the endosome, probably due to phagosome-ER fusion (d). The peptide fragments bind to the MHC class I molecules (e) and transported into the cell surface (f). **Third pathway** is the classical route of MHC class II antigen presentation (right panel), where phagocytosed particles (a) move into the interior of the cells in the endocytic pathway (b). In the acidified endosomes, PLGA-NPs hydrolyze and release the encapsulated proteins (c) which are degraded by the activated acid proteases (d) into smaller peptide fragments. In the ER, the newly synthesized MHC class II molecules bind to a protein known as the MHC class II-associated invariant (Ii) chain, which direct the transportation of MHC class II molecules from the ER into the endocytic pathway (e). Within the endocytic vesicles, the acid proteases cleave the in variant chain, leaving a short peptide fragment called CLIP (class II associated in variant chain peptide) still bound to the peptide binding groove of MHC class II molecule. CLIP is then exchanged with the antigenic peptide (f). The resulting peptide/MHC class II complexes are then transported to the cell surface (g). A fraction of endocytosed particles undergo exocytosis (h), where they can degrade and release their content outside the cells.

1.7 Thesis proposal

1.7.1 Rationale

Despite advancement of several cancer vaccines from bench to bed side, the extent of success immunotherapy of cancer has been limited in clinical trials. The two major obstacles against development of successful cancer vaccine formulations are: 1. Tolerance to cancer self-antigens; 2. The presence of immunosuppressive tumor microenvironment that inhibits anti-tumor T cell responses [143,144]. An elegant review by Rosenberg *et al* have analysed the overall response among 1306 cancer patients treated with different cancer vaccination strategies (e.g tumor cells, DC-based vaccines, peptides, virus, HSP). Unfortunately, the overall objective response rate to current cancer vaccine formulations was only 3.3% [26]. Altogether, these results emphasize the need for developing novel immunotherapy strategies that can break tolerance to self cancer antigens, induce effective anti-tumor T cell immune responses, while reversing the immunosuppressive network at the tumor microenvironment, at the same time.

L-BLP25 is a cancer vaccine formulation that was originally developed in our lab in 1998 [145] and is currently in a clinical phase III trial for non-small cell lung cancer (NSCLC). L-BLP25 consists of synthetic human MUC I 25-mer peptide and the immunoadjuvant MPLA both enclosed in a liposomal vehicle. Results from clinical phase IIB trial suggested a potential survival advantages for L-BLP25 treated group [146]. Despite these promising results, L-BLP25 formulation harbors several drawbacks that may limit its applicability in large clinical settings. Some of these drawbacks are related to liposomal formulation; such as tedious and expensive process of preparation, scale-up problems and

difficulty in producing sterile products. In fact, an extensive amount of research have been undertaken on liposomes, but only a limited number of liposomal formulations have been approved in humans. As a logical step, our long-term goal is to develop a novel PLGA-based cancer vaccine formulation that in addition to just actively targeting antigens/adjuvants to DCs could circumvent all the problems associated with the L-BLP25 liposomal formulation. In contrast to liposomes, the process of PLGA-NPs formulation and scaling-up are much easier and cost-effective [122]. In addition, the use of PLGA co-polymer provide additional advantage over liposomes, in terms of the ability to manipulate various physico-chemical properties of the carrier and tailor its rate of degradation and release pattern (as discussed in section 1.6.2).

Other drawbacks of L-BLP25 are related to the presence of natural lipid A (MPLA). MPLA is produced from bacterial culture and consists of a mixture of heterogeneous molecules. This heterogeneity is the main cause of large batch-to-batch variations in terms of composition and activity. As a result, its use in clinic may results in inconsistency of vaccine efficacy among cancer patients who have been vaccinated with L-BLP25. To circumvent this problem, our industrial co-partner; Oncothyreon Inc. (formerly Biomira), Edmonton, AB have chemically synthesized lipid A moiety with minor modification into it, allowing for the development of several synthetic lipid A analogues. These synthetic analogues are highly pure, stable and well-defined single structures that have comparable immunostimulatory effects to MPLA, and harbor additional advantages in terms of reproducibility, feasible large scale production, better control over purity of the final products, and minimal variations from batch to batch

[147]. The current series of investigations explore the immunostimulatory properties of one of those synthetic lipid A analogues (called 7-acyl lipid A) and further assess its potential to serve as a powerful companion to antigens in PLGA-based cancer vaccine formulation.

1.7.2 Objective

The long-term objective of this research is to develop effective cancer vaccines based on PLGA-NPs. The current dissertation aimed to investigate the efficacy of PLGA-NPs as a vaccine delivery system for co-delivery of antigens along with 7-acyl lipid A (as adjuvant) in eliciting robust antigen specific T cell responses against cancer associated self antigens in both normal and tumor-bearing mice.

1.7.3 Research outline

In these series of investigations, we have designed and characterized pathogen-mimicking PLGA-NPs containing OVA, as a model antigen and an analog of bacterial products (7- acyl lipid A) as an adjuvant. These NPs were designed to target DCs both *in vitro* and *in vivo*. We have assessed both quantitative (increase in the percentage of antigen-specific T cells) and functional (increase in expression of activation markers and cytokine secretion) aspects of T cell responses following s.c. vaccination of PLGA-NPs. As a rigorous test for our vaccination strategy, we have extended our studies to work with a real tumor antigen. Interestingly, both human and murine tyrosinase-related protein 2 (TRP2) were recently identified as melanoma antigens recognized by $CD8^+$ T cells. One epitope of TRP2 ($TRP2_{180\text{-}188}$) is of special interest. $TRP2_{180\text{-}188}$ can bind both human

human leukocyte antigen (HLA)-A*0201 and murine MHC class I molecule H2-K^b making it an attractive model antigen that is very relevant to human use. In these studies, we have formulated and characterized PLGA-NP formulation co-encapsulating $TRP2_{180-188}$ peptide along with 7-acyl lipid A. The potential of this formulation to elicit antigen specific T cell response that can lead to therapeutic anti-tumor effect was investigated in murine B16 melanoma tumor model.

1.7.4 Hypotheses

1) PLGA-NPs encapsulating either OVA (model antigen) or TRP2 peptide (cancer antigen) along with TLR ligand (7-acyl lipid A) will be internalized by DCs both *in vitro* and *in vivo*.
2) Following the uptake, PLGA-NPs containing OVA will be biodegraded and the OVA will be processed to produce the well defined $CD4^+$ T cell epitope ($OVA_{323-339}$) and $CD8^+$ T cell epitope ($OVA_{257-264}$) or SIINFEKL which will be presented by the DC MHC class II- and MHC class I-restricted pathway, respectively, leading to the induction of strong OVA specific $CD4^+$ and $CD8^+$ T cell responses. Incorporation of TLR ligand in the same nanoprticle formulation will have pronounced effects on the magnitude and the quality of generated T cell responses.
3) Co-delivery of TRP2 melanoma antigen and TLR ligand in PLGA-NPs will break the self tolerance against the TRP2 epitope and generate therapeutic anti-tumor $CD8^+$ T cell responses in murine B16 melanoma model.

1.7.5 Specific aims

1) To develop an easy, sensitive and reliable assay for analysis of synthetic lipid A analogues in PLGA-NPs.
2) To co-encapsulate OVA and 7-acyl lipid A in PLGA-NPs and characterize the formulation.
3) To investigate *in vivo* $CD4^+$ T cell responses following delivery of OVA and 7-acyl lipid A in PLGA-NPs through assessing the kinetics of clonal expansion of antigen specific $CD4^+$ T cells, increase in activation/memory surface phenotype and cytokine production.
4) To assess *in vitro* $CD8^+$ T cell responses following delivery of OVA and 7-acyl lipid A in PLGA-NPs investigating the clonal expansion of antigen specific CD8 T cells, increase in activation/memory surface phenotype (such as CD11a, CD25 and CD44) and cytokine production (such as IFN-γ).
5) To co-encapsulate a real cancer antigen (TRP2 peptide) and 7-acyl lipid A in PLGA-NPs and characterize the formulation.
6) To evaluate the efficacy of TRP2/7-acyl lipid A-NPs as a therapeutic strategy in an *in vivo* B16 murine melanoma model.

1.8 References:

[1] M. Schuster, A. Nechansky, R. Kircheis, Cancer immunotherapy, Biotechnol J 1 (2006) 138-47.

[2] A. Casadevall, Passive antibody therapies: progress and continuing challenges, Clin Immunol 93 (1999) 5-15.

[3] P. Neeson, Y. Paterson, Effects of the tumor microenvironment on the efficacy of tumor immunotherapy, Immunol Invest 35 (2006) 359-94.

[4] J. Gong, D. Chen, M. Kashiwaba, D. Kufe, Induction of antitumor activity by immunization with fusions of dendritic and carcinoma cells, Nat Med 3 (1997) 558-61.

[5] D.W. Kowalczyk, P.J. Wysocki, A. Mackiewicz, Cancer immunotherapy using cells modified with cytokine genes, Acta Biochim Pol 50 (2003) 613-24.

[6] T. Tuting, W.J. Storkus, M.T. Lotze, Gene-based strategies for the immunotherapy of cancer, J Mol Med 75 (1997) 478-91.

[7] M.L. Albert, B. Sauter, N. Bhardwaj, Dendritic cells acquire antigen from apoptotic cells and induce class I-restricted CTLs, Nature 392 (1998) 86-9.

[8] F.O. Nestle, S. Alijagic, M. Gilliet, Y. Sun, S. Grabbe, R. Dummer, G. Burg, D. Schadendorf, Vaccination of melanoma patients with peptide- or tumor lysate-pulsed dendritic cells, Nat Med 4 (1998) 328-32.

[9] Y. Tamura, P. Peng, K. Liu, M. Daou, P.K. Srivastava, Immunotherapy of tumors with autologous tumor-derived heat shock protein preparations, Science 278 (1997) 117-20.

[10] R. Bernards, A. Destree, S. McKenzie, E. Gordon, R.A. Weinberg, D. Panicali, Effective tumor immunotherapy directed against an oncogene-encoded product using a vaccinia virus vector, Proc Natl Acad Sci U S A 84 (1987) 6854-8.

[11] R. Lathe, M.P. Kieny, P. Gerlinger, P. Clertant, I. Guizani, F. Cuzin, P. Chambon, Tumour prevention and rejection with recombinant vaccinia, Nature 326 (1987) 878-80.

[12] C.A. Mack, W.R. Song, H. Carpenter, T.J. Wickham, I. Kovesdi, B.G. Harvey, C.J. Magovern, O.W. Isom, T. Rosengart, E. Falck-Pedersen, N.R. Hackett, R.G. Crystal, A. Mastrangeli, Circumvention of anti-adenovirus neutralizing immunity by administration of an adenoviral vector of an alternate serotype, Hum Gene Ther 8 (1997) 99-109.

[13] A. Razzaque, E. Dye, R.K. Puri, Characterization of tumor vaccines during product development, Vaccine 19 (2000) 644-7.

[14] R.J. Amato, Heat-shock protein-peptide complex-96 for the treatment of cancer, Expert Opin Biol Ther 7 (2007) 1267-73.

[15] Y. Takakura, S. Takemoto, M. Nishikawa, Hsp-based tumor vaccines: state-of-the-art and future directions, Curr Opin Mol Ther 9 (2007) 385-91.

[16] D.T. O'Hagan, N.M. Valiante, Recent advances in the discovery and delivery of vaccine adjuvants, Nat Rev Drug Discov 2 (2003) 727-35.

[17] E.M. Sotomayor, I. Borrello, H.I. Levitsky, Tolerance and cancer: a critical issue in tumor immunology, Crit Rev Oncog 7 (1996) 433-56.

[18] G.A. Rabinovich, D. Gabrilovich, E.M. Sotomayor, Immunosuppressive strategies that are mediated by tumor cells, Annu Rev Immunol 25 (2007) 267-96.

[19] D.J. Hicklin, F.M. Marincola, S. Ferrone, HLA class I antigen downregulation in human cancers: T-cell immunotherapy revives an old story, Mol Med Today 5 (1999) 178-86.

[20] D.I. Gabrilovich, H.L. Chen, K.R. Girgis, H.T. Cunningham, G.M. Meny, S. Nadaf, D. Kavanaugh, D.P. Carbone, Production of vascular endothelial growth factor by human tumors inhibits the functional maturation of dendritic cells, Nat Med 2 (1996) 1096-103.

[21] M.R. Hussein, Transforming growth factor-beta and malignant melanoma: molecular mechanisms, J Cutan Pathol 32 (2005) 389-95.

[22] G. Gerlini, A. Tun-Kyi, C. Dudli, G. Burg, N. Pimpinelli, F.O. Nestle, Metastatic melanoma secreted IL-10 down-regulates CD1 molecules on dendritic cells in metastatic tumor lesions, Am J Pathol 165 (2004) 1853-63.

[23] J.A. Vrana, E.S. Cleaveland, A. Eastman, R.W. Craig, Inducer-and cell type-specific regulation of antiapoptotic MCL1 in myeloid leukemia and multiple myeloma cells exposed to differentiation-inducing or microtubule-disrupting agents, Apoptosis 11 (2006) 1275-88.

[24] S. Kusmartsev, D.I. Gabrilovich, Role of immature myeloid cells in mechanisms of immune evasion in cancer, Cancer Immunol Immunother 55 (2006) 237-45.

[25] S. Sakaguchi, Naturally arising CD4+ regulatory t cells for immunologic self-tolerance and negative control of immune responses, Annu Rev Immunol 22 (2004) 531-62.

[26] S.A. Rosenberg, J.C. Yang, N.P. Restifo, Cancer immunotherapy: moving beyond current vaccines, Nat Med 10 (2004) 909-15.

[27] E. Giarelli, Cancer vaccines: a new frontier in prevention and treatment, Oncology (Williston Park) 21 (2007) 11-7; discussion 18.

[28] M.H. Chang, Decreasing incidence of hepatocellular carcinoma among children following universal hepatitis B immunization; Liver Int 23 (2003) 309-14.

[29] F.A. Garcia, D. Saslow, Prophylactic human papillomavirus vaccination: a breakthrough in primary cervical cancer prevention, Obstet Gynecol Clin North Am 34 (2007) 761-81, ix.

[30] P.S. Writer, in Pharmaceutical Business Review, 2008.

[31] M. Singh, J. Kazzaz, M. Ugozzoli, J. Chesko, D.T. O'Hagan, Charged polylactide co-glycolide microparticles as antigen delivery systems, Expert Opin Biol Ther 4 (2004) 483-91.

[32] E.S. Trombetta, I. Mellman, Cell biology of antigen processing in vitro and in vivo, Annu Rev Immunol 23 (2005) 975-1028.

[33] T.J.K.B.A.O.R.A. Goldsby, Kuby Immunology, W.H Freeman, New York, 2006.

[34] I. Mellman, S.J. Turley, R.M. Steinman, Antigen processing for amateurs and professionals, Trends Cell Biol 8 (1998) 231-7.

[35] K. Shortman, Y.J. Liu, Mouse and human dendritic cell subtypes, Nat Rev Immunol 2 (2002) 151-61.

[36] D.M. Underhill, A. Ozinsky, Phagocytosis of microbes: complexity in action, Annu Rev Immunol 20 (2002) 825-52.

[37] A.D. Luster, The role of chemokines in linking innate and adaptive immunity, Curr Opin Immunol 14 (2002) 129-35.

[38] M.C. Dieu, B. Vanbervliet, A. Vicari, J.M. Bridon, E. Oldham, S. Ait-Yahia, F. Briere, A. Zlotnik, S. Lebecque, C. Caux, Selective recruitment of immature and mature dendritic cells by distinct chemokines expressed in different anatomic sites, J Exp Med 188 (1998) 373-86.

[39] V.W. Chan, S. Kothakota, M.C. Rohan, L. Panganiban-Lustan, J.P. Gardner, M.S. Wachowicz, J.A. Winter, L.T. Williams, Secondary lymphoid-tissue chemokine (SLC) is chemotactic for mature dendritic cells, Blood 93 (1999) 3610-6.

[40] S. Garg, A. Oran, J. Wajchman, S. Sasaki, C.H. Maris, J.A. Kapp, J. Jacob, Genetic tagging shows increased frequency and longevity of antigen-presenting, skin-derived dendritic cells in vivo, Nat Immunol 4 (2003) 907-12.

[41] P. Bousso, E. Robey, Dynamics of CD8+ T cell priming by dendritic cells in intact lymph nodes, Nat Immunol 4 (2003) 579-85.

[42] C. Winzler, P. Rovere, M. Rescigno, F. Granucci, G. Penna, L. Adorini, V.S. Zimmermann, J. Davoust, P. Ricciardi-Castagnoli, Maturation stages of mouse dendritic cells in growth factor-dependent long-term cultures, J Exp Med 185 (1997) 317-28.

[43] P. Kalinski, C.M. Hilkens, E.A. Wierenga, M.L. Kapsenberg, T-cell priming by type-1 and type-2 polarized dendritic cells: the concept of a third signal, Immunol Today 20 (1999) 561-7.

[44] M. Bouvier, Accessory proteins and the assembly of human class I MHC molecules: a molecular and structural perspective, Mol Immunol 39 (2003) 697-706.

[45] F. Sallusto, M. Cella, C. Danieli, A. Lanzavecchia, Dendritic cells use macropinocytosis and the mannose receptor to concentrate macromolecules in the major

histocompatibility complex class II compartment: downregulation by cytokines and bacterial products, J Exp Med 182 (1995) 389-400.

[46] E. Castellino, R.N. Germain, Extensive trafficking of MHC class II-invariant chain complexes in the endocytic pathway and appearance of peptide-loaded class II in multiple compartments, Immunity 2 (1995) 73-88.

[47] G.P. Shi, R.A. Bryant, R. Riese, S. Verhelst, C. Driessen, Z. Li, D. Bromme, H.L. Ploegh, H.A. Chapman, Role for cathepsin F in invariant chain processing and major histocompatibility complex class II peptide loading by macrophages, J Exp Med 191 (2000) 1177-86.

[48] P. Guermonprez, J. Valladeau, L. Zitvogel, C. Thery, S. Amigorena, Antigen presentation and T cell stimulation by dendritic cells, Annu Rev Immunol 20 (2002) 621-67.

[49] P. Morris, J. Shaman, M. Attaya, M. Amaya, S. Goodman, C. Bergman, J.J. Monaco, E. Mellins, An essential role for HLA-DM in antigen presentation by class II major histocompatibility molecules, Nature 368 (1994) 551-4.

[50] C. Kurts, Cross-presentation: inducing CD8 T cell immunity and tolerance, J Mol Med 78 (2000) 326-32.

[51] W.R. Heath, F.R. Carbone, Cross-presentation, dendritic cells, tolerance and immunity, Annu Rev Immunol 19 (2001) 47-64.

[52] K.L. Rock, L. Shen, Cross-presentation: underlying mechanisms and role in immune surveillance, Immunol Rev 207 (2005) 166-83.

[53] A.L. Ackerman, C. Kyritsis, R. Tampe, P. Cresswell, Early phagosomes in dendritic cells form a cellular compartment sufficient for cross presentation of exogenous antigens, Proc Natl Acad Sci U S A 100 (2003) 12889-94.

[54] P. Guermonprez, L. Saveanu, M. Kleijmeer, J. Davoust, P. Van Endert, S. Amigorena, ER-phagosome fusion defines an MHC class I cross-presentation compartment in dendritic cells, Nature 425 (2003) 397-402.

[55] M. Houde, S. Bertholet, E. Gagnon, S. Brunet, G. Goyette, A. Laplante, M.F. Princiotta, P. Thibault, D. Sacks, M. Desjardins, Phagosomes are competent organelles for antigen cross-presentation, Nature 425 (2003) 402-6.

[56] R.R. Kopito, ER quality control: the cytoplasmic connection, Cell 88 (1997) 427-30.

[57] C.R. Roy, Immunology: professional secrets, Nature 425 (2003) 351-2.

[58] R. Song, C.V. Harding, Roles of proteasomes, transporter for antigen presentation (TAP), and beta 2-microglobulin in the processing of bacterial or particulate antigens via an alternate class I MHC processing pathway, J Immunol 156 (1996) 4182-90.

[59] E. Gagnon, S. Duclos, C. Rondeau, E. Chevet, P.H. Cameron, O. Steele-Mortimer, J. Paiement, J.J. Bergeron, M. Desjardins, Endoplasmic reticulum-mediated phagocytosis is a mechanism of entry into macrophages, Cell 110 (2002) 119-31.

[60] K.L. Rock, A new foreign policy: MHC class I molecules monitor the outside world, Immunol Today 17 (1996) 131-7.

[61] L. Shen, L.J. Sigal, M. Boes, K.L. Rock, Important role of cathepsin S in generating peptides for TAP-independent MHC class I crosspresentation in vivo, Immunity 21 (2004) 155-65.

[62] A.L. DeFranco, R.M. Locksley, M. Robertson, Immunity, The immune response in infectious and inflammatory disease, New Science Press Ltd, 2007.

[63] A. Pinzon-Charry, C.S. Ho, T. Maxwell, M.A. McGuckin, C. Schmidt, C. Furnival, C.M. Pyke, J.A. Lopez, Numerical and functional defects of blood dendritic cells in early- and late-stage breast cancer, Br J Cancer 97 (2007) 1251-9.

[64] C. Mesa, L.E. Fernandez, Challenges facing adjuvants for cancer immunotherapy, Immunol Cell Biol 82 (2004) 644-50.

[65] E. Celis, Toll-like receptor ligands energize peptide vaccines through multiple paths, Cancer Res 67 (2007) 7945-7.

[66] M. Schroder, A.G. Bowie, TLR3 in antiviral immunity: key player or bystander? Trends Immunol 26 (2005) 462-8.

[67] C. Pasare, R. Medzhitov, Toll pathway-dependent blockade of CD4+CD25+ T cell-mediated suppression by dendritic cells, Science 299 (2003) 1033-6.

[68] Z. Fehervari, S. Sakaguchi, Control of Foxp3+ CD25+CD4+ regulatory cell activation and function by dendritic cells, Int Immunol 16 (2004) 1769-80.

[69] T. Kubo, R.D. Hatton, J. Oliver, X. Liu, C.O. Elson, C.T. Weaver, Regulatory T cell suppression and anergy are differentially regulated by proinflammatory cytokines produced by TLR-activated dendritic cells, J Immunol 173 (2004) 7249-58.

[70] J. Schletter, H. Heine, A.J. Ulmer, E.T. Rietschel, Molecular mechanisms of endotoxin activity, Arch Microbiol 164 (1995) 383-9.

[71] H. Takada, S. Kotani, Structural requirements of lipid A for endotoxicity and other biological activities, Crit Rev Microbiol 16 (1989) 477-523.

[72] K. Miyake, Innate immune sensing of pathogens and danger signals by cell surface Toll-like receptors, Semin Immunol 19 (2007) 3-10.

[73] S. Akira, K. Takeda, Toll-like receptor signalling, Nat Rev Immunol 4 (2004) 499-511.

[74] K. Takeda, S. Akira, TLR signaling pathways, Semin Immunol 16 (2004) 3-9.

[75] S.M. Dauphinee, A. Karsan, Lipopolysaccharide signaling in endothelial cells, Lab Invest 86 (2006) 9-22.

[76] A.G. Stover, J. Da Silva Correia, J.T. Evans, C.W. Cluff, M.W. Elliott, E.W. Jeffery, D.A. Johnson, M.J. Lacy, J.R. Baldridge, P. Probst, R.J. Ulevitch, D.H. Persing, R.M. Hershberg, Structure-activity relationship of synthetic toll-like receptor 4 agonists, J Biol Chem 279 (2004) 4440-9.

[77] K. Brandenburg, A. Wiese, Endotoxins: relationships between structure, function, and activity, Curr Top Med Chem 4 (2004) 1127-46.

[78] E.T. Rietschel, T. Kirikae, F.U. Schade, U. Mamat, G. Schmidt, H. Loppnow, A.J. Ulmer, U. Zahringer, U. Seydel, F. Di Padova, et al., Bacterial endotoxin: molecular relationships of structure to activity and function, Faseb J 8 (1994) 217-25.

[79] N. Qureshi, K. Takayama, E. Ribi, Purification and structural determination of nontoxic lipid A obtained from the lipopolysaccharide of Salmonella typhimurium, J Biol Chem 257 (1982) 11808-15.

[80] D.H. Persing, R.N. Coler, M.J. Lacy, D.A. Johnson, J.R. Baldridge, R.M. Hershberg, S.G. Reed, Taking toll: lipid A mimetics as adjuvants and immunomodulators, Trends Microbiol 10 (2002) S32-7.

[81] K.R. Myers, A.T. Truchot, J. Ward, Y. Hudson, J.T. Ulrich, in Cellular and Molecular Aspects of Endotoxin Reactions, Elsevier Science, Amsterdam, 1990.

[82] H. Bjorkbacka, K.A. Fitzgerald, F. Huet, X. Li, J.A. Gregory, M.A. Lee, C.M. Ordija, N.E. Dowley, D.T. Golenbock, M.W. Freeman, The induction of macrophage gene expression by LPS predominantly utilizes Myd88-independent signaling cascades, Physiol Genomics 19 (2004) 319-30.

[83] B.E. Henricson, W.R. Benjamin, S.N. Vogel, Differential cytokine induction by doses of lipopolysaccharide and monophosphoryl lipid A that result in equivalent early endotoxin tolerance, Infect Immun 58 (1990) 2429-37.

[84] C.A. Salkowski, G.R. Detore, S.N. Vogel, Lipopolysaccharide and monophosphoryl lipid A differentially regulate interleukin-12, gamma interferon, and interleukin-10 mRNA production in murine macrophages, Infect Immun 65 (1997) 3239-47.

[85] V. Mata-Haro, C. Cekic, M. Martin, P.M. Chilton, C.R. Casella, T.C. Mitchell, The vaccine adjuvant monophosphoryl lipid A as a TRIF-biased agonist of TLR4, Science 316 (2007) 1628-32.

[86] K.A. Fitzgerald, D.T. Golenbock, Immunology. The shape of things to come, Science 316 (2007) 1574-6.

[87] J.T. Evans, C.W. Cluff, D.A. Johnson, M.J. Lacy, D.H. Persing, J.R. Baldridge, Enhancement of antigen-specific immunity via the TLR4 ligands MPL adjuvant and Ribi.529, Expert Rev Vaccines 2 (2003) 219-29.

[88] J.T. Ulrich, K.R. Myers, Monophosphoryl lipid A as an adjuvant. Past experiences and new directions, Pharm Biotechnol 6 (1995) 495-524.

[89] J.R. Baldridge, P. McGowan, J.T. Evans, C. Cluff, S. Mossman, D. Johnson, D. Persing, Taking a Toll on human disease: Toll-like receptor 4 agonists as vaccine adjuvants and monotherapeutic agents, Expert Opin Biol Ther 4 (2004) 1129-38.

[90] N. Romani, S. Gruner, D. Brang, E. Kampgen, A. Lenz, B. Trockenbacher, G. Konwalinka, P.O. Fritsch, R.M. Steinman, G. Schuler, Proliferating dendritic cell progenitors in human blood, J Exp Med 180 (1994) 83-93.

[91] A. Mackensen, B. Herbst, J.L. Chen, G. Kohler, C. Noppen, W. Herr, G.C. Spagnoli, V. Cerundolo, A. Lindemann, Phase I study in melanoma patients of a vaccine with peptide-pulsed dendritic cells generated in vitro from CD34(+) hematopoietic progenitor cells, Int J Cancer 86 (2000) 385-92.

[92] J. Banchereau, A.K. Palucka, M. Dhodapkar, S. Burkeholder, N. Taquet, A. Rolland, S. Taquet, S. Coquery, K.M. Wittkowski, N. Bhardwaj, L. Pineiro, R. Steinman, J. Fay, Immune and clinical responses in patients with metastatic melanoma to CD34(+) progenitor-derived dendritic cell vaccine, Cancer Res 61 (2001) 6451-8.

[93] L. Fong, Y. Hou, A. Rivas, C. Benike, A. Yuen, G.A. Fisher, M.M. Davis, E.G. Engleman, Altered peptide ligand vaccination with Flt3 ligand expanded dendritic cells for tumor immunotherapy, Proc Natl Acad Sci U S A 98 (2001) 8809-14.

[94] J. Nash, A. Pini, Making the connections in nerve regeneration, Nat Med 2 (1996) 25-6.

[95] M.A. Morse, Y. Deng, D. Coleman, S. Hull, E. Kitrell-Fisher, S. Nair, J. Schlom, M.E. Ryback, H.K. Lyerly, A Phase I study of active immunotherapy with carcinoembryonic antigen peptide (CAP-1)-pulsed, autologous human cultured dendritic

cells in patients with metastatic malignancies expressing carcinoembryonic antigen, Clin Cancer Res 5 (1999) 1331-8.

[96] Y. Osman, M. Takahashi, Z. Zheng, T. Koike, K. Toba, A. Liu, T. Furukawa, S. Aoki, Y. Aizawa, Generation of bcr-abl specific cytotoxic T-lymphocytes by using dendritic cells pulsed with bcr-abl (b3a2) peptide: its applicability for donor leukocyte transfusions in marrow grafted CML patients, Leukemia 13 (1999) 166-74.

[97] J. Pinilla-Ibarz, K. Cathcart, T. Korontsvit, S. Soignet, M. Bocchia, J. Caggiano, L. Lai, J. Jimenez, J. Kolitz, D.A. Scheinberg, Vaccination of patients with chronic myelogenous leukemia with bcr-abl oncogene breakpoint fusion peptides generates specific immune responses, Blood 95 (2000) 1781-7.

[98] R.C. Fields, K. Shimizu, J.J. Mule, Murine dendritic cells pulsed with whole tumor lysates mediate potent antitumor immune responses in vitro and in vivo, Proc Natl Acad Sci U S A 95 (1998) 9482-7.

[99] S.G. Smith, P.M. Patel, J. Porte, P.J. Selby, A.M. Jackson, Human dendritic cells genetically engineered to express a melanoma polyepitope DNA vaccine induce multiple cytotoxic T-cell responses, Clin Cancer Res 7 (2001) 4253-61.

[100] A. Kugler, G. Stuhler, P. Walden, G. Zoller, A. Zobywalski, P. Brossart, U. Trefzer, S. Ullrich, C.A. Muller, V. Becker, A.J. Gross, B. Hemmerlein, L. Kanz, G.A. Muller, R.H. Ringert, Regression of human metastatic renal cell carcinoma after vaccination with tumor cell-dendritic cell hybrids, Nat Med 6 (2000) 332-6.

[101] T. Ogihara, H. Iinuma, K. Okinaga, Usefulness of immunomodulators for maturation of dendritic cells, Int J Oncol 25 (2004) 453-9.

[102] M. Onaitis, M.F. Kalady, S. Pruitt, D.S. Tyler, Dendritic cell gene therapy, Surg Oncol Clin N Am 11 (2002) 645-60.

[103] P.J. Tacken, I.J. de Vries, R. Torensma, C.G. Figdor, Dendritic-cell immunotherapy: from ex vivo loading to in vivo targeting, Nat Rev Immunol 7 (2007) 790-802.

[104] I.J. De Vries, D.J. Krooshoop, N.M. Scharenborg, W.J. Lesterhuis, J.H. Diepstra, G.N. Van Muijen, S.P. Strijk, T.J. Ruers, O.C. Boerman, W.J. Oyen, G.J. Adema, C.J. Punt, C.G. Figdor, Effective migration of antigen-pulsed dendritic cells to lymph nodes in melanoma patients is determined by their maturation state, Cancer Res 63 (2003) 12-7.

[105] D.T. O'Hagan, M. Singh, Microparticles as vaccine adjuvants and delivery systems, Expert Rev Vaccines 2 (2003) 269-83.

[106] D.T. O'Hagan, M. Singh, J.B. Ulmer, Microparticles for the delivery of DNA vaccines, Immunol Rev 199 (2004) 191-200.

[107] A. Saupe, W. McBurney, T. Rades, S. Hook, Immunostimulatory colloidal delivery systems for cancer vaccines, Expert Opin Drug Deliv 3 (2006) 345-54.

[108] R.A. Jain, The manufacturing techniques of various drug loaded biodegradable poly(lactide-co-glycolide) (PLGA) devices, Biomaterials 21 (2000) 2475-90.

[109] I. Bala, S. Hariharan, M.N. Kumar, PLGA nanoparticles in drug delivery: the state of the art, Crit Rev Ther Drug Carrier Syst 21 (2004) 387-422.

[110] J. Samuel, G.S. kwon, Polymeric Nanoparticle Delivery of Cancer Vaccines, Informa Healthcare, USA, 2005.

[111] S.K. Hunter, M.E. Andracki, A.M. Krieg, Biodegradable microspheres containing group B Streptococcus vaccine: immune response in mice, Am J Obstet Gynecol 185 (2001) 1174-9.

[112] M.J. Alonso, R.K. Gupta, C. Min, G.R. Siber, R. Langer, Biodegradable microspheres as controlled-release tetanus toxoid delivery systems, Vaccine 12 (1994) 299-306.

[113] K.D. Newman, J. Samuel, G. Kwon, Ovalbumin peptide encapsulated in poly(d,l lactic-co-glycolic acid) microspheres is capable of inducing a T helper type 1 immune response, J Control Release 54 (1998) 49-59.

[114] K.D. Newman, D.L. Sosnowski, G.S. Kwon, J. Samuel, Delivery of MUC1 mucin peptide by Poly(d,l-lactic-co-glycolic acid) microspheres induces type 1 T helper immune responses, J Pharm Sci 87 (1998) 1421-7.

[115] M. Diwan, M. Tafaghodi, J. Samuel, Enhancement of immune responses by co-delivery of a CpG oligodeoxynucleotide and tetanus toxoid in biodegradable nanospheres, J Control Release 85 (2002) 247-62.

[116] D. Wang, D.R. Robinson, G.S. Kwon, J. Samuel, Encapsulation of plasmid DNA in biodegradable poly(D, L-lactic-co-glycolic acid) microspheres as a novel approach for immunogene delivery, J Control Release 57 (1999) 9-18.

[117] S.D. Putney, P.A. Burke, Improving protein therapeutics with sustained-release formulations, Nat Biotechnol 16 (1998) 153-7.

[118] T. Uchida, S. Goto, Oral delivery of poly(lactide-co-glycolide) microspheres containing ovalbumin as vaccine formulation: particle size study, Biol Pharm Bull 17 (1994) 1272-6.

[119] J.H. Eldridge, J.K. Staas, J.A. Meulbroek, J.R. McGhee, T.R. Tice, R.M. Gilley, Biodegradable microspheres as a vaccine delivery system, Mol Immunol 28 (1991) 287-94.

[120] R.A. Miller, J.M. Brady, D.E. Cutright, Degradation rates of oral resorbable implants (polylactates and polyglycolates): rate modification with changes in PLA/PGA copolymer ratios, J Biomed Mater Res 11 (1977) 711-9.

[121] D.E. Cutright, B. Perez, J.D. Beasley, 3rd, W.J. Larson, W.R. Posey, Degradation rates of polymers and copolymers of polylactic and polyglycolic acids, Oral Surg Oral Med Oral Pathol 37 (1974) 142-52.

[122] S. Cohen, M.J. Alonso, R. Langer, Novel approaches to controlled-release antigen delivery, Int J Technol Assess Health Care 10 (1994) 121-30.

[123] F.G. Hutchinson, B.J. Furr, Biodegradable polymers for the sustained release of peptides, Biochem Soc Trans 13 (1985) 520-3.

[124] W.R. Gombotz, D.K. Pettit, Biodegradable polymers for protein and peptide drug delivery, Bioconjug Chem 6 (1995) 332-51.

[125] M. Diwan, P. Elamanchili, H. Lane, A. Gainer, J. Samuel, Biodegradable nanoparticle mediated antigen delivery to human cord blood derived dendritic cells for induction of primary T cell responses, J Drug Target 11 (2003) 495-507.

[126] E. Walter, D. Dreher, M. Kok, L. Thiele, S.G. Kiama, P. Gehr, H.P. Merkle, Hydrophilic poly(DL-lactide-co-glycolide) microspheres for the delivery of DNA to human-derived macrophages and dendritic cells, J Control Release 76 (2001) 149-68.

[127] M.E. Lutsiak, D.R. Robinson, C. Coester, G.S. Kwon, J. Samuel, Analysis of poly(D,L-lactic-co-glycolic acid) nanosphere uptake by human dendritic cells and macrophages in vitro, Pharm Res 19 (2002) 1480-7.

[128] P. Elamanchili, M. Diwan, M. Cao, J. Samuel, Characterization of poly(D,L-lactic-co-glycolic acid) based nanoparticulate system for enhanced delivery of antigens to dendritic cells, Vaccine 22 (2004) 2406-12.

[129] Y. Waeckerle-Men, M. Groettrup, PLGA microspheres for improved antigen delivery to dendritic cells as cellular vaccines, Adv Drug Deliv Rev 57 (2005) 475-82.

[130] C. Foged, A. Sundblad, L. Hovgaard, Targeting vaccines to dendritic cells, Pharm Res 19 (2002) 229-38.

[131] S.T. Reddy, M.A. Swartz, J.A. Hubbell, Targeting dendritic cells with biomaterials: developing the next generation of vaccines, Trends Immunol 27 (2006) 573-9.

[132] K.D. Newman, P. Elamanchili, G.S. Kwon, J. Samuel, Uptake of poly(D,L-lactic-co-glycolic acid) microspheres by antigen-presenting cells in vivo, J Biomed Mater Res 60 (2002) 480-6.

[133] H.O. Alpar, Strategies for vaccine delivery, J Drug Target 11 (2003) 459-61.

[134] A. Gamvrellis, D. Leong, J.C. Hanley, S.D. Xiang, P. Mottram, M. Plebanski, Vaccines that facilitate antigen entry into dendritic cells, Immunol Cell Biol 82 (2004) 506-16.

[135] J.C. Reece, N.J. Vardaxis, J.A. Marshall, S.M. Crowe, P.U. Cameron, Uptake of HIV and latex particles by fresh and cultured dendritic cells and monocytes, Immunol Cell Biol 79 (2001) 255-63.

[136] D.F. Nixon, C. Hioe, P.D. Chen, Z. Bian, P. Kuebler, M.L. Li, H. Qiu, X.M. Li, M. Singh, J. Richardson, P. McGee, T. Zamb, W. Koff, C.Y. Wang, D. O'Hagan, Synthetic peptides entrapped in microparticles can elicit cytotoxic T cell activity, Vaccine 14 (1996) 1523-30.

[137] L. Josephson, C.H. Tung, A. Moore, R. Weissleder, High-efficiency intracellular magnetic labeling with novel superparamagnetic-Tat peptide conjugates, Bioconjug Chem 10 (1999) 186-91.

[138] J. Panyam, W.Z. Zhou, S. Prabha, S.K. Sahoo, V. Labhasetwar, Rapid endo-lysosomal escape of poly(DL-lactide-co-glycolide) nanoparticles: implications for drug and gene delivery, Faseb J 16 (2002) 1217-26.

[139] D.W. Pack, A.S. Hoffman, S. Pun, P.S. Stayton, Design and development of polymers for gene delivery, Nat Rev Drug Discov 4 (2005) 581-93.

[140] T.L. Whiteside, J. Stanson, M.R. Shurin, S. Ferrone, Antigen-processing machinery in human dendritic cells: up-regulation by maturation and down-regulation by tumor cells, J Immunol 173 (2004) 1526-34.

[141] H. Pandha, A. Rigg, J. John, N. Lemoine, Loss of expression of antigen-presenting molecules in human pancreatic cancer and pancreatic cancer cell lines, Clin Exp Immunol 148 (2007) 127-35.

[142] B. Lankat-Buttgereit, R. Tampe, The transporter associated with antigen processing: function and implications in human diseases, Physiol Rev 82 (2002) 187-204.

[143] W. Zou, Immunosuppressive networks in the tumour environment and their therapeutic relevance, Nat Rev Cancer 5 (2005) 263-74.

[144] H.L. Kaufman, M.L. Disis, Immune system versus tumor: shifting the balance in favor of DCs and effective immunity, J Clin Invest 113 (2004) 664-7.

[145] J. Samuel, W.A. Budzynski, M.A. Reddish, L. Ding, G.L. Zimmermann, M.J. Krantz, R.R. Koganty, B.M. Longenecker, Immunogenicity and antitumor activity of a liposomal MUC1 peptide-based vaccine, Int J Cancer 75 (1998) 295-302.

[146] R. Sangha, C. Butts, L-BLP25: a peptide vaccine strategy in non small cell lung cancer, Clin Cancer Res 13 (2007) s4652-4.

[147] Z.H. Jiang, W.A. Budzynski, D. Qiu, D. Yalamati, R.R. Koganty, Monophosphoryl lipid A analogues with varying 3-O-substitution: synthesis and potent adjuvant activity, Carbohydr Res 342 (2007) 784-96.

Chapter Two

Development of liquid chromatography-mass spectrometry (LC-MS) method for quantification of synthetic lipid A analogues in PLGA-NPs

A version of this chapter has been published in

Journal of Pharmaceutical and Biomedical Analysis

Hamdy S, Haddadi A, Somayaji V, Ruan D and Samuel J, Faculty of Pharmacy & Pharmaceutical Sciences, University of Alberta, Edmonton, AB, Canada, T6G2N8

and

presented as a poster in Candian Society for Pharmaceutical Sciences (CSPS) Montréal, Québec Canada, May 30-June 2, 2007

2.1 Introduction

Owing to the clinical success of MPLA, preparation of chemical analogues of lipid A has been the focus of large interest in vaccine development research. Such analogues can induce comparable immune responses to that of MPLA, but their synthesis is reproducible, feasible for large scale production, can be purified more easily and have minimal differences from batch to batch. In line with these investigations, Oncothyreon (previously known as Biomira) has introduced two novel synthetic lipid A analogues; 7-acyl lipid A and pentaerythritol- based (PET) lipid A. 7-acyl lipid A (Figure 2-1A) is a comprised of β-(1→6) diglucosamine moiety bearing three identical (R)-tetradecanoyl-oxytetradecanoyl residues on the 2, 2' and 3' positions and one (R)-3-hydroxytetradecanoyl group on 3 position. Structurally this analogue is closer to the natural lipid A (MPLA) but differs from it in having all acyl chains of uniform length and acylated at 3 position. Where as in PET lipid A (Figure 2-1B), a penta erythritol moiety mimics the first sugar and comprised of three identical (R)-tetradecanoyloxy-tetradecanoyl residues similar to that of 7-acyl lipid A.

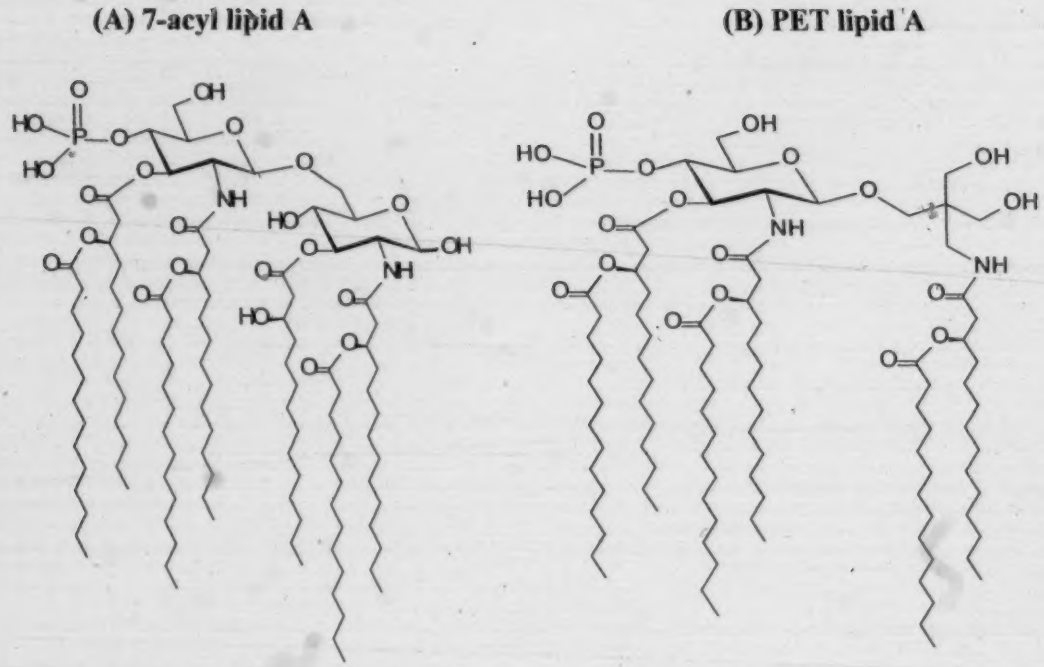

Figure 2-1. Chemical structure of 7-acyl lipid A and PET lipid A

We have previously shown that treatment of BMDCs with either LPS or 7-acyl lipid A could induce DC maturation/activation [1]. In the current report we are showing that PET lipid A is as effective as 7-acyl lipid A in its ability to activate DCs, as evidenced by secretion of pro-inflammatory cytokines and up-regulation of key maturation/activation DC surface markers.

Natural and synthetic lipid A analogues have been successfully encapsulated in a variety of particulate vaccine delivery systems, including emulsions, liposomes [2,3], and PLGA-NPs [4-7]. However, full characterization and optimization of lipid A-encapsulating vaccine formulations have been hampered by lack of sensitive and reliable methods for lipid A analysis. In fact, Lipid A is not a good chromophore. Therefore, spectrophotometric detection of lipid A by the conventional high performance liquid chromatography (HPLC)-based methods had been hindered by its poor ultraviolet (UV) absorption. In an attempt to improve the sensitivity of its spectrophotometric detection, derivatization reaction with dinitrobenzyloxyamine prior to analysis had been performed [4,8]. Such tedious derivatization process was accomplished in 3 hours (h) at 60°C [4,8]. In the present study, we present a sensitive, reliable and fast method for the analysis of lipid A-based adjuvants by liquid chromatography coupled with mass spectrometry (LC-MS). This method overcame all the potential problems associated with the poor UV-absorbance of lipid A derivatives, and pre-column derivatization. As a preliminary application, this method has been successfully applied to the determination of 7-acyl lipid A and PET lipid A content in PLGA-NPs.

2.2 Materials and Methods

2.2.1 Mice

C57Bl/6 mice were bred and maintained at the University of Alberta's Health Science's Laboratory Animal Facility. All experiments were performed in accordance to the University of Alberta guidelines for the care and use of laboratory animals. All experiments were performed using 6 to 12 week old male mice.

2.2.2 Materials

7-acyl lipid A, PET lipid A and aspartic (Asp) PET lipid A, (molecular weights (Mwt): 1956.5, 1685.70 and 1699.2 Dalton (Da), respectively) were kindly provided by Oncothyreon Inc. (formerly Biomira Inc., Edmonton, AB, Canada). Polyvinyl alcohol (PVA), Mwt 31,000-50,000 Da. PLGA co-polymer, monomer ratio 50:50, Mwt 7000 Da, was purchased from Absorbable Polymers International, (Pelham, AL, USA). Recombinant murine Granulocyte Monocyte Colony Stimulating Factor (GM-CSF) was purchased from Peprotech (Rocky Hill, NJ, USA). Murine IL-6 and TNF-α enzyme-linked immunosorbent assay (ELISA) kits were purchased from E-Bioscience (San Diego, CA, USA). Murine IL-12 ELISA kit was purchased from BD Biosciences (Mississauga, ON, Canada), respectively. RPMI-1640, L-glutamine, and gentamycin were purchased from Gibco-BRL (Burlington, ON, Canada). Fetal Calf Serum (FCS) was obtained from Hyclone Laboratories (Logan, UT, USA). Anti mouse CD16/CD32, CD40, and CD86 mAbs, and their respective isotype controls were purchased from BD Biosciences (Mississauga, ON, Canada. Chloroform, methanol, acetonitrile, water (all HPLC grades) were purchased from Fisher Scientific (Fair Lawn, NJ, USA).

2.2.3 Preparation of BMDCs

DC primary cultures were generated from murine bone marrow precursors from femurs of C57BL/6 mice in complete media in presence of GM-CSF as described earlier [9]. Briefly, femurs were removed and cleaned from the surrounding muscle and fatty tissues. For disinfection, intact bones were put in 70% ethanol for 2 minutes (min) and then washed with phosphate buffer saline (PBS). Afterwards, both ends of the femur were cut with sterile scissors and the marrow was flushed with PBS-containing insulin syringe. After one wash in PBS, about $1–2\times10^7$ leukocytes were obtained per femur. Cell culture medium was complete RPMI-1640 [RPMI-1640 supplemented with gentamycin (80 µg/mL), L-glutamine (2 mM), and 10% heat-inactivated FCS]. At day 0 bone marrow leukocytes were seeded at 2×10^6 per 100 mm dish in 10 mL complete medium containing 20 ng/mL GM-CSF. At day 3 another 10 mL complete medium containing 20 ng/mL GM-CSF were added to the plates. At days 6 half of the culture supernatant was collected, centrifuged, and the cell pellet re-suspended in 10 mL fresh medium containing 20 ng/mL GM-CSF, and given back into the original plate. At day 7 cells can be used already. The purity of the DC population on day 7 was found to be between 70-75% based on the expression of CD11c on the semi-adherent and non-adherent cell populations.

2.2.4 DCs activation/maturation studies

Cytokine secretion

On day 7 of the primary culture, the semi-adherent and non-adherent cell populations were harvested and re-suspended at 4×10^5 cells/mL in complete RPMI media containing 20 ng/mL of GM-CSF. Stock solutions of 7-acyl lipid A and PET lipid A were prepared at 1 mg/mL in tertiary butanol, then diluted with plain RPMI media to give the corresponding concentration (0.05, 0.1 0.5, 1, 5 and 10 μg/mL of culture media) when added to the cells. DCs treated with tertiary butanol (diluted similarly with plain RPMI media) were used as vehicle control. After an overnight incubation, culture supernatants were analyzed for IL-6, IL-12p70, and TNF-α secretion by ELISA kits in a 96 well microplate using a microplate reader (Powerwave with KC Junior software; Bio-Tek, Winooski, VT) at optical density (OD) of 450 nm with reference set at 570 nm according to the manufacturer's directions. All samples were analyzed in duplicates. The minimum detection levels of the cytokines were: IL-12p70, 5 pg/mL; IL-6, 10 pg/mL; TNF-α, 15 pg/mL.

Flow cytometry

DCs pulsed with 0.1 μg/mL of either 7-acyl lipid A or PET lipid A were harvested (after overnight incubation), and tested for up-regulation of maturation surface markers (CD40 and CD86). Briefly, 2.5×10^5 cells were suspended in FACS buffer (PBS with 5% FCS, and 0.09% sodium azide) and incubated with anti mouse CD16/CD32 mAb to block Fc receptors and then stained appropriate fluorescence conjugated antibodies. DCs pulsed

was 1 μg/mL LPS was used as a positive control. All samples were finally acquired on a Becton-Dickinson Facsort and analyzed by Cell-Quest software.

2.2.5 Establishment of LC-MS method for quantification of lipid A analogues

LC-MS method parameters

LC-MS analyses were performed using a Waters Micromass ZQ 4000 spectrometer, coupled to a Waters 2795 separations module with an autosampler (Milford, MA, USA). The mass spectrometer was operated in negative ionization mode with selected ion recording (SIR) acquisition. The nebulizer gas was obtained from an in house high purity nitrogen source. The temperature of source was set at 150 °C, and the voltages of the capillary and cone were 3.11 kilovolt (KV) and 60 volt (V), respectively. The gas flow of desolvation and the cone were set at 550 and 90 liter per hour (L/h), respectively. Chromatographic separation was achieved using an Agilent Technologies (Palo Alto, CA, USA) Zorbax eclipse XDB C8 3.5 μm column (2.1×50 mm) as the stationary phase. The mobile phase was consisting of 2 solutions; *Solution A* is 0.1% glacial acetic acid, 0.1% triethylamine in methanol and *Solution B* is 0.1% glacial acetic acid, 0.1% triethylamine, 10% methanol in tetrahydrofuran (THF). The mobile phases were delivered at a constant flow rate of 0.2 mL/min. The gradient conditions are shown in Table 2-1. Asp-PET lipid A (another synthetic lipid A derivative) (Figure 2-2) was used as an internal standard (IS). SIR at m/z 1955.5, 1684.7 and 1698.2, related to M-H were selected for quantification of 7-acyl lipid A, PET lipid A and the internal standard, respectively.

Table 2-1
Chromatographic gradient program over LC-MS analysis time; 15 min

Time (min)	Mobile phase A* %	Mobile phase B** %	Flow rate mL/min	Gradient curve
0	100	0	0.2	1
10	50	50	0.2	6
10.2	100	0	0.2	1

*Mobile phase A is methanol containing 0.1% glacial acetic acid and 0.1% triethylamine.

**Mobile phase B is 10% methanol in tetrahydrofuran containing 0.1% glacial acetic acid and 0.1% triethylamine.

Aspartic (Asp)-PET lipid A

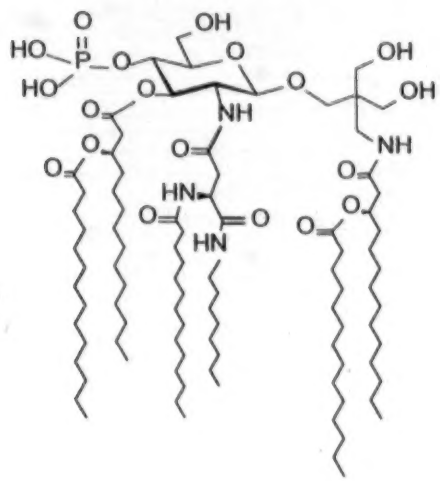

Figure 2-2. Chemical structure of the internal standard; Asp-PET lipid A

Standard and stock solutions

The stock solutions were prepared by dissolving 2 mg of 7-acyl lipid A or PET lipid A in 1 mL of chloroform: methanol mixture (4:1, volume (v):v). The stock solutions were stored at -20 °C between experiments. The working solutions of 7-acyl lipid A and PET lipid A were prepared fresh each day by making a 50-fold dilution of the stock solution in chloroform: methanol mixture (4:1, v: v), and (1:4, v: v), respectively. The calibration standards were then prepared by serial dilution of the working solution. The stock solution of the internal standard was prepared by dissolving 2 mg of Asp-PET lipid A in 1 mL chloroform: methanol mixture (4:1, v: v), followed by the preparation of a working solution of 20 μg/mL by a further 100-fold dilution of the stock solution. The stock solution of the internal standard was stored at -20 °C between experiments, and the working solution was prepared fresh at each experiment.

Accuracy and precision of the LC-MS method

Each sample was prepared in triplicates on three different days. The accuracy (the nearness of a measured value to the true value) was expressed as the mean percentage error, [mean measured concentration/ expected concentration x 100]. The precision (agreement between replicate measurements) was evaluated as inter and intra-day coefficient of variation (CV), which was calculated as: [%CV= (standard deviation (SD)/mean) x 100]. Least-squared regression method was used to determine the regression coefficient and the equation for the best fitting line.

2.2.6 Preparation and characterization of lipid A-containing PLGA-NPs

Preparation of NPs

PLGA-NPs containing 7-acyl lipid A or PET lipid A were prepared as oil/water (o/w) single emulsion formulation by the solvent evaporation method (Figure 2-3). Briefly, 100 µL of 1:4 methanol-chloroform mixture (v: v) (containing either 200 µg 7-acyl lipid A or 600 µg PET lipid A) was added to the polymer-chloroform solution (100 mg polymer in 300 µL chloroform). The resulting solution was then was emulsified in 2 ml of PVA solution (9% w/v PVA in PBS) by sonication for 45 seconds (sec) at level 4, using a microtip sonicator (Heat systems Inc., Farmingdale, NY, USA). The emulsion was added drop-wise into 8 ml of stirring PVA solution. NPs were collected after 3 h of stirring by centrifugation of the emulsion at 40000 x gravitation force (*g*) for 10 min at 4°C. The NPs were washed twice with cold deionized water and lyophilized.

Particle size analysis

NPs were suspended in filtered PBS and the mean hydrodynamic diameter and polydispersity determined by dynamic light scattering methodology using a particle size analyzer (Zetasizer 3000, Malvern, UK).

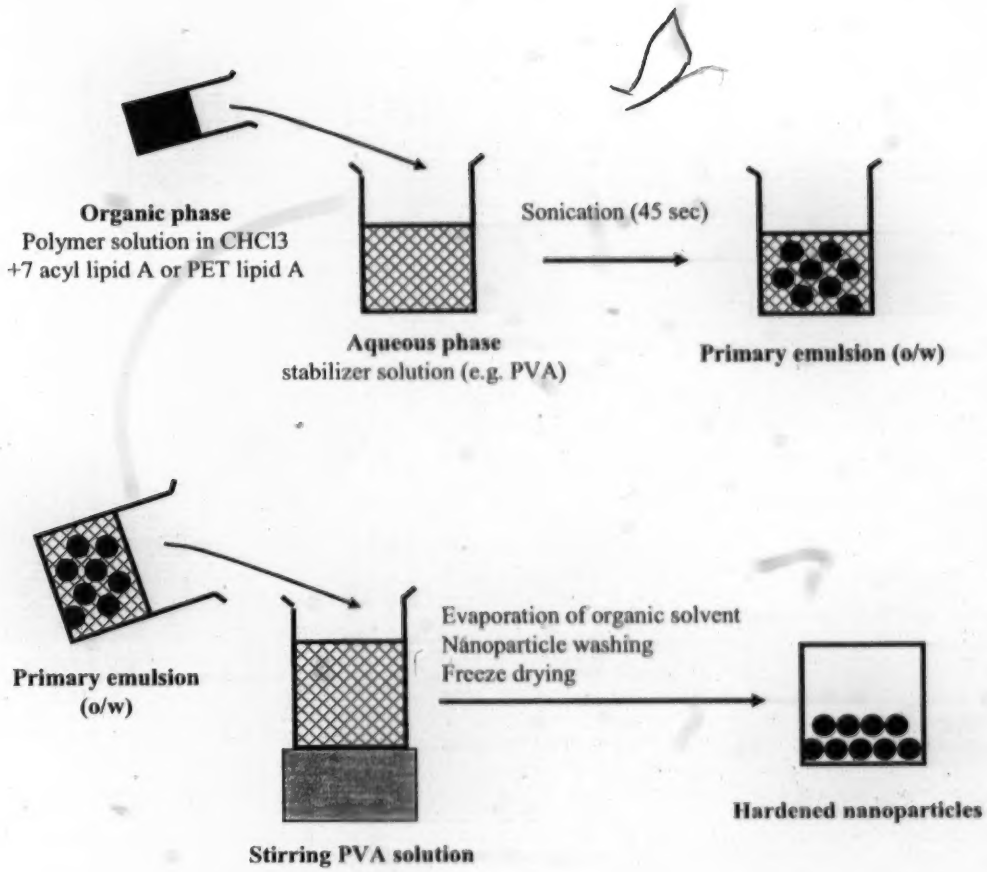

Figure 2-3. Single emulsification-solvent evaporation technique for preparation of PLGA-NPs containing either 7-acyl lipid A or PET lipid A- Briefly, 200 µg 7-acyl lipid A or 600 µg PET lipid A in 100 µL of 1:4 methanol-chloroform mixture (v:v) is mixed with the polymer-chloroform solution (100 mg polymer in 300 µL chloroform). The resulting solution was then was emulsified in 2 mL of PVA solution (9% w/v PVA in PBS) by sonication for 45 sec. The emulsion was added drop-wise into 8 mL of stirring PVA solution. NPs were then collected after 3 h of stirring by centrifugation of the emulsion at 40000 x *g* for 10 min at 4° C. The NPs were washed twice with cold deionized water and lyophilized.

Extraction and quantification of lipid A content

Unlike PLGA, 7-acyl lipid A is not soluble in acetonitrile. Therefore, extraction was done by first dispersing 10 mg of NPs in 400 µL of acetonitrile, followed by centrifugation at 15000 x *g* for 15 min. The supernatant was removed. The residue was then extracted by adding 500 µL of 1:4 methanol-chloroform mixture. The sample was centrifuged at 15000 x *g* for 15 minutes and the supernatant was assayed for 7-acyl lipid A by LC-MS. In contrast to 7-acyl lipid A, PET lipid A is soluble in acteonitrile, so the extraction of PET lipid A from PLGA-NPs was done by slightly different method. Briefly, 10 mg of NPs were dispersed in 100 µL of acetonitrile. After brief sonication (2-3 sec), both the polymer and PET lipid A were dissolved. PET lipid A was then extracted by adding 1400 µL ethanol followed by centrifugation at 15000× *g* for 15 minutes. After centrifugation, polymer was precipitated and the supernatant was analyzed by LC-MS. The supernatant containing extracted 7-acyl lipid A or PET lipid A, were then mixed in (1:1, v:v ratio) with working solution (20 µg/mL) of the internal standard. An aliquot of 10 µL of this mixture was then injected into the LC-MS system. Based on the measured concentration, the encapsulation efficiency was calculated as the amount of encapsulated 7-acyl lipid A or PET lipid A relative to the total amount of 7-acyl lipid A or PET lipid A used during NP preparation, respectively. The loading was calculated from the weight of the NPs and the amount of 7-acyl lipid A or PET lipid A incorporated.

2.2.7 Statistical Analysis

Student's t-test was used to compare data sets for statistical significance ($p<0.05$).

2.3 Results

2.3.1 Soluble lipid A analogues induce DCs activation/maturation

The process of DCs maturation is crucial for the stimulation of antigen specific T cell responses and may be essential for developing cancer vaccine formulations relying on T cell immunity [10]. In this study, we have investigated the effects of soluble form of two synthetic lipid A analogues (7-acyl lipid A and PET lipid A) on their ability to mature BMDCs both phenotypically (up-regulation of key markers, CD40 and CD86) and functionally (secretion of pro-inflammatory cytokines; IL-12p70, TNF-α and IL-6).

Stimulation of DCs with either 0.1 μg/mL of 7-acyl lipid A or PET lipid A enhanced the expression of CD40 and CD86 to a similar extent (Figure 2-4). Numbers at the right corner of histograms in Figure 2-4 represent percentages of positive cells/mean florescence intensity (MFI). Teriary butanol alone (vehicle control) didn't have any effect on either percentage of cells or MFI. The expression of CD40 was highly up-regulated following treatment with either 7-acyl lipid A or PET lipid A, as evidenced by more than 2 folds increase in the percentage of positive cells (relative to the unpulsed DCs), and also 3.2 and 3.9 folds increase in the MFI, respectively of CD40, respectively. Both adjuvants resulted also in up-regulation of CD86 expression, as more than 3 folds increase in the percentage of positive cells for CD86 have been observed relative to the unpulsed DCs.

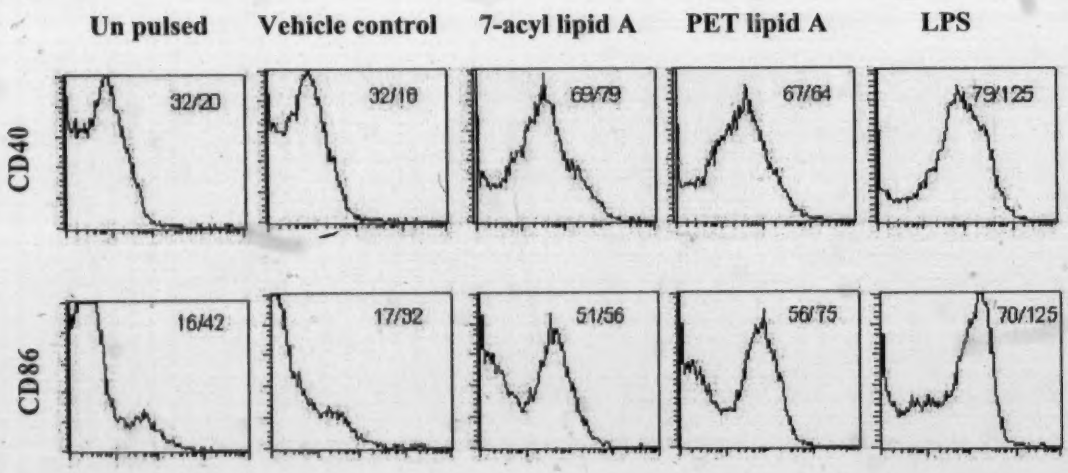

Figure 2-4. Effect of 7-acyl lipid A and PET lipid A on up-regulation of CD40 and CD86 on BMDCs- Day 7 BMDCs were incubated in complete media containing GM-CSF and left untreated (unpulsed) or treated with 0.1 μg/mL of 7-acyl lipid A, PET lipid A, or LPS. After overnight incubation, non-adherent cells were harvested and stained with the antibodies and analyzed by FACS. Stock solutions of 7-acyl lipid A and PET lipid A were prepared at 1 mg/mL in tertiary butanol, then, diluted with plain RPMI media to give the corresponding concentration. DCs treated with teriary butanol (diluted with RPMI media) were used as vehicle control. Numbers at the right corner of histograms represent percentages of positive cells/mean florescence intensity (MFI). One representative out of three individual experiments is shown.

Along with up-regulation of co-stimulatory molecules, fully mature DCs also secrete pro-inflammatory cytokines in response to a danger signal [11]. For this purpose, the production of IL-12p70, IL-6 and TNF-α upon exposure to 7-acyl lipid A or PET lipid A was assessed by quantitative ELISA kits. Immature DCs from day 7 of *in vitro* propagation were cultured overnight in the presence of titrating concentration of 7-acyl lipid A or PET lipid A (0.05 μg/mL-10 μg/mL of culture medium). Vehicle control was DCs treated with tertiary butanol (diluted similarly with culture medium). After overnight incubation supernatant was analyzed for cytokine secretion. Results are shown in Figure 2-5. As observed in the phenotype maturation studies, both 7-acyl lipid A and PET lipid A have very similar dose response effect on the secretion of pro-inflammatory cytokines. However, at the lowest concentration (0.05 μg/mL), PET lipid A produced significantly higher amount of IL-12p70, TNF-α, and IL-6 ($p<0.05$) than 7-acyl lipid A. As the concentration of adjuvants increased both 7-acyl lipid A and PET lipid A showed similar cytokine secretion profile. All three cytokine have reached their highest peak concentration when DCs were stimulated with 1 μg/mL of either 7-acyl lipid A or PET lipid A. When the concentration of adjuvants was further increased, secretions of the cytokines have started to decrease. However, more sudden and sharp decrease have been observed by 7-acyl lipid A at 5 μg/mL, especially in the secretion of IL-12p70 (Figure 2-5A) and TNF-α (Figure 2-5B), whereas PET lipid A was still resulting in significantly higher secretion of those cytokines ($p<0.05$). At 10 μg/mL, 7-acyl lipid A resulted in slight increase in TNF-α secretion. However, this increase was not significantly different from what was observed at 5 μg/ml ($p>0.05$). Minimum level of cytokine secretion has been observed at the highest concentration (10 μg/mL).

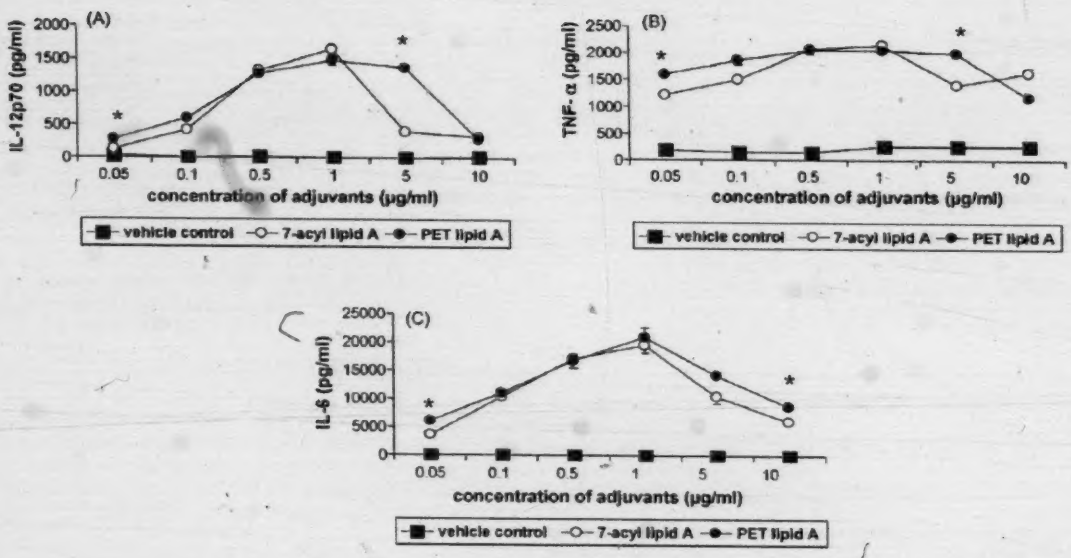

Figure 2-5. Effect of titrating doses of 7-acyl lipid A and PET lipid A on the secretion of pro-inflammatory cytokines by BMDCs- On day 7 of the primary culture, the semi-adherent and non-adherent cell populations were harvested and re-suspended at 4×10^5 cells/mL in complete media containing 20 ng/mL of GM-CSF. Stock solutions of 7-acyl lipid A and PET lipid A were prepared at 1 mg/mL in tertiary butanol, then diluted with plain RPMI media to give the corresponding concentration (0.05, 0.1 0.5, 1, 5 and 10 µg/mL of culture media) before adding to the cells (in duplicates). DCs treated with tertiary butanol were used as vehicle control. After an over night incubation, culture supernatants were analyzed for cytokine secretion, IL-12p70 (A), TNF-α (B) and IL-6 (C). One representative out of three individual experiments is shown. * denotes significance between 7-acyl lipid A and Pet lipid A treated DCs ($p < 0.05$).

Taken together these data (Figures 2-4 and 2-5) demonstrate that PET lipid A is as effective as 7-acyl lipid A at least in terms of BMDCs cells and secretion of pro-inflammatory cytokines that induce Th1-biased immune responses.

2.3.2 Validation of the newly developed LC-MS method

The mass spectra of 7-acyl lipid A, PET lipid A and Asp-PET lipid A (IS) dissolved in 50:50 (v: v) solution A: solution B is shown in Figure 2-6. The molecular ions at m/z of 1955.5, 1684.7 and 1698.2 corresponding to [M-H] were selected for quantification of 7-acyl lipid A, PET lipid A, and the IS, respectively.

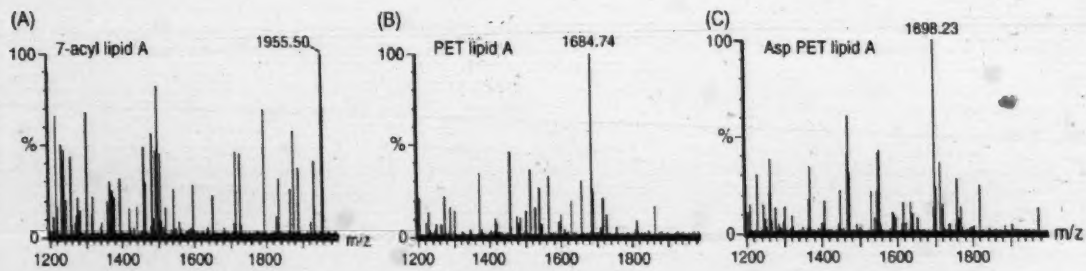

Figure 2-6. Mass spectra of 7-acyl lipid A (A), PET lipid A (B) and Asp-PET lipid A (C)- 7-acyl lipid A, PET lipid A and Asp-PET lipid A were dissolved in 50:50 (v: v) Solution A: Solution B. *Solution A* is methanol containing 0.1% glacial acetic acid and 0.1% triethylamine, *Solution B* is 10% methanol in tetrahydrofuran containing 0.1% glacial acetic acid and 0.1% triethylamine.

Figure 2-7 shows the SIR chromatograms of either 7-acyl lipid A and IS (Figure 2-7A) or PET lipid A and IS (Figure 2-7B). The peaks of both 7-acyl lipid A and PET lipid A were well separated from that of the IS in the established chromatographic condition. The retention times of 7-acyl lipid A, PET lipid A and IS were approximately 10.2, 9.2 and 8 min, respectively. The analytical run time was 15 min.

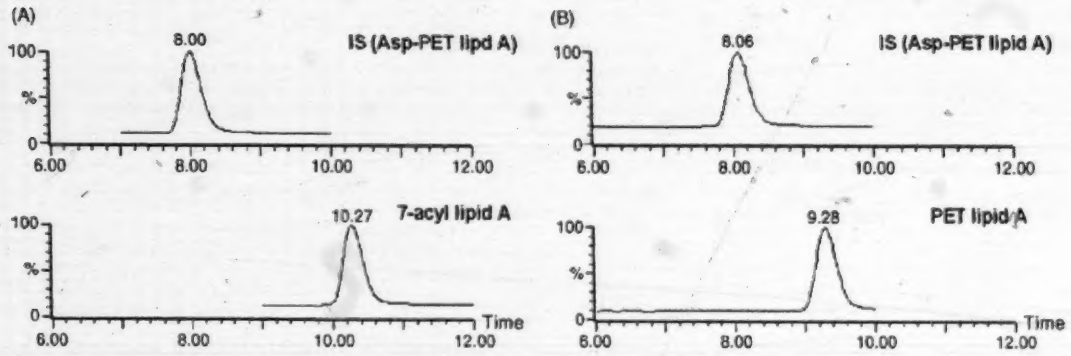

Figure 2-7. Single ion recorder (SIR) chromatograms of Asp PET lipid A (IS), with either 7-acyl lipid A (A) or PET lipid A (B)

Linearity range

The regression analysis was constructed by plotting the peak-area ratio of either 7-acyl lipid A or PET lipid A to IS (response factor) *versus* analyte concentration (μg/mL). The calibration curve was linear within the range of 1.25-20 μg/mL (Figure 2-8). The correlation coefficient (r^2) was always greater than 0.999, indicating a good linearity.

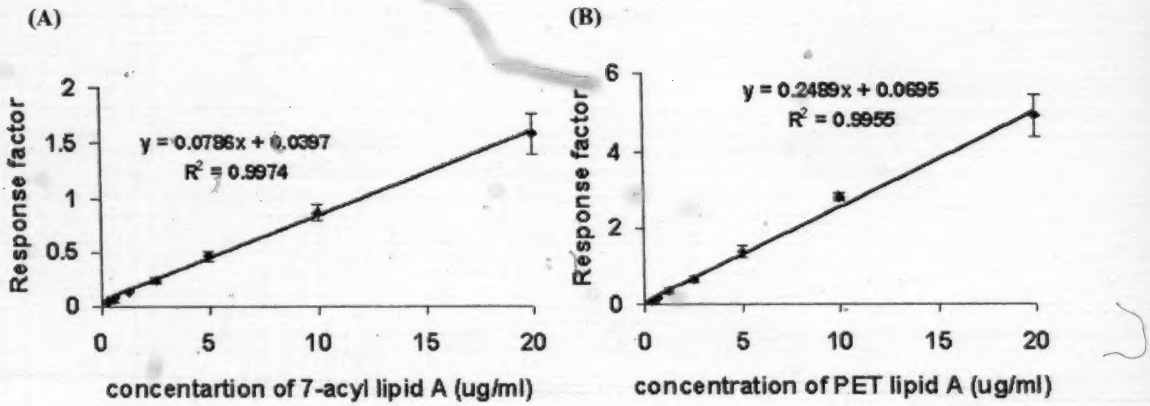

Figure 2-8. A representative standard curve for 7-acyl lipid A (A) and PET lipid A (B) extending from 0.3125-20 µg/mL- The calibration curves were constructed by plotting peak-area ratio of either 7-acyl lipid A or PET lipid A to the internal standard (response factor) on y-axis *versus* analyte concentration (µg/mL) on x-axis. Chromatographic gradient conditions are described in Table 2-1.

Sensitivity

The limit of detection (LOD) was assessed based on Signal-to-Noise (S/N) ratio. Determination of the S/N ratio was performed by comparing measured signals from samples with known low concentrations of 7-acyl lipid A or PET lipid A with those of blank samples and establishing the minimum concentration at which the signal can be reliably detected. A S/N ratio between 4:1 or 3:1 is generally acceptable for estimating the detection limit. The LOD for 7-acyl lipid A and PET lipid A was found to be 0.035, 0.015 µg/mL, respectively. Based on 10 µL injection volume, that corresponds to an amount of 0.35 ng and 0.15 ng, respectively. The limit of quantification (LOQ) or the minimum level at which 7-acyl lipid A or PET lipid A could be quantified with acceptable accuracy and precision have been found to be 1.25 µg/mL for both of them. Based on 10 µL injection volume, that corresponds to an amount of 12.5 ng.

Accuracy and precision

Intra- and inter-day precision were determined using different concentrations of 7-acyl lipid A or PET lipid A standards (1.25, 2.5, 5, 10 and 20 µg/mL). These concentrations were assayed in triplicates on three different days. The assay coefficient of variation at all of the intra-day and inter-day assessment was less than 13%. The accuracy of the assay at different concentrations tested ranged from 89-108% and from 92-107% for 7-acyl lipid A and PET lipid A, respectively, and the measured amounts were not significantly different than expected, based on Student's *t*-test (α=0.05). All validation results are reported in Table 2-2 and 2-3 for 7-acyl lipid A and PET lipid A, respectively.

Selectivity

Injection of reagent blanks showed no interfering peaks in the 7-acyl lipid A or PET lipid A region of the chromatograms. Furthermore, a structure analogue used as an internal standard (Asp-PET lipid A) was well separated from both test compounds.

Table 2-2
Assay validation data for 7-acyl lipid A

(A) Intra-day precision (coefficient of variation, CV) and accuracy (mean percent error) (n=3)

Expected concentration (µg/mL)	Measured concentration ±SD (µg/mL)	CV %	Accuracy %
1.25	1.1± 0.069	6.2	89
2.5	2.3± 0.200	8.6	92
5	5.0± 0.646	12.9	100
10	9.6± 0.880	9.1	96
20	18.8± 1.678	8.9	94

(B) Inter-day precision (coefficient of variation, CV) and accuracy (mean percent error) (n=3)

Expected concentration (µg/mL)	Measured concentration ±SD (µg/mL)	CV %	Accuracy %
1.25	1.1± 0.061	5.3	91
2.5	2.5± 0.223	8.7	102
5	5.4± 0.385	7.1	108
10	10.5± 0.828	7.8	105
20	19.4± 1.350	6.9	97

Table 2-3
Assay validation data for PET lipid A

(A) Intra-day precision (coefficient of variation, CV) and accuracy (mean percent error) (n=3)

Expected concentration (μg/mL)	Measured concentration ±SD (μg/mL)	CV %	Accuracy %
1.25	1.3± 0.123	9.4	105
2.5	2.7± 0.101	3.6	110
5	5.3± 0.491	9.2	106
10	10.2± 0.28	2.7	102
20	19.7± 1.15	5.8	98

B) Inter-day precision (coefficient of variation, CV) and accuracy (mean percent error) (n=3)

Expected concentration (μg/mL)	Measured concentration ±SD (μg/mL)	CV %	Accuracy %
1.25	1.15± 0.13	11.7	92
2.5	2.5± 0.29	11.3	102
5	5.3± 0.4	7.4	107
10	10.6± 0.55	5.2	106
20	19.0± 0.7	3.6	95

2.3.3 Particle size analysis of lipid A-containing PLGA-NPs

Lipid A-containing PLGA-NPs were less than 300 nm in size and poly dispersity was less than 0.2. The results of particle size analysis are summarized in Figure 2-9.

(A) 7-acyl lipid A PLGA-NPs

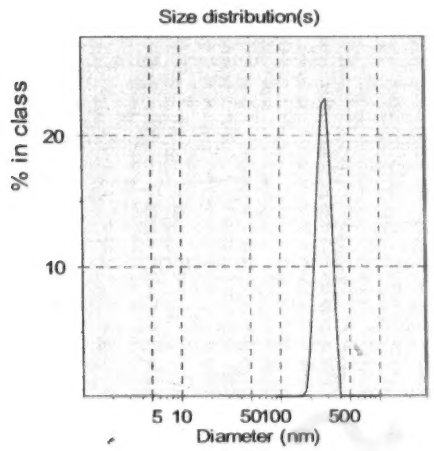

Size: 280± 11 nm

Polydispersity: 0.06± 0.01

(B) PET lipid A PLGA-NPs

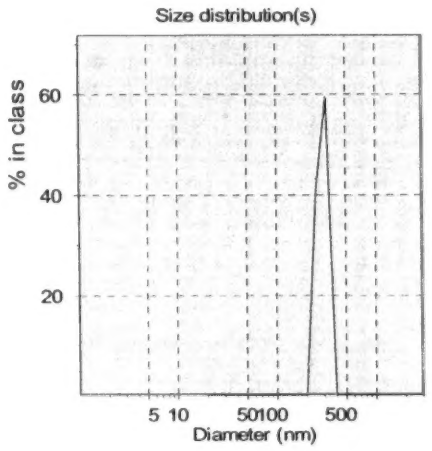

Size: 282± 16 nm

Polydispersity: 0.12± 0.02

Figure 2-9. The intensity size distribution of PLGA-NPs containing either 7-acyl lipid A (A) or PET lipid A (B)

2.3.4 Extraction and quantification of lipid A content in PLGA-NPs

We have used the LC-MS method to analyze 7-acyl lipid A and PET lipid A content in PLGA-NPs. The results of the analysis are summarized in Table 2-4. The efficiency of the extraction procedure was measured by a spiking study, where known amounts of 7-acyl lipid A or PET lipid A were added to empty PLGA-NPs. Following extraction, the supernatant was injected to the LC-MS system and the extraction recovery was calculated as the amount detected/ amount used in spiking x 100. The procedures of extraction of 7-acyl lipid A and PET lipid A was easy and was performed in less than one hour, the recoveries were ~100% and ~80%, respectively.

Table 2-4
Analysis of 7-acyl lipid A and PET lipid A content in PLGA-NPs

Adjuvant	Total amount used in preparation	Extraction Recovery	Loading*	Encapsulation** Efficiency
7-acyl lipid A	200 μg	~ 100 %	1.79 ± 0.18 μg	67.3 ± 6.9 %
PET lipid A	600 μg	~ 80%	1.76 ± 0.10 μg	22.0 ± 1.2 %

*The amount of 7-acyl lipid A or PET lipid A incorporated per 1 mg of the NPs.

** Based on 75 % polymer recovery, encapsulation efficiency was calculated as the amount of encapsulated 7-acyl lipid A or PET lipid A relative to the total amount of 7-acyl lipid A or PET lipid A used during nanoparticle preparation, (200 μg and 600 μg, respectively).

PET lipid A is smaller in size (6 fatty acid chains versus 7 in 7-acyl lipid A), thus it is less hydrophobic than 7-acyl lipid A. Accordingly, the encapsulation efficiency inside PLGA-NPs was less than that of 7-acyl lipid A (22.0% versus 67.3%, respectively). During the preparation of NPs, 600 μg of PET lipid A was used (versus 200 μg of 7-acyl lipid A), so that the loading of both 7-acyl lipid A and PET lipid A was almost the same; 1.79 μg and 1.76 μg per 1 mg dry weight of NPs, respectively (Table 2-4).

2.4 Discussion

All together, our results support the potential use of lipid A-based adjuvants in clinic and also introduce two promising members from lipid A family (7-acyl lipid A and PET lipid A), as candidates for further studies in future vaccine trials. The successful clinical development of MPLA or any lipid A analogue requires the establishment and validation of an appropriate analytical method for the conduction and evaluation of pharmaceutical and/or pharmacokinetic studies. MPLA is a heterogenous product composed of several lipid A species which differ in the degree and type of fatty acid acylation and also in fatty acid chain length [12]. Previous attempts to analyze MPLA with conventional reversed-phase HPLC (RP-HPLC) have utilized either UV-visible (Vis) detection at 210 nm, where MPLA is poorly absorbing, or radiodetction by metabolically-labeled preparations [13,14]. In addition to the low sensitivity of MPLA, UV-Vis detection of MPLA has been unfavorable because of the different species present in MPLA, which may have variable molar extinction coefficients. The process of radiolabeling is also unfavorable for safety concerns and is obviously inappropriate for vaccines used in clinic [8]. An additional complication in the use of RP-HPLC to analyze MPLA is that the phosphomonoester

group in MPLA interferes with elution from RP columns. In the present study, we present a quick, sensitive, accurate and reliable method for the analysis of lipid A analogues by LC-MS. This method can overcome all the potential problems associated with the poor UV-absorbance, use of radiolabeling, difficulty in elution from RP columns, and pre-column derivatization of lipid A compounds. In addition, our method can detect 4 samples/ h (analysis time is only 15 min), which is much faster than the conventional HPLC method in which the analysis time was 45 min per one run plus three hours for the pre-column derivatization reaction. This method is also much more sensitive than HPLC, as evidenced by LOD (0.35 ng and 0.15 ng for 7-acyl lipid A and PET lipid A, respectively as compared to 540 ng in previously reported HPLC method for MPLA analysis) [8]. One additional advantage to our method is that, it is easily applicable to various lipid A analogues (7-acyl lipid A, PET lipid A and Asp-PET lipid A) without changing any parameters. Lipid A analogues have been employed in various vaccine formulations either alone or combined with other adjuvants [15,16]. In fact, AS04 adjuvant system (a combination of MPLA and aluminium salt) have induced superior and long lasting immune responses compared to a vaccine formulated with aluminium salt only [16]. Therfore, if more than one lipid A analogue is going to be combined in the same vaccine formulation, the developed LC-MS method can easily differentiate them, enabling simultaneous quantification of both analogues in a considerably short time.

Encapsulation of lipid A-based adjuvants within PLGA-NPs dramatically enhances their immunostimulatory properties [17,18]. However, the difficulty in extracting and quantifying lipid A analogues in PLGA-NPs have restricted our capacity in finding ways

to optimize loading, release and stability of lipid A in PLGA-NPs. Pre-column derivatization process required at least 1 mg of MPLA [8]. In a preparation of PLGA-NPs containing 7-acyl lipid A, a total of 200 µg 7-acyl lipid A is added to 100 mg polymer. That means, in order to analyze the 7-acyl lipid A content from PLGA-NPs, we have to use at least 500 mg PLGA-NPs to be able to extract 1 mg of 7-acyl lipid A to start the derivatization process (assuming 100% encapsulation, 100% polymer recovery and 100% extraction recovery, which is not practically true). However, our method enabled us to extract and quantify both 7-acyl lipid A and PET lipid A from only 10 mg PLGA-NPs and in less than one hour, which is a significant practical advantage.

In earlier studies, the encapsulation efficiency of MPLA in PLGA-NPs has been estimated to be 100%, as it is a very hydrophobic and lipid soluble molecule [19]. In the present study we have formulated both 7-acyl lipid A and PET lipid A in PLGA-NPs. Although both compounds are lipid soluble and very similar in size and structure, but the encapsulation efficiency of PET lipid A was significantly lower than that of 7-acyl lipid A inside PLGA-NPs (Table 4) ($p< 0.05$). The amount of PET lipid A that was used in the preparation (600 µg) was three fold higher than the amount of 7-acyl lipid A (200 µg), however both formulations had the same loading (almost 1.7 µg of 7-acyl lipid A or PET lipid A per 1 mg dry weight NPs). The reason of the low encapsulation of PET lipid A could be because it is more hydrophilic molecule than 7-acyl lipid A. In fact, the more hydrophilic the compound, the lower affinity it has to the polymer. Such low affinity results in the movement of this molecule from the organic phase to the outer aqueous phase, where it is washed away and not efficiently encapsulated inside the NPs.

In conclusion, we have succeeded in developing high-speed, sensitive and reliable method for lipid A analysis. This method enabled us to determine loading and encapsulation efficiencies of two synthetic lipid A analogues in PLGA-NPs. Our results showed that minor modifications of the lipid A molecule can result in considerable change in its encapsulation efficiency at least in PLGA-based formulation. These results have pointed out into one common misconception that lipophilic compounds can be always encapsulated in PLGA-NPs with 100 % encapsulation efficiency. Finally, we believe that employing the developed LC-MS method will lay the foundation for further characterization and optimization of lipid A-based vaccine formulations.

2.5 References

[1] P. Elamanchili, C.M. Lutsiak, S. Hamdy, M. Diwan, J. Samuel, "Pathogen-mimicking" nanoparticles for vaccine delivery to dendritic cells, J Immunother 30 (2007) 378-95.

[2] R.L. Richards, M. Rao, N.M. Wassef, G.M. Glenn, S.W. Rothwell, C.R. Alving, Liposomes containing lipid A serve as an adjuvant for induction of antibody and cytotoxic T-cell responses against RTS,S malaria antigen, Infect Immun 66 (1998) 2859-65.

[3] J. Neidhart, K.O. Allen, D.L. Barlow, M. Carpenter, D.R. Shaw, P.L. Triozzi, R.M. Conry, Immunization of colorectal cancer patients with recombinant baculovirus-derived KSA (Ep-CAM) formulated with monophosphoryl lipid A in liposomal emulsion, with and without granulocyte-macrophage colony-stimulating factor, Vaccine 22 (2004) 773-80.

[4] C.S. Chong, M. Cao, W.W. Wong, K.P. Fischer, W.R. Addison, G.S. Kwon, D.L. Tyrrell, J. Samuel, Enhancement of T helper type 1 immune responses against hepatitis B virus core antigen by PLGA nanoparticle vaccine delivery, J Control Release 102 (2005) 85-99.

[5] M. Diwan, P. Elamanchili, H. Lane, A. Gainer, J. Samuel, Biodegradable nanoparticle mediated antigen delivery to human cord blood derived dendritic cells for induction of primary T cell responses, J Drug Target 11 (2003) 495-507.

[6] P. Elamanchili, M. Diwan, M. Cao, J. Samuel, Characterization of poly(D,L-lactic-co-glycolic acid) based nanoparticulate system for enhanced delivery of antigens to dendritic cells, Vaccine 22 (2004) 2406-12.

[7] M.E. Lutsiak, G.S. Kwon, J. Samuel, Biodegradable nanoparticle delivery of a Th2-biased peptide for induction of Th1 immune responses, J Pharm Pharmacol 58 (2006) 739-47.

[8] S.R. Hagen, J.D. Thompson, D.S. Snyder, K.R. Myers, Analysis of a monophosphoryl lipid A immunostimulant preparation from Salmonella minnesota R595 by high-performance liquid chromatography, J Chromatogr A 767 (1997) 53-61.

[9] M.B. Lutz, N. Kukutsch, A.L. Ogilvie, S. Rossner, F. Koch, N. Romani, G. Schuler, An advanced culture method for generating large quantities of highly pure dendritic cells from mouse bone marrow, J Immunol Methods 223 (1999) 77-92.

[10] J. Ismaili, J. Rennesson, E. Aksoy, J. Vekemans, B. Vincart, Z. Amraoui, F. Van Laethem, M. Goldman, P.M. Dubois, Monophosphoryl lipid A activates both human dendritic cells and T cells, J Immunol 168 (2002) 926-32.

[11] T. De Smedt, B. Pajak, E. Muraille, L. Lespagnard, E. Heinen, P. De Baetselier, J. Urbain, O. Leo, M. Moser, Regulation of dendritic cell numbers and maturation by lipopolysaccharide in vivo, J Exp Med 184 (1996) 1413-24.

[12] D.T. O'Hagan, M. Singh, Microparticles as vaccine adjuvants and delivery systems, Expert Rev Vaccines 2 (2003) 269-83.

[13] N. Qureshi, K. Takayama, E. Ribi, Purification and structural determination of nontoxic lipid A obtained from the lipopolysaccharide of Salmonella typhimurium, J Biol Chem 257 (1982) 11808-15.

[14] N. Qureshi, P. Mascagni, E. Ribi, K. Takayama, Monophosphoryl lipid A obtained from lipopolysaccharides of Salmonella minnesota R595. Purification of the dimethyl

derivative by high performance liquid chromatography and complete structural determination, J Biol Chem 260 (1985) 5271-8.

[15] J.P. Valensi, J.R. Carlson, G.A. Van Nest, Systemic cytokine profiles in BALB/c mice immunized with trivalent influenza vaccine containing MF59 oil emulsion and other advanced adjuvants, J Immunol 153 (1994) 4029-39.

[16] S.L. Giannini, E. Hanon, P. Moris, M. Van Mechelen, S. Morel, F. Dessy, M.A. Fourneau, B. Colau, J. Suzich, G. Losonksy, M.T. Martin, G. Dubin, M.A. Wettendorff, Enhanced humoral and memory B cellular immunity using HPV16/18 L1 VLP vaccine formulated with the MPL/aluminium salt combination (AS04) compared to aluminium salt only, Vaccine 24 (2006) 5937-49.

[17] P.E. Samar Hamdy, Aws Alshamsan, Ommoleila Molavi, Tadaaki Satou, John Samuel., Enhanced antigen-specific primary CD4+ and CD8+ responses by co-delivery of ovalbumin and Toll-like receptor ligand monophosphoryl lipid A in poly(D,L-lactic-co-glycolic acid) nanoparticles, Journal of Biomedical Materials Research Part A in press (2006).

[18] J. Kazzaz, M. Singh, M. Ugozzoli, J. Chesko, E. Soenawan, T. O'Hagan D, Encapsulation of the immune potentiators MPL and RC529 in PLG micropartieles enhances their potency, J Control Release 110 (2006) 566-73.

[19] K.D. Newman, J. Samuel, G. Kwon, Ovalbumin peptide encapsulated in poly(d,l lactic-co-glycolic acid) microspheres is capable of inducing a T helper type 1 immune response, J Control Release 54 (1998) 49-59.

Chapter Three

Enhanced antigen-specific primary $CD4^+$ and $CD8^+$ T cell responses by co-delivery of OVA and 7-acyl lipid A in PLGA-NPs

A version of this chapter has been published in

Journal of Biomaterial Medical Research A 2007; 81(3):652-62

Hamdy S, Elamanchili P, Haddadi A, Alshamsan A, Molavi O, Satou T, Ma Z, and John Samuel, Faculty of Pharmacy & Pharmaceutical Sciences, University of Alberta, Edmonton, AB, Canada, T6G2N8

and

presented as a poster in Keystone Symposia, The Potent New Anti-Tumor Immunotherapies Banff, Alberta, March 28-April 2, 2007

3.1 Introduction

Numerous animal models and several clinical studies highlight the important roles of T cells in mediating cancer rejection [1-5]. The T cell-mediated arm of the adaptive immune system is comprised from both $CD4^+$ Th cells and $CD8^+$ CTLs. Although $CD8^+$ T cells were initially considered as primary mediators of anti-tumor activity, more recent studies highlight the significance of $CD4^+$ Th cells (especially Th1) in controlling the anti-tumor responses [6]. Th1 cells secrete IL-2 and IFN-γ, which help $CD8^+$ T cells to differentiate into CTLs, capable of killing MHC class I positive tumors. In addition to the direct anti-tumor effect of IFN-γ (through inhibition of angiogenesis), IFN-γ secretion further activates innate immune cells that can also mediate anti-tumor activity e.g. NK cells. Cancer vaccine formulations that can activate $CD4^+$ cell (together with $CD8^+$ T cells) response are expected to give better CTL response with the assistance of IFN-γ secreting Th1 cells.

Here we are investigating a vaccine delivery approach that can target DCs both *in vitro* and *in vivo* in order to activate potent antigen specific $CD4^+$ and $CD8^+$ T cell responses. This approach is based on the co-encapsulation of OVA, as a model antigen, in combination with an immunostimulatory adjuvant (7-acyl lipid A) in PLGA-NPs. OVA-containing PLGA-NPs are internalized by DCs through phagocytosis, as they have similar size to those of pathogens. Following uptake, we hypothesized that encapsulated OVA is released and degraded inside the DCs to produce both CD4 and CD8 T cell epitopes ($OVA_{323-339}$ and OVA_{257-26}) that can reach both MHC II and MHC I pathways, with simultaneous activation of both $CD4^+$ and $CD8^+$ T cell responses, respectively.

Co-delivery of OVA and 7-acyl lipid A in the same NP formulation would result in concurrent antigen processing and presentation plus triggering of TLR signaling pathways leading to the generation of properly activated DCs capable of inducing robust T cell responses [7-9]. Previous study in our lab showed that PLGA delivery of OVA induced an increase in the primary $CD4^+$ T cell proliferative response *in vitro* by 500-1000 fold, and incorporation of 7-acyl lipid A in the NP formulation increased the T cell activation potential of DCs and reduced the dose of OVA necessary for efficient T cell priming [10]. In the current series of experiments, we extended our studies to investigate whether our vaccination strategy (OVA/7-acyl lipid A in PLGA-NPs) would induce activation of primary $CD4^+$ T cell activation to the same extent *in vivo*. We were also interested to see the effect of particulate delivery of OVA and 7-acyl lipid A to BMDCs on their ability to prime naïve $CD8^+$ T cell responses. Finally, the simultaneous activation of OVA specific $CD4^+$ and $CD8^+$ T cell responses following vaccinating wild-type mice with our vaccine formulation was investigated.

3.2 Materials and Methods

3.2.1 Mice

Balb/c mice were bred and maintained at the University of Alberta's Health Science's Laboratory Animal Facility. C57Bl/6 mice and both DO11.10 and OT-1 TCR transgenic mice were purchased from the Jackson Laboratory (Bar Harbor, ME, USA). All experiments were performed in accordance to the University of Alberta guidelines for the care and use of laboratory animals. All experiments were performed using 6 to 12 week old male mice.

3.2.2 Reagents

Synthetic 7-acyl lipid A, Mwt, 1955.5 Da and MUC1 lipopeptide were kindly provided by Oncothyreon Inc., Edmonton, AB, Canada. OVA protein (Grade-V), PVA, Mwt, 31,000-50,000 Da, Freund Adjuvant Complete (CFA) and Incomplete Freund Adjuvant (IFA) were obtained from Sigma Aldrich co. (Oakville, ON, Canada). PLGA co-polymer (monomer ratio 50:50) Mwt, 7000 Da, was purchased from Absorbable Polymers International, (Pelham, AL, USA). Recombinant GM-CSF was purchased from Peprotech (Rocky Hill, NJ, USA). Murine CD4 and CD8 isolation kits were purchased from StemCell Technologies (Vancouver, BC, Canada). Murine IFN-γ ELISA and ELISPOT kit were purchased from E-Bioscience (San Diego, CA, USA). RPMI-1640, L-glutamine, and gentamycin were purchased from Gibco-BRL (Burlington, ON, Canada). FCS was obtained from Hyclone Laboratories (Logan, UT, USA). Micro bicinchoninic acid (BCA) protein assay kit was purchased from BioLynx Inc. (Brockville, ON, Canada). Anti mouse CD16/CD32 mAb and Phycoerythrin (PE)-Cy5-conjugated anti mouse CD8 mAb

were purchased from BD Biosciences (Mississauga, ON, Canada). Fluorescein isothiocyanate (FITC)-conjugated anti mouse CD90.2 mAb and PE-conjugated anti mouse CD4, CD11a, CD25, CD44 and CD62L mAbs and their respective isotype controls, were purchased from E-Bioscience (San Diego, CA, USA). Clonotype specific DO11.10 TCR transgenic mAb (KJ1-26) and its isotype control were purchased from Caltag Laboratories (Burlingame, CA, USA).

3.2.3 Preparation of murine BMDCs

DC primary cultures were generated from murine bone marrow precursors from femurs of C57BL/6 mice in complete RPMI media in the presence of GM-CSF as described earlier in chapter 2.

3.2.4 Preparation and characterization of OVA-containing PLGA-NPs

PLGA-NPs containing OVA protein with or without 7-acyl lipid A were prepared as water/oil/water (w/o/w) double emulsion formulation by the solvent evaporation method [11]. Two kinds of OVA-containing PLGA-NPs were employed in the current studies: one was loaded with lower amount of OVA and the other was loaded with higher amount. Both formulations were loaded with equal amount of 7-acyl lipid A. In brief, 50 μL of OVA/PBS solution (containing either 10 mg or 25 mg OVA) was emulsified with PLGA solution in chloroform (100 mg polymer in 300 μL chloroform) for 15 sec at level 4, using a microtip sonicator (Heat systems Inc., Farmingdale, NY, USA) to form a primary water/oil emulsion (w/o). For the preparation of NPs containing 7-acyl lipid A, 200 μg of 7-acyl lipid A in 100 μL of 1:4 methanol-chloroform mixture was added to the polymer-

chloroform solution. The resulting primary emulsion was further emulsified in 2 mL of PVA solution (9% w/v PVA in PBS) by sonication for 45 sec at level 4 to form a seconday water/oil/water (w/o/w) emulsion. The secondary emulsion was added drop-wise into 8 mL of stirring PVA solution. NPs were collected and washed as previously described in chapter 2. Particle size was determined by dynamic light scattering technique (using a Zetasizer 3000 (Malvern, UK)). Schematic illustration of double emulsion solvent evaporation technique is shown in Figure 3-1.

OVA content in the NPs was determined by BCA protein assay. Briefly, 5 mg of NPs was re-dispersed in 3.0 ml of 0.1 M NaOH containing 5% (w/v) sodium dodecyl sulfate (SDS). The mixture was incubated overnight in an orbital shaker. The supernatant was then collected by centrifugation at 15000 x *g* for 10 minutes (min). Finally, a BCA protein assay was used to determine the protein concentration in the supernatant. Quantification of 7-acyl lipid A in NPs was done by a newly developed LC-MS method as described in chapter 2. The approximate amounts of particulate or soluble (Sol) OVA and 7-acyl lipid A used per mice (for *in vivo* experiments) or per mL (for *in vitro* experiments) are indicated in each figure legend.

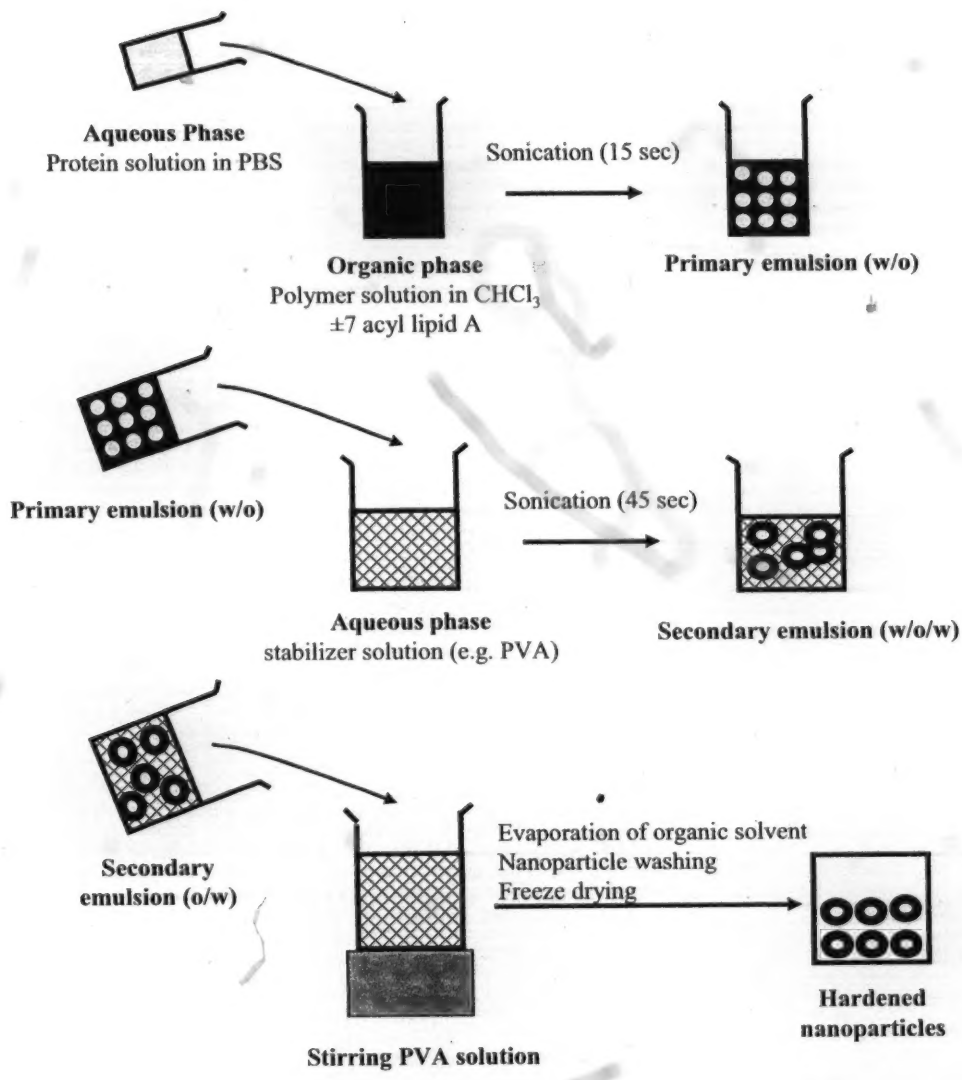

Figure 3-1. Double emulsification solvent evaporation technique for the preparation of OVA-containing PLGA-NPs- Briefly, 50 µL of OVA/PBS solution was emulsified with PLGA solution in chloroform (100 mg polymer in 300 µL chloroform) by sonication for 15 sec at level 4, to form a primary water-in-oil (w/o) emulsion. For the preparation of NPs containing 7-acyl lipid A, 200 µg of 7-acyl lipid A in 100 µL of 1:4 methanol-chloroform mixture was added to the polymer-chloroform solution. The resulting primary emulsion was further emulsified in 2 mL of PVA solution (9% w/v PVA in PBS) by sonication for 45 sec at level 4 to form a secondary water-in-oil-in water (w/o/w) emulsion. The secondary emulsion was added drop-wise into 8 mL of stirring PVA solution. NPs were collected after 3 h of stirring by centrifugation of the emulsion at 40000 x *g* for 10 min at 4°C. The NPs were washed twice with cold deionized water and lyophilized.

3.2.5 Flow cytometry

For $CD4^+$ and $CD8^+$ T cell activation studies, 1×10^6 cells were suspended in FACS buffer (PBS with 5% FCS, and 0.09% sodium azide) and incubated with anti mouse CD16/CD32 monoclonal antibody (mAb) to block Fc receptors and then stained with appropriate fluorescence conjugated antibodies as described in each section. All samples were finally acquired on a Becton-Dickinson Facsort and analyzed by Cell-Quest software.

3.2.6 Transgenic $CD4^+$ T cell adoptive transfer and immunization

$CD4^+$ T cells from the spleens of DO11.10 mice were isolated by negative selection using the EasySep® mouse CD4 isolation kit according to the manufacturer's instructions. BALB/c mice were adoptively transferred with 3.5×10^6 DO11.10 $CD4^+$ T cells. One day later; groups of mice were immunized i.p. with either, PBS, Sol OVA, Sol 7-acyl lipid A, Sol OVA/7-acyl lipid A, Empty-NPs, 7-acyl lipid A-NPs, OVA-NPs or OVA/7-acyl lipid A-NP (3 mice per group). After 72 h, the spleens of the vaccinated mice were harvested and single cell suspensions were prepared and blocked with CD16/32 mAb. For antigen specific clonal expansion studies, the spleenocytes were stained with CD4 and KJ1-26 mAbs. The percentages of double positive ($CD4^+$/KJ1-26^+) T cells were calculated for each group. Fold increase in the percentage of $CD4^+$/KJ1-26^+ T cells for each group was calculated as the percentage of $CD4^+$/KJ1-26^+ T cells in test group divided by the percentage of $CD4^+$/KJ1-26^+ T cells in the PBS immunized group. For T cell phenotyping studies, the spleenocytes were stained with CD90, KJ1-26 and either CD11a, CD44, or CD62L mAbs.

In another set of experiments, BALB/c mice were adoptively transferred with 3.5 x 10^6 DO11.10 TCR transgenic $CD4^+$ T cells. One day later, groups of mice were immunized s.c. in the right flank region with either OVA-NPs or OVA/7-acyl lipid-NPs. Negative control mice received PBS. Positive control mice received 200 μg OVA emulsified in CFA. To characterize the antigen specific clonal expansion, the draining lymph node of the vaccinated mice were harvested at 3, 5 and 7 days after vaccination and stained with CD4 and KJ1-26 mAbs. Percentages of $CD4^+$/KJ1-26^+ T cells in the pooled draining lymph nodes for each group at the different times tested were reported (3 mice/group/time point). For T cell phenotyping studies, 5 days after vaccinations, the lymphocytes were stained with CD90, KJ1-26 and either CD11a, CD44, or CD62L mAbs.

3.2.7 Transgenic $CD8^+$ T cell activation studies

For assessing the $CD8^+$ responses, another transgenic mouse model was used, (OT-I). OT-I $CD8^+$ T cells recognize the OVA $peptide_{257-264}$ (SIINFEKL) in association with H-2^b MHC class I molecules. In brief, day 7 BMDCs were incubated with 1 μg/mL OVA (test antigen) either soluble or encapsulated in PLGA-NPs, both in the presence or absence of 7-acyl lipid A. Negative controls includes untreated (unpulsed) DCs, DCs incubated with either Empty-NPs, 7-acyl lipid A-NPs or NPs containing MUC1 lipopeptide as an irrelevant antigen, with or without 7-acyl lipid A (MUC1/7-acyl lipid A-NPs and MUC1-NPs, respectively). After overnight incubation, all DC groups were harvested, irradiated, washed, and plated (in triplicates) in a 96-well plate (2 x 10^4 DCs/well). $CD8^+$ T cells isolated from the spleens of OT-1 mice were then co-cultured

with different DC groups (2 x 10^5 T cells/well) in a DC:T cell ratio of 1:10. Three parallel assays were performed to assess the extent of OT-1 T cell activation (T cell proliferation, analysis of the expression of the activation markers on $CD8^+$ T cells and detection of IFN-γ secretion in the co-culture supernatants).

OT-1 $CD8^+$ T cell proliferation

The extent of T cell proliferation was assessed after adding ^{3}H-thymidine during the last 18 h of a 60 h co-culture. Stimulation Index (S.I) for each group was calculated as the ratio of counts per minute (cpm) of T cells co-cultured with DCs pulsed with different formulations (test groups) divided by the cpm of T cells co-cultured with un-pulsed DCs (control group).

OT-1 $CD8^+$ T cell phenotypic activation

The expression of different activation markers (CD11a, CD25, CD44 and CD62L) on the expanded OT-1 $CD8^+$ T cells (after 90 h DC/T cell co-culture) was tested. Among the different groups employed in T cell proliferation studies, only two groups had been phenotypicaly analyzed; T cells co-cultured with OVA-NPs treated DCs and T cells co-cultured with OVA/7-acyl lipid A-NPs treated DCs. The extent of clonal expansion (proliferation) of other T cell groups; T cells co-cultured with untreated DCs or DCs treated with Empty-NPs, Sol OVA, Sol OVA/7-acyl lipid A or MUC1 containing NPs was very low. As a result, the number of T cells at the end of the co-culture period was not enough to be used in performing the flow cytometry studies. Freshly isolated $CD8^+$ T

cells (from OT-1 spleenocytes) served as a negative control to show the basal level of expression for these activating markers in naïve OT-1 $CD8^+$ T cells.

Detection of IFN-γ secretion by activated OT-1 $CD8^+$ T cells

Supernatants from the test groups; i.e., T cells co-cultured with OVA-NPs treated DCs and T cells co-cultured with OVA/7-acyl lipid A-NPs treated DCs were collected over a period of 0-96 h and analyzed for IFN-γ production by ELISA kit. Supernatants from T cells co-cultured with unpulsed DCs served as a negative control. The assay was performed in a 96 well microplate using a microplate reader (Powerwave with KC Junior software; Bio-Tek, Winooski, VT) at OD of 450 nm with reference set at 570 nm according to the manufacturer's directions. All samples were analyzed in duplicates. The minimum level for IFN-γ detection was 15 pg/mL.

3.2.8 Wild-type mice studies

Immunization

In these studies we have used wild type C57BL/6 mice. Five groups (4-6 mice/group) were immunized twice (s.c., two weeks apart) in right flank region with either Empty-NPs, 7-acyl lipid A-NPs, OVA-NPs, OVA/7-acyl lipid A-NPs or OVA/CFA. One week after the last immunization, mice were euthanized and draining inguinal lymph nodes harvested, pooled and washed three times in PBS. Lymphocytes were re-suspended in complete RPMI media for ELISPOT assay, as described below.

ELISPOT assay

Ninety-six-well MultiScreen™ filter plates (Millipore, Bedford, MA, USA) were coated overnight at 4 °C with 100 µl/well of anti-mouse IFN-γ capture antibody (diluted in sterile PBS according to the manufacturer's instructions). After the overnight incubation, the coating antibody solution was decanted from the plates. The plates were washed twice with 200 µL/well PBS and then blocked for 1 hour at room temperature with 200 µL/well of complete RPMI-1640. After blocking, plates were decanted and lymphocytes were added into individual wells (as described below).

Pooled lymphocytes from each treatment group were suspended in complete RPMI media at $1x10^7$ cells/mL. From those lymphocyte cell suspensions, 100 µL (containing $1x10^6$ lymphocytes) were added into ELISPOT plates. Lymphocytes from each treatment group were stimulated (in duplicates) with either of the following peptide formulations (20 µM peptide in 100 µL complete RPMI media): $OVA_{323-339}$ epitope (CD4 test peptide), MUC 1 lipopeptide (irrelevant CD4 epitope), $OVA_{257-264}$ epitope (CD8 test peptide) or HB-YD (irrelevant CD8 epitope) (listed in Table 3-1). The cells were incubated at 37°C for 18 hours in the presence of 5% CO_2 and then washed three times with 0.05% Tween in PBS (PBS-Tween). The anti-mouse IFN-γ detection antibody was diluted in 1% bovine serum albumin (BSA) in PBS according to the manufacturer's instructions. Diluted solution was added at a volume of 100 µL per well. After two hours incubation at room temperature, plates were washed four times with PBS-Tween and incubated for 45 min at room temperature with Streptavidin-HRP. Plates were then washed three times with PBS-Tween followed by two times wash with PBS. Spots were developed by adding 100

μL/well of freshly prepared AEC substrate solution. Stopping the substrate reaction was done after 20-30 min by washing the plates three times with distilled water. Plates were then dried and spots were counted in a BioReader 3000 (BioSys, Karben, Germany).The background level was measured in wells containing lymphocytes stimulated by the irrelevant peptide. The number of OVA-specific spots was obtained by subtracting the background (number of spots appearing after irrelevant peptide stimulation) from the number of spots appearing after OVA peptide stimulation. Results are presented as mean values obtained for duplicate wells ± SD.

Table 3-1. List of the different peptides used for stimulation of isolated lymphocytes in the *ex-vivo* ELSPOT assay (described in Figure 3-8)

Peptide name	Peptide type	Sequence
MUC1	CD4 irrelevant epitope	STAPPAHGVTSAPDTRPAPGSTAPP-Lysine (palmitoyl)G
HY-BD	CD8 irrelevant epitope	WMHHNMDLI
$OVA_{323-339}$	CD4 test epitope	ISQAVHAAHAEINEAGR
$OVA_{257-264}$	CD8 test epitope	SIINFEKL

3.2.9 Statistical analysis

The significance of differences among groups was analyzed either by one-way analysis of variance (ANOVA) followed by the Student-Newman-Keuls post hoc test for multiple comparisons. *P* value of ≤ 0.05 was set for the significance of difference among groups. The statistical analysis was performed with SigmaStat software (Systat Software Inc. San Jose, California, USA).

3.3 Results

3.3.1 Characterization of PLGA-NP formulations

The mean intensity diameter of all prepared NP formulations [Empty-NPs, 7-acyl lipid A-NPs, OVA-NPs and OVA-7-acyl lipid A-NPs] ranged between 350-450 nm with a polydispersity below 0.2. In this series of investigations, 2 different concentrations of OVA were employed in the process of NP formulation. Based on BCA assay, the encapsulation efficiency for OVA in both types of formulations was ~15 % and the loading was either ~ 20 μg or ~50 μg entrapped per 1 mg dry weight of NPs. On the other hand, 7-acyl lipid A was equally loaded in all the NP formulations. Based on LC-MS analysis, the encapsulation efficiency for 7-acyl lipid A was ~70 % and the loading was ~ 1.7 μg 7- acyl lipid A entrapped per 1 mg dry weight of NPs.

3.3.2 Activation of primary $CD4^+$ T cell responses

For studying $CD4^+$ T cell responses, we have used a transgenic mouse model (known as DO11.10), which has T cell receptor (TCR) specific for OVA epitope; $OVA_{323-339}$. This model as previously described by Kearney *et al* [12] enables the detection of small numbers of $CD4^+$ T cells when adoptively transferred from DO11.10 mice into wild type mice using a clonotype-specific mAb (KJ1-26) that specifically binds to this transgenic TCR. In our studies, $CD4^+$ T cells were isolated from DO11.10 mice by negative selection using the EasySep® mouse CD4 isolation kit. The purity of the isolated $CD4^+$ T cells was >92% (Figure 3-2A) and greater than 87% of the $CD4^+$ T cells were stained positive for the clonotype specific KJ1-26 mAb (Figure 3-2B). Figure 3-2C, shows the absence of these transgenic $CD4^+$ T cells in the wild-type Balb/c mice.

After isolation from DO11.10 mice, transgenic $CD4^+$ T cells were adoptively transferred to naïve Balb/c mice. One day later, recipient mice were vaccinated with different combinations of OVA-containing formulations. The *in vivo* activation of OVA-specific $CD4^+$ T cell immune responses was assessed both quantitatively (through measuring the clonal expansion of the adoptively transferred $CD4^+$ T cells) and qualitatively (by assessing the up-regulation of activation markers on the expanded $CD4^+$ T cells).

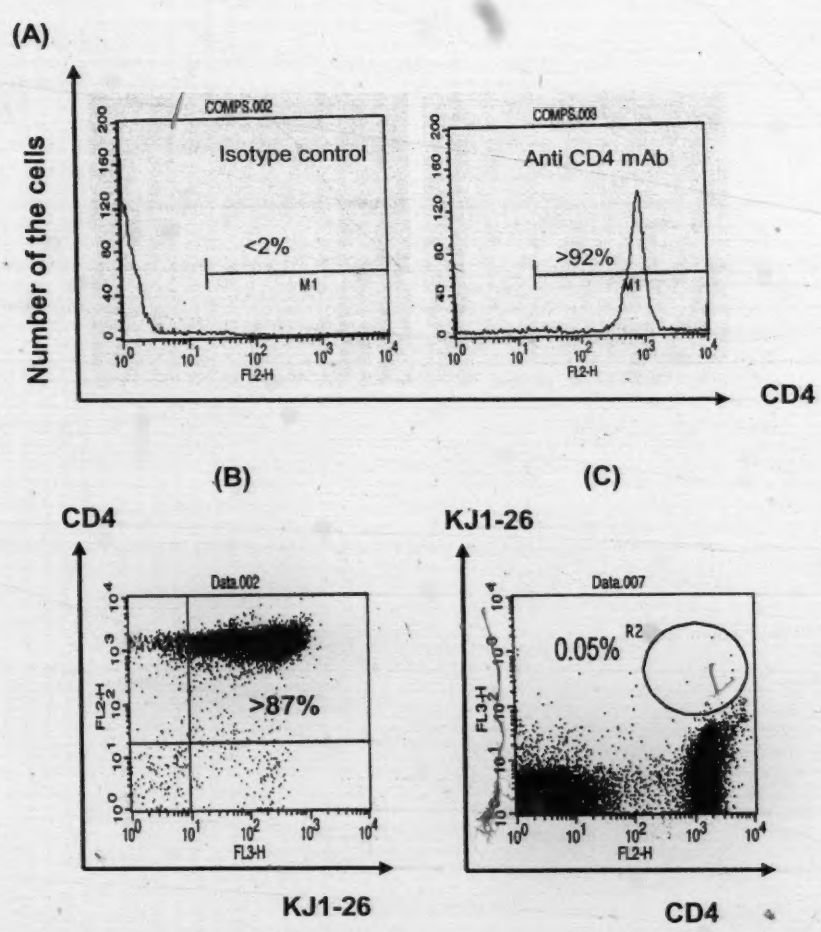

Figure 3-2. Flow cytometric analysis of isolated CD4$^+$ T cells from transgenic DO11.10 mice- CD4$^+$ T cells were isolated from spleens of DO11.10 mice by negative selection using the EasySep® mouse CD4 isolation kit. The purity of the isolated CD4$^+$ T cells was >92% (A) and greater than 87% of the CD4$^+$ T cells stained positive for the clonotype specific KJ1-26 mAb (B). These transgenic CD4$^+$ T cells were not detectable in the spleens isolated from wild-type Balb/c mice as evidence by the absence of CD4$^+$/KJ1-26$^+$ T cells (C).

Adoptive transfer studies followed by i.p. vaccination

To assess the ability of our vaccination strategy to induce clonal expansion of the adoptively transferred transgenic $CD4^+$ T cells, the percentages of double positive ($CD4^+$/KJ1-26^+) T cells were determined for each immunization group. Figure 3-3A demonstrates the fold increase in the percentage of $CD4^+$/KJ1-26^+ T cells for each group relative to PBS immunized group. Only a trace population of $CD4^+$/ KJ1-26^+ T cells was observed in groups immunized with Sol formulations. Such trace populations were comparable to what we observed in the PBS immunized group. As shown in Figure 3-3A, the fold increase in the percentage of $CD4^+$/KJ1-26^+ T cells for Sol OVA, Sol 7-acyl lipid A and Sol OVA/7-acyl lipid A immunized mice were ~1.5, 1 and 1.1, respectively. Same pattern was observed in the mice immunized with control NP formulations, such as Empty-NPs (~0.6) and 7-acyl lipid A-NPs (~1.6). Remarkably, OVA-containing NPs were far more potent than soluble formulations in inducing clonal expansion of the adoptively transferred $CD4^+$ T cells. In fact, ~7 fold increase in the percentages of $CD4^+$/ KJ1-26^+ cells was observed in the OVA-NPs immunized group. The presence of 7-acyl lipid A along with OVA in the same formulation (OVA/7-acyl lipid A-NPs) significantly increased the extent of *in vivo* clonal expansion of adoptively transferred T cells, as evidenced by ~15 fold increase in the percentages of $CD4^+$/ KJ1-26^+ T cells ($p< 0.05$).

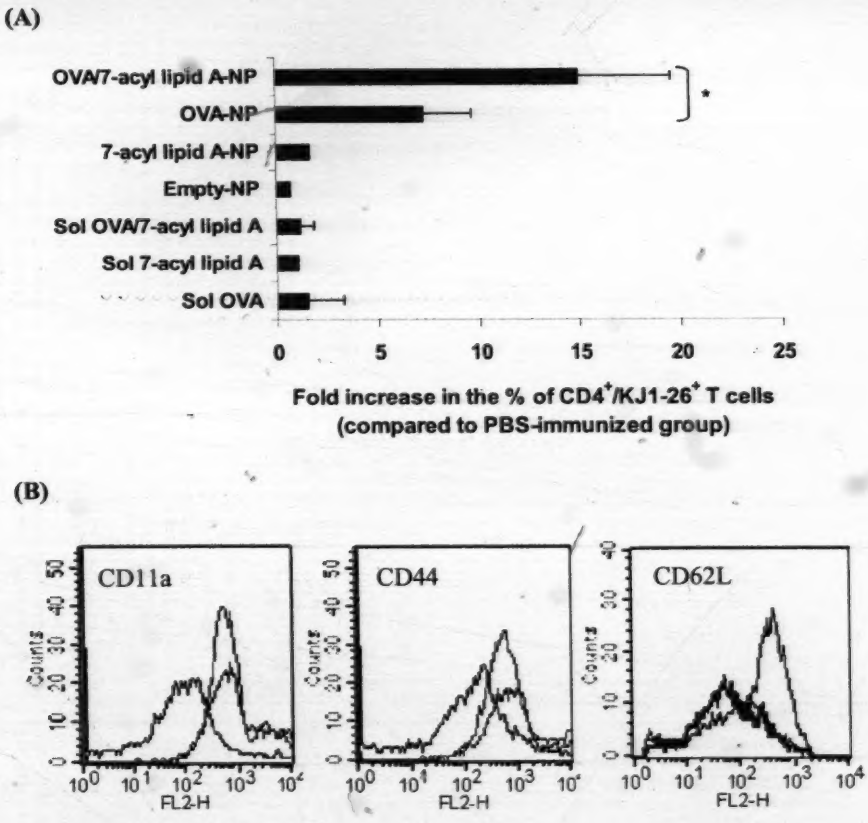

Figure 3-3. Clonal expansion and activation of adoptively transferred OVA-specific $CD4^+$ T cells following i.p. vaccination with OVA-containing formulations- BALB/c mice were adoptively transferred with 3.5 x 10^6 DO11.10 $CD4^+$ T cells. One day later, groups of mice were immunized i.p. (3 mice per group) with one of the following formulations: PBS, Sol OVA, Sol 7-acyl lipid A and Sol OVA/7-acyl lipid A, Empty-NPs, OVA-NPs and OVA/7-acyl lipid A-NPs. The approximate dosages of OVA and 7-acyl lipid 7-acyl lipid A (per mouse) were 20 μg and 1.7 μg, respectively. Three days following the vaccinations, the animals were scarified and spleens were isolated. Spleens from each treatment group were pooled together, washed and tested for the clonal expansion of the adoptively transferred T cells (A) and the presence of activation markers on the expanded T cells (B). Fold increase in the percentage of $CD4^+$/KJ1-26^+ T cells for each group was calculated as the percentage of $CD4^+$/KJ1-26^+ T cells in test group divided by the percentage of $CD4^+$/KJ1-26^+ T cells in the PBS immunized group (A). Represented data are averages of up to 4 independent experiments. Error bars represent S.D between data obtained from independent experiments. For T cell phenotyping studies (B), spleenocytes from naïve DO11.10 mice was used as negative control (black line). These transgenic spleenocytes and spleenocytes from mice vaccinated with OVA-NPs (blue line), and OVA/7-acyl lipid A-NPs (red line) were stained with CD90, KJ1-26 and either CD11a, CD44 or CD62L mAbs. Histograms of the activation markers represent $CD90^+$/KJ1-26^+ gated population. * denotes significance between OVA-NPs and OVA/7-acyl lipid A-NPs ($p < 0.05$).

Our next objective was to determine whether the expanded OVA-specific $CD4^+$ T cells would display an activated phenotype. Spleenocytes isolated from naïve DO11.10 mice served as a negative control. Staining of these transgenic spleenocytes showed that naïve DO11.10 T cells display a $CD62L^{hi}$, $CD11a^{lo}$ and $CD44^{lo}$ surface phenotype. On the other hand, T cells isolated from recipient mice that have been immunized with either OVA-NPs or OVA/7-acyl lipid A-NPs possessed a $CD62L^{lo}$, $CD11a^{hi}$ and $CD44^{hi}$ surface phenotype characteristic of activated effector T cells (Figure 3-3B). Flow cytometric analysis of T cells in the mice that received control NPs or Sol formulations was not feasible due to their presence in extremely low frequencies.

Adoptive transfer studies followed by s.c. vaccination

Previous experiments with i.p. mode of vaccine delivery demonstrated the superior activation of $CD4^+$ T cells following particulate delivery of antigens (compared to Sol formulations). In the current set of experiments, we were interested to test the s.c. route of immunization, which is more clinically relevant than the i.p. administration. We have also extended our studies to examine the kinetics of clonal expansion of adoptively transferred $CD4^+$ T cells at different time points following vaccination.

Our results showed that the injection of OVA-NPs alone caused 9-10 fold increase in the percentage of OVA specific $CD4^+$/KJ1-26^+ cells relative to PBS immunized group at day 3 (2.9%). This percentage started to decline at day 5 (1.54%) and finally reached 1.27% at day 7. On the other hand, the injection of OVA/7-acyl lipid A-NPs showed its peak at day 5, where 13-fold increase in the percentage of $CD4^+$/KJ1-26^+ cells was observed

(4.32%). At day 7, three-fold reduction of the percentage and absolute numbers of DO11.10 cells was detected (1.41%). Interestingly, similar pattern was observed for the OVA/CFA positive control group, while the DO11.10 cells peaked at day 5 (12.70%) and contracted at day 7 (3.96%) with three fold reduction in their percentage. Taking into account that the amount of OVA in the OVA/CFA group was 4-fold higher than the amount of OVA encapsulated in the PLGA-NPs (200 and 50 μg, respectively), we can conclude that, at least in terms of $CD4^+$ T cell expansion, co-encapsulation of protein and 7-acyl lipid A in PLGA-NPs can induce a response which is comparable to that induced by protein emulsified in CFA, one of the strongest adjuvants used in animal studies. These results also demonstrate that delivery of the antigen, its acquisition by DCs and its presentation to naïve $CD4^+$ T cells all had occurred within this 7-day period. Furthermore, the presence of 7-acyl lipid A along with OVA in the same NP formulation resulted in an increase in the number of antigen specific T cells at the peak of clonal expansion and after clonal contraction had occurred.

We have also determined whether these expanded $CD4^+$ T cells would display an activated effector phenotype. Lymphocytes from recipient mice 5 days after s.c. immunization with OVA-NPs or OVA/7-acyl lipid A-NPs showed that the DO11.10 donor T cells express $CD62L^{lo}$, $CD11a^{hi}$ and $CD44^{hi}$ surface phenotype (Figure 3-4B), similar to the phenotype observed in the spleenocytes of the i.p. vaccinated mice (Figure 3-3B). Such a phenotype is characteristic to the activated effector T cells.

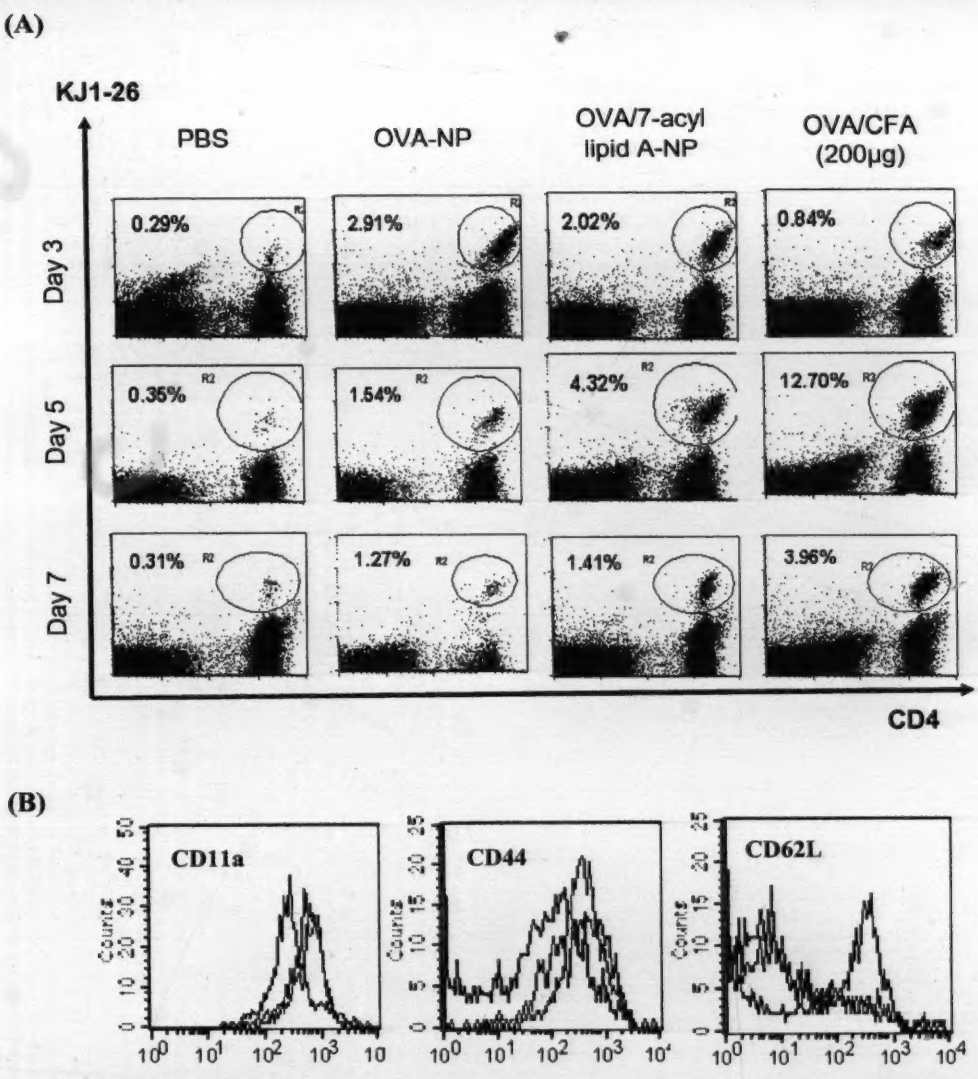

Figure 3-4. Kinetics of *in vivo* clonal expansion of antigen specific T cells after particulate delivery of OVA and 7-acyl lipid A- BALB/c mice were adoptively transferred with 3.5 x 10^6 DO11.10 $CD4^+$ T cells. One day later; groups of mice were immunized s.c. in the right flank region with 50 µg OVA encapsulated with or without 1.7 µg 7-acyl lipid A in PLGA-NPs. Negative control mice received PBS. Positive control mice received 200 µg OVA emulsified in CFA. To characterize the antigen specific clonal expansion, the draining lymph node of the vaccinated mice were harvested at 3, 5 and 7 days after vaccination (3 mice/group/time point) and stained with CD4 and KJ1-26 mAbs (A). For T cell phenotyping studies (B), lymphocytes from mice immunized with OVA-NPs (blue line), and OVA/7-acyl lipid A-NPs (red line) were harvested 5 days after vaccination and stained with CD90, KJ1-26 and either CD11a, CD44 or CD62L mAbs. Lymphocytes from naïve DO11.10 mice were stained similarly and used as negative control (black line). Histograms of the activation markers represent $CD90^+/KJ1\text{-}26^+$ gated populations. Data are representative of three independent experiments.

3.3.3 Activation of primary $CD8^+$ T cell responses

OT-1 $CD8^+$ T cell proliferation

As illustrated in Figure 3-5, incubating DCs with 1 μg/mL Sol protein, either alone (Sol OVA) or together with Sol 7-acyl lipid A (Sol OVA/7-acyl lipid A) did not result in any detectable priming of OVA specific $CD8^+$ T cells. However, delivery of OVA encapsulated in PLGA-NPs (OVA-NPs) to DCs efficiently primed naïve T cells as evidenced by stimulation index (S.I) of 600. Co-delivery of 7-acyl lipid A along with OVA in the same NP formulation (OVA/7-acyl lipid A-NPs) dramatically increased the extent of T cell stimulation (S.I >3000). Our results imply that 7-acyl lipid A could directly activate DCs to cross-present encapsulated OVA to $CD8^+$ T cells, and this process could occur in the absence of $CD4^+$ T cells. These results are in agreement with the findings of Datta *et al.* [13], which suggest that certain TLR ligands could enhance antigen escape into the cytosol, where they access the MHC class I antigen processing pathway for presentation to $CD8^+$ T cells. The robust activation of primary $CD8^+$ T cell responses observed in the current study is similar to what we have reported earlier on the ability of OVA/7-acyl lipid A-NPs treated DCs to induce robust activation of primary $CD4^+$ T cell responses [14].

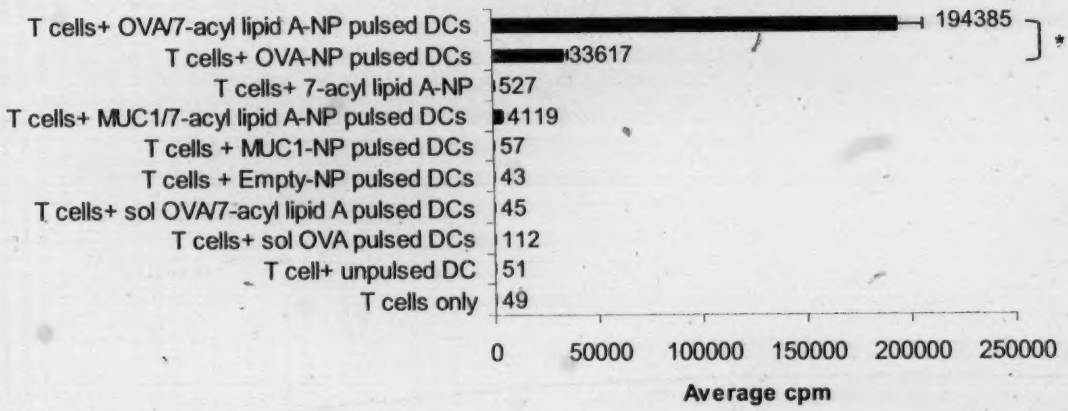

Figure 3-5. Treatment of DCs with particulate OVA dramatically enhances primary antigen specific OT-1 $CD8^+$ T cell proliferation- Day 7 BMDCs were incubated with 1 μg/mL OVA (test antigen) either soluble or encapsulated in PLGA-NPs, both in the presence or absence of 7-acyl lipid A. Negative controls include untreated (unpulsed) DCs, DCs incubated with either Empty-NPs, 7-acyl lipid A-NPs or NPs containing MUC1 lipopeptide as an irrelevant antigen, with or without 7-acyl lipid A (MUC1/7-acyl lipid A-NPs and MUC1-NPs, respectively). After overnight incubation, non adherent cells were harvested and co-cultured with $CD8^+$ T cells from OT-1 mice in a DC:T cell ratio of 1:10. T cell proliferation was assessed after adding ^{3}H-thymidine during the last 18 h of a 60 h co-culture. The values are mean of triplicates ± SD. Mean of each group is shown above its corresponding bar. Data shown are representative of three independent experiments (all gave similar results).

* denotes significance between T cells co-cultured with OVA-NPs pulsed DCs and T cells co-cultured with OVA/7-acyl lipid A-NPs pulsed DCs ($p< 0.05$).

OT-1 $CD8^+$ T cell phenotypic activation

Particulate delivery of OVA and 7-acyl lipid A to DCs generated a large population of OVA specific $CD8^+$ T cells (Figure 3-5). We then asked whether such expanded $CD8^+$ transgenic T cells possess an activated phenotype. As shown in Figure 3-6, $CD8^+$ T cells harvested from spleen of OT-1 mice displayed the naïve phenotype of $CD8^+$ T cells: CD11a ^{lo}CD25$^-$CD62L^{hi}CD44^{lo} [15]. Upon co-culture with OVA/7-acyl lipid A-NPs pulsed DCs, these OT-1 T cells exhibited the typical effector CTL phenotype: CD11a ^{hi}CD25$^+$CD62L^{lo}CD44^{hi}. Co-culture of $CD8^+$ T cells with DCs pulsed with OVA-NPs alone (without 7-acyl lipid A) resulted in similar level of expression of CD11a, CD44, CD62L as in effector T cell phenotype; however, lower expression of CD25 was observed (Figure 3-6).

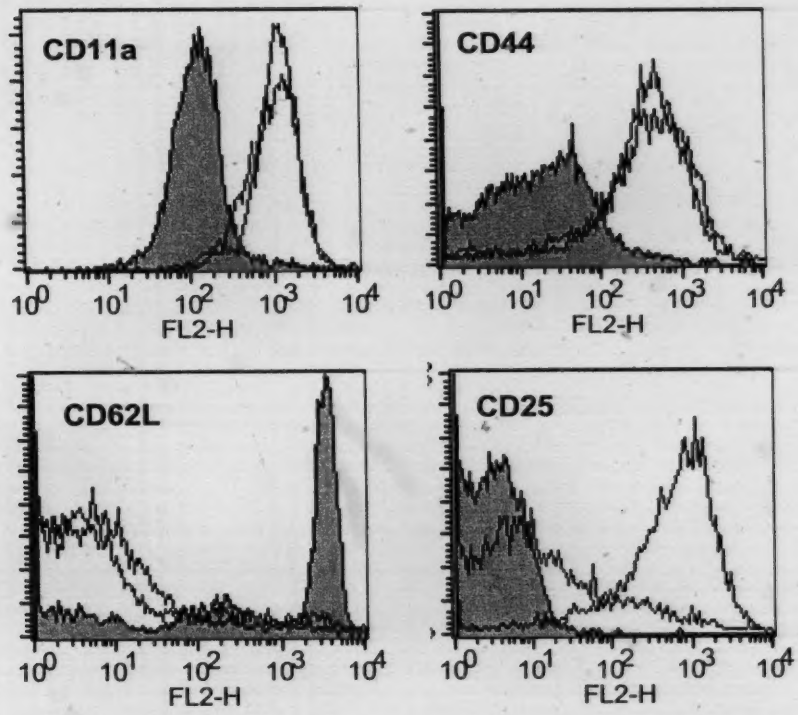

Figure 3-6. Expanded antigen specific OT-1 $CD8^+$ T cells express activated effector T cell phenotype- Day 7 BMDCs were incubated with either OVA-NPs or OVA/7-acyl lipid A-NPs. After an overnight incubation, non adherent cells were harvested and co-cultured with $CD8^+$ T cells from OT-1 mice in a DC:T cell ratio of 1:10. After 90 h co-culture, the cells were stained with CD8, CD90 and either CD11a, CD25, CD44 or CD62L mAbs, and analyzed by flow cytometry. Shaded histograms represent naïve $CD8^+$ T cells isolated from OT-1 spleenocytes. Blue lines and red lines represent $CD8^+$ OT-1 co-cultured with DCs pulsed with OVA-NPs and OVA/7-acyl lipid A-NPs, respectively. Histograms represent $CD90^+/CD8^+$ gated populations.

IFN-γ secretion by activated OT-1 $CD8^+$ T cells

The amount of proliferation (Figure 3-5) and activation (Figure 3-6) were also correlated with IFN-γ production (Figure 3-7). OT-1 T cells co-cultured with un-pulsed DCs didn't produce any detectable level of IFN-γ at all time points. OVA-NPs induced moderate secretion of IFN-γ, which appeared after 24 h from co-culture and sustained at similar level up to 96 h. Co-delivery of OVA and 7-acyl lipid A (OVA/7-acyl lipid A-NPs) resulted in a dramatic increase in IFN-γ production, especially after 72-96 h from co-culture.

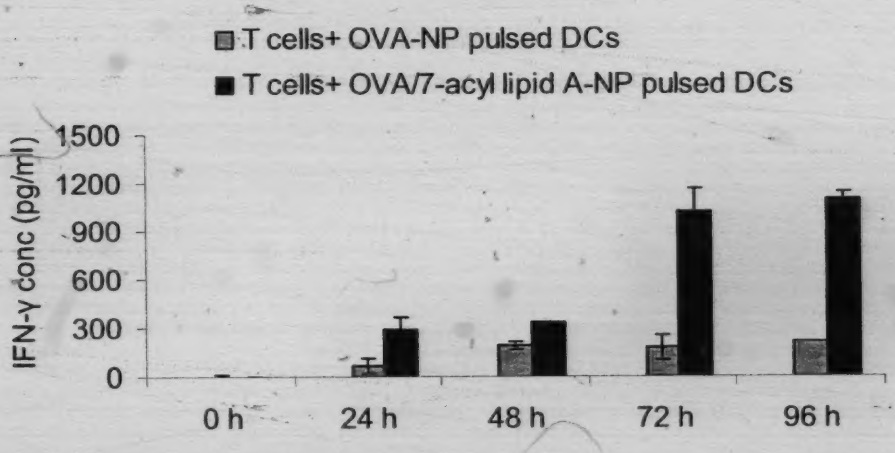

Figure 3-7. IFN-γ secretion pattern of OT1-$CD8^+$ T cells over 96 h co-culture period with antigen treated DCs- Day 7 BMDCs were incubated with either OVA-NPs or OVA/7-acyl lipid A-NPs. After an overnight incubation, non adherent cells were harvested and co-cultured with $CD8^+$ T cells from OT-1 mice in a DC:T cell ratio of 1:10. IFN-γ secretion was detected in the supernatant after 0, 24, 48, 72 and 96 h from co-culture using routine ELISA technique per the manufacture's instruction. OT-1 T cells co-cultured with un-pulsed DCs didn't produce any detectable level of IFN-γ at all time points. Gray and black bars represent DCs pulsed with OVA-NPs and OVA/7-acyl lipid A-NPs, respectively. The values are means of duplicates ± S.D.

3.3.4 Simultaneous activation of $CD4^+$ and $CD8^+$ T cell responses

Results obtained from DO11.10 and OT-1 transgenic mouse models have demonstrated the superior ability of particulate delivery of OVA and 7-acyl lipid A to induce robust primary antigen specific $CD4^+$ and $CD8^+$ T cell responses, respectively. In the current set of experiments, we purposed to assess the ability of our vaccine to induce simultaneous activation of antigen specific $CD4^+$ and $CD8^+$ T cell responses in wild-type mice (without any artificial manipulation, use of transgenic mice or adoptive transfer of antigen specific T cells). In these studies, wild-type C57Bl/6 mice were vaccinated twice (2 weeks apart) and the induction of IFN-γ secretion by OVA specific $CD4^+$ and $CD8^+$ T cells was investigated by a single-cell, *ex vivo* ELISPOT assay (Figure 3-8).

Immunization with strong adjuvants such as 7-acyl lipid A or CFA may induce non specific inflammatory response at the site of injection and/or in the draining lymph nodes. In the ELISPOT assay, such inflammation may cause relatively high background readings in the wells stimulated with the medium alone or with irrelevant peptides, probably due to the non-specific IFN-γ secretion by innate immune cells in those wells. To circumvent this problem and in order to get the actual number of OVA-specific IFN-γ secreting cells, we subtracted the background (number of spots appearing after irrelevant peptide stimulation) from the number of spots appearing after OVA peptide stimulation.

(A)

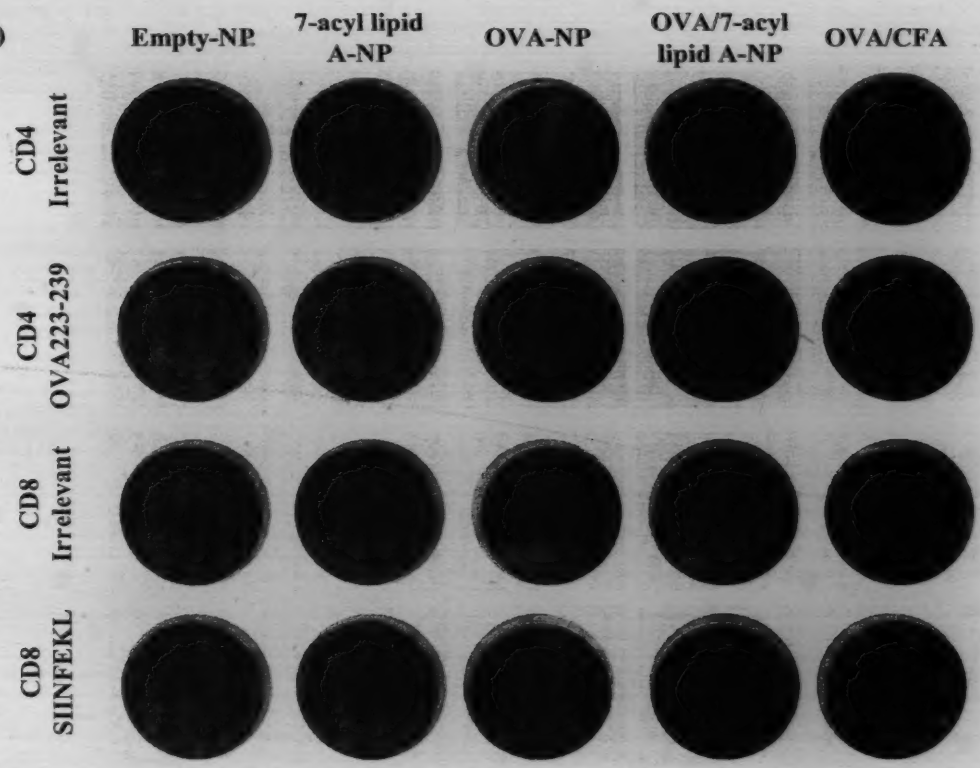
Empty-NP
7-acyl lipid A-NP
OVA-NP
OVA/7-acyl lipid A-NP
OVA/CFA
CD4 Irrelevant
CD4 OVA223-239
CD8 Irrelevant
CD8 SIINFEKL

(B)

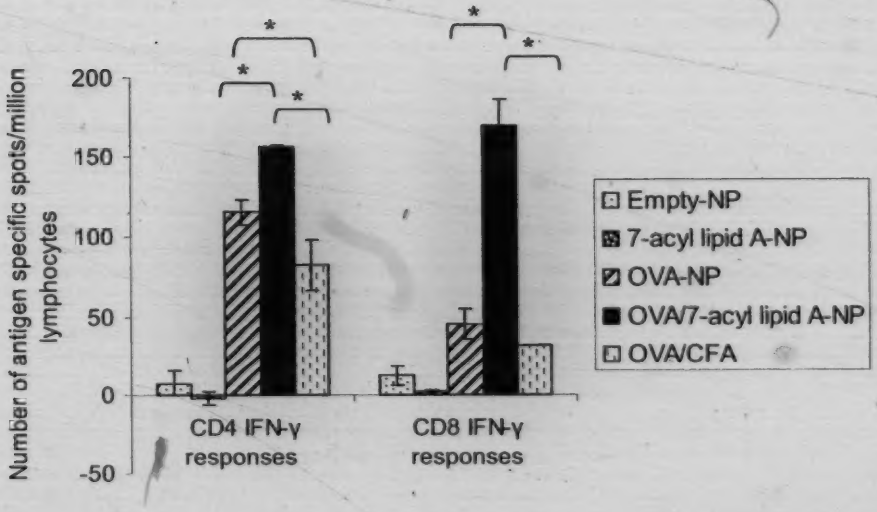
Number of antigen specific spots/million lymphocytes
200
150
100
50
0
-50
CD4 IFN-γ responses
CD8 IFN-γ responses
Empty-NP
7-acyl lipid A-NP
OVA-NP
OVA/7-acyl lipid A-NP
OVA/CFA

Figure 3-8. Wild-type mice s.c. vaccinated with OVA/7-acyl lipid A-NPs simultaneously develop robust OVA specific $CD4^+$ and $CD8^+$ T cell responses- Wild-type C57Bl/6 mice were s.c. vaccinated in right flank region with either Empty-NPs, 7-acyl lipid A-NPs, OVA-NPs, OVA/7-acyl lipid A-NPs or OVA/CFA (4-6 mice per group). The approximate dosages of OVA and 7-acyl lipid 7-acyl lipid A (per mouse) were 200 μg and 17 μg, respectively. Fourteen days later, the mice got booster vaccination of similar formulations (with the exception of OVA/CFA group that got OVA/IFA in the second immunization). One week after, draining lymph nodes of vaccinated mice were isolated, pooled and the ELISPOT assay for the determination of IFN-γ secretion was performed (as described in Materials and Methods section). In brief, $1x10^6$ lymphocytes were stimulated with 20 μM of either irrelevant or test peptides for both $CD4^+$ and $CD8^+$ T cells (duplicate wells per stimulation). Names and sequences of peptides used are given in Table 3-1. For all vaccinated mice, a picture of one representative well per each stimulation is shown (A). The background level was measured in wells containing lymphocytes stimulated by the irrelevant peptide. The number of OVA-specific spots was obtained by subtracting the background from the number of spots appearing after OVA peptide stimulation. Results are presented as mean values obtained for duplicate wells± SD. (B) Data are representative of two independent experiments.

* denotes significance between different groups ($p< 0.05$).

Consistent with our previous results (sections 3.3.2 and 3.3.3), co-delivery of OVA and 7-acyl lipid A in PLGA-NPs promoted OVA specific IFN-γ secretion by both $CD4^+$ T cells and $CD8^+$ T cells. Figure 3-8, shows the number of OVA specific IFN-γ secreting $CD4^+$ or $CD8^+$ T cells/million lymphocytes for all the groups. Immunization with either Empty-NPs or 7-acyl lipid A-NPs didn't induce any OVA specific IFN-γ secretion. The highest IFN-γ secretion by OVA specific $CD4^+$ and $CD8^+$ T cells was observed in OVA/7-acyl lipid A-NPs immunized mice, which was significantly higher than what observed in OVA-NPs and OVA/CFA immunized groups ($p < 0.05$).

3.4 Discussion

Designing cancer vaccines capable of inducing robust T cell-mediated immune responses is a primary focus of research in the field of immunotherapy. Another primary focus for immunotherapy is the development of efficient and safe adjuvants, which initiate and control the induction of the appropriate type and magnitude of immune response. The ultimate goal of the current study was to evaluate the efficacy of PLGA-based vaccines in priming antigen specific $CD4^+$ and $CD8^+$ T cell responses. We hypothesized that PLGA-NPs co-encapsulating OVA (as a model antigen) and 7-acyl lipid A (immunostimulatory adjuvant) will be taken up efficiently by DCs both *in vitro* and *in vivo,* resulting in DC maturation/activation and induction of potent T cell responses.

While several previous studies have evaluated the effect of PLGA-NPs on $CD4^+$ T cell functions [14,16,17], there have not been any reports that directly monitored their effects on the activation of antigen specific $CD4^+$ T cells *in vivo*. A primary hallmark of *in vivo*

$CD4^+$ T cell activation is the ability of a trace population of naïve $CD4^+$ T cells to undergo massive clonal expansion after they encounter their cognate antigen. In the current studies, we have employed the DO11.10 adoptive transfer model to directly assess the effect of particulate delivery of OVA together with 7-acyl lipid A on the primary antigen specific $CD4^+$ T cell responses *in vivo*. Using this model, evidence of T cell encounter with the antigen have been observed, as reflected by the clonal expansion of OVA-specific $CD4^+$ T cells following either i.p. or s.c. route of immunization, and the activated surface phenotype ($CD11a^{hi}CD44^{hi}CD62L^{lo}$) of the expanded $CD4^+$ T cells. The ability of 7-acyl lipid A to induce rapid activation and clonal expansion of DO11.10 T cells, is comparable to that reported previously using CFA, lipopolysaccharide (LPS), inflammatory cytokines, DNA microparticles, bacterial flagellin as adjuvants in the same adoptive transfer model [18-22].

The ability of 7-acyl lipid A activated DCs to activate $CD4^+$ T cell response and shape a Th1- biased immune responses has been well described [16,17,23]. However the role of particulate delivery of 7-acyl lipid A in priming $CD8^+$ T cells had not been investigated. In the present study, using OT-1 transgenic mouse model, we showed that targeting DCs with PLGA-NPs co-encapsulating OVA and 7-acyl lipid A dramatically increased the extent of antigen specific primary $CD8^+$ T cell immune stimulation as measured by proliferative response, phenotypic activation and IFN-γ production. These results imply that PLGA-NPs had efficiently delivered the encapsulated antigen into the MHC class I pathway to be processed and cross-presented to the $CD8^+$ T cells. Furthermore, the

presence of 7-acyl lipid A in the same NP formulation has increased the magnitude and /or efficiency of cross-presentation.

Delivering 7-acyl lipid A to DCs likely leads to multiple effects on DCs that may promote cross-presentation. 7-acyl lipid A up-regulates co-stimulatory molecules and induces cytokine secretion by DCs, both of which play pivotal role in T cell activation. Other TLR ligands (such as immunostimulatory sequence (ISS) DNA) may enhance cross-presentation by alternative ways, e.g. inducing the expression of essential components of the class I antigen processing machinery (including TAP and MHC class I molecules) [24], or facilitate the escape of endocytosed antigens to the cytosol [13]. The exact subcellular mechanisms underlying improved cross-presentation with co-encapsulated antigen and 7-acyl lipid A are yet to be elucidated.

The simultaneous induction of robust Th1 and CTL responses is a crucial goal of vaccination. In the current study, we have shown that targeting DCs with OVA/7-acyl lipid A-NPs resulted in robust activation of T cell responses *in vivo*. Activated antigen specific $CD4^+$ and $CD8^+$ T cells were capable of secreting large amounts of IFN-γ upon *ex vivo* stimulation. IFN-γ is the hallmark cytokine of Th1-biased immune responses. Beside its well-known ability to activate various immune cells (such as macrophages, NK cells), IFN-γ up-regulates the expression of multiple components of MHC I and MHC II antigen processing/presentation machineries in DCs [25]. This cross-talk between antigen bearing DCs and IFN-γ secreting T cells could lead to further amplification of vaccine-induced immune responses.

Our results are in agreement with a recent study by Blander *et al* [26], which showed that physical association of TLR4 ligand (LPS) and antigen (OVA) is required for efficient $CD4^+$ T cell activation. Interestingly, co-localization of OVA and LPS in the same phagosome have led to enhanced phagosomal maturation and activation of hydrolytic enzymes that cleave the invariant chain and generate the antigenic peptides, resulting in more efficient presentation on MHC class II molecules [26]. All together, these results highlight the significance of co-delivery of antigen along with adjuvant in the same vaccine formulation for optimal activation of $CD4^+$ T cell responses. Meanwhile, a recent study by Schlosser *et al* [27] has demonstrated that mice immunized with PLGA-NPs co-encapsulating TLR ligand and antigen (OVA) developed stronger CTL responses than mice immunized with a mixture of two NP formulations (loaded separately with antigen or adjuvant). This effect was observed for two TLR ligands (TLR3 ligand, Poly I:C; and TLR9 ligand, CpG) [27]. These findings suggest that may be there is a similar requirement for antigen and adjuvant to be co-localized in the same phagosome for optimal activation of $CD8^+$ T cell responses.

In conclusion, the experiments presented here are the first to study the ability of combining a clinically acceptable vaccine delivery system (PLGA) with novel synthetic lipid A analog (7-acyl lipid A) to prime antigen-specific T cells at the cellular level. Our results demonstrate that, PLGA-NPs represent effective means to deliver protein antigens along with immunomodulators to DCs for the induction of $CD4^+$ and $CD8^+$ antigen specific T cell responses.

3.5 References:

[1] G. Zeng, MHC Class II-Restricted Tumor Antigens Recognized by CD4+ T Cells: New Strategies for Cancer Vaccine Design, J Immunother 24 (2001) 195-204.

[2] G. Parmiani, Melanoma antigens and their recognition by T cells, Keio J Med 50 (2001) 86-90.

[3] F.M. Foss, Immunologic mechanisms of antitumor activity, Semin Oncol 29 (2002) 5-11.

[4] C.J. Kirk, D. Hartigan-O'Connor, B.J. Nickoloff, J.S. Chamberlain, M. Giedlin, L. Aukerman, J.J. Mule, T cell-dependent antitumor immunity mediated by secondary lymphoid tissue chemokine: augmentation of dendritic cell-based immunotherapy, Cancer Res 61 (2001) 2062-70.

[5] M.C. Panelli, E. Wang, V. Monsurro, P. Jin, K. Zavaglia, K. Smith, Y. Ngalame, F.M. Marincola, Vaccination with T cell-defined antigens, Expert Opin Biol Ther 4 (2004) 697-707.

[6] A. Perez-Diez, N.T. Joncker, K. Choi, W.F. Chan, C.C. Anderson, O. Lantz, P. Matzinger, CD4 cells can be more efficient at tumor rejection than CD8 cells, Blood 109 (2007) 5346-54.

[7] T. Kaisho, S. Akira, Toll-like receptors as adjuvant receptors, Biochim Biophys Acta 1589 (2002) 1-13.

[8] T. Kaisho, S. Akira, Regulation of dendritic cell function through toll-like receptors, Curr Mol Med 3 (2003) 759-71.

[9] K. Schwarz, T. Storni, V. Manolova, A. Didierlaurent, J.C. Sirard, P. Rothlisberger, M.F. Bachmann, Role of Toll-like receptors in costimulating cytotoxic T cell responses, Eur J Immunol 33 (2003) 1465-70.

[10] P. Elamanchili, Lutsiak, C., Hamdy, S., Diwan, J., & Samuel, J., Pathogen-mimicking' Nanoparticles for vaccine delivery to dendritic cells, J Immunother (in press).

[11] Y. Ogawa, M. Yamamoto, H. Okada, T. Yashiki, T. Shimamoto, A new technique to efficiently entrap leuprolide acetate into microcapsules of polylactic acid or copoly(lactic/glycolic) acid, Chem Pharm Bull (Tokyo) 36 (1988) 1095-103.

[12] E.R. Kearney, K.A. Pape, D.Y. Loh, M.K. Jenkins, Visualization of peptide-specific T cell immunity and peripheral tolerance induction in vivo, Immunity 1 (1994) 327-39.

[13] S.K. Datta, V. Redecke, K.R. Prilliman, K. Takabayashi, M. Corr, T. Tallant, J. DiDonato, R. Dziarski, S. Akira, S.P. Schoenberger, E. Raz, A subset of Toll-like receptor ligands induces cross-presentation by bone marrow-derived dendritic cells, J Immunol 170 (2003) 4102-10.

[14] P. Elamanchili, C.M. Lutsiak, S. Hamdy, M. Diwan, J. Samuel, "Pathogen-mimicking" nanoparticles for vaccine delivery to dendritic cells, J Immunother 30 (2007) 378-95.

[15] L. Yang, D. Baltimore, Long-term in vivo provision of antigen-specific T cell immunity by programming hematopoietic stem cells, Proc Natl Acad Sci U S A 102 (2005) 4518-23.

[16] C.S. Chong, M. Cao, W.W. Wong, K.P. Fischer, W.R. Addison, G.S. Kwon, D.L. Tyrrell, J. Samuel, Enhancement of T helper type 1 immune responses against hepatitis B

virus core antigen by PLGA nanoparticle vaccine delivery, J Control Release 102 (2005) 85-99.

[17] M.E. Lutsiak, G.S. Kwon, J. Samuel, Biodegradable nanoparticle delivery of a Th2-biased peptide for induction of Th1 immune responses, J Pharm Pharmacol 58 (2006) 739-47.

[18] K.A. Pape, A. Khoruts, A. Mondino, M.K. Jenkins, Inflammatory cytokines enhance the in vivo clonal expansion and differentiation of antigen-activated CD4+ T cells, J Immunol 159 (1997) 591-8.

[19] R. Merica, A. Khoruts, K.A. Pape, R.L. Reinhardt, M.K. Jenkins, Antigen-experienced CD4 T cells display a reduced capacity for clonal expansion in vivo that is imposed by factors present in the immune host, J Immunol 164 (2000) 4551-7.

[20] J. Sun, B. Dirden-Kramer, K. Ito, P.B. Ernst, N. Van Houten, Antigen-specific T cell activation and proliferation during oral tolerance induction, J Immunol 162 (1999) 5868-75.

[21] R.J. Creusot, L.L. Thomsen, C.A. van Wely, P. Topley, J.P. Tite, B.M. Chain, Early commitment of adoptively transferred CD4+ T cells following particle-mediated DNA vaccination: implications for the study of immunomodulation, Vaccine 19 (2001) 1678-87.

[22] S.J. McSorley, B.D. Ehst, Y. Yu, A.T. Gewirtz, Bacterial flagellin is an effective adjuvant for CD4+ T cells in vivo, J Immunol 169 (2002) 3914-9.

[23] K.D. Newman, J. Samuel, G. Kwon, Ovalbumin peptide encapsulated in poly(d,l lactic-co-glycolic acid) microspheres is capable of inducing a T helper type 1 immune response, J Control Release 54 (1998) 49-59.

[24] H.J. Cho, T. Hayashi, S.K. Datta, K. Takabayashi, J.H. Van Uden, A. Horner, M. Corr, E. Raz, IFN-alpha beta promote priming of antigen-specific CD8+ and CD4+ T lymphocytes by immunostimulatory DNA-based vaccines, J Immunol 168 (2002) 4907-13.

[25] K. Schroder, P.J. Hertzog, T. Ravasi, D.A. Hume, Interferon-gamma: an overview of signals, mechanisms and functions, J Leukoc Biol 75 (2004) 163-89.

[26] J.M. Blander, R. Medzhitov, Toll-dependent selection of microbial antigens for presentation by dendritic cells, Nature 440 (2006) 808-12.

[27] E. Schlosser, M. Mueller, S. Fischer, S. Basta, D.H. Busch, B. Gander, M. Groettrup, TLR ligands and antigen need to be coencapsulated into the same biodegradable microsphere for the generation of potent cytotoxic T lymphocyte responses, Vaccine 26 (2008) 1626-37.

Chapter 4

Co-delivery of cancer associated antigens and 7-acyl lipid A in PLGA-NPs induces potent $CD8^+$ T cell mediated anti-tumor immunity

A version of this chapter has been accepted for publication in

Vaccine

Hamdy S, Molavi O, Ma Z, Haddadi A, Alshamsan A, Ghobti Z, EL Hasi S, Samuel J and Lavasanifar A, Faculty of Pharmacy & Pharmaceutical Sciences, University of Alberta, Edmonton, AB, Canada, T6G2N8

and

presented as a poster in 11th Canadian Society for Pharmaceutical Science (CSPS) Symposium Banff, Alberta, May 22-25, 2008

4.1 Introduction

The long term objective of this research is to achieve vaccines based on PLGA-NPs that can induce effective T cell immune responses against cancer. Our research group has recently shown that co-delivery of OVA as model antigen, and 7-acyl lipid A in PLGA-NPs enhances DC maturation and dramatically induces robust OVA specific primary $CD4^+$ and $CD8^+$ T cell proliferative responses [1,2] (& chapter 3). Moreover, vaccinating healthy C57Bl/6 mice with PLGA-NPs co-encapsulating OVA and 7-acyl lipid A dramatically enhanced IFN-γ secretion by both OVA specific $CD4^+$ and $CD8^+$ T cells draining lymph nodes of vaccinated mice. This activation was superior to what we observed in mice immunized with OVA emulsified in CFA, one of the most powerful adjuvants used in animal studies (chapter 3). Consistent with these results, in a recent study by Heit *et al* [3] a single injection of PLGA microparticles co-encapsulating OVA and TLR9 ligand (CpG) efficiently activated OVA-specific T cells and caused complete tumor regression in 80% of animals bearing OVA-expressing B16 melanoma (B16-OVA). These results clearly demonstrate the efficacy of PLGA nano/microparticles in delivering exogenous antigens and adjuvants into DCs and initiating robust T cell responses. However, the vigorous T cell activation can be partially attributed to the fact that chicken OVA is recognized as a foreign antigen (non-self) in mice. As a result, OVA-specific T cells could be easily activated, as they are not subjected to the regulations of central and peripheral tolerance. By contrast, the majority of cancer antigens belong to self. Accordingly, stimulating the immune system against those antigens requires breaking of self-tolerance mechanisms, which is more challenging and difficult to achieve. An elegant study by Belone *et al* [4], had compared the efficacy of

three vaccination strategies (naked DNA, peptide-pulsed DCs or mixture of peptide and the *Escherichia coli* toxin LTR72) using either the foreign antigen OVA or the naturally expressed tumor antigen (TRP2) in the B16-OVA or B16 melanoma models, respectively. They found similar level of CTL activation and tumor protection against B16-OVA melanoma by all the three vaccines that used OVA antigen. However, when TRP2, a self tumor-associated antigen, was employed, all vaccines elicited B16-specific CTLs, but only the TRP2-pulsed DCs were able to protect against B16 melanoma. Two conclusions can be made from these results; 1. The induction of *in vitro* CTL activity doesn't correlate with the *in vivo* anti-tumor activity. 2. Foreign (non-self) antigens used in evaluating immunotherapeutic strategies can overestimate the therapeutic outcome and lead to bias in the validation of vaccine efficacy. In the light of these findings, the purpose of the present study was to rigorously evaluate the efficacy of PLGA-based cancer vaccines using a realistic and clinically relevant tumor antigen, i.e., TRP2.

4.2 Materials and Methods

4.2.1 Reagents

Synthetic 7-acyl lipid A, Mwt., 1955.5 Da was kindly provided by Oncothyreon Inc. (formerly Biomira Inc.), Edmonton, AB, Canada. TRP2 peptide$_{180\text{-}188}$ was purchased from BioSynthesis Inc. (Lewisville, TX, USA). PVA, Mwt., 31,000-50,000 Da was obtained from Sigma Aldrich co. (Oakville, ON, Canada). PLGA co-polymer (monomer ratio 50:50, Mwt., 7000 Da) was purchased from Absorbable Polymers International, (Pelham, AL, USA). Chloroform, methanol, acetonitrile, water (all HPLC grades) were purchased from Fisher Scientific (Fair Lawn, NJ, USA). Murine CD8 isolation kit was purchased

from StemCell Technologies (Vancouver, BC, Canada). Murine IFN-γ ELISPOT kit was purchased from E-Bioscience (San Diego, CA, USA). ELISPOT ninety-six-well MultiScreen™ filter plates was obtained from Millipore (Bedford, MA, USA). AEC (3-amino-9-ethyl carbazole) substrate solution was purchased from BD Biosciences (Mississauga, ON, Canada). DMEM, RPMI media, L-glutamine, and gentamicin were purchased from Gibco-BRL (Burlington, ON, Canada). FCS was obtained from Hyclone Laboratories (Logan, UT, USA). Murine IL-6, IL-2, IFN-γ and TNF-α ELISA kits were purchased from E-Bioscience (San Diego, CA, USA). Murine IL-12 and VEGF ELISA kits were purchased from BD Biosciences (Mississauga, ON, Canada) and R&D Systems (Minneapolis, USA), respectively.

4.2.2 Preparation of PLGA-NPs encapsulating $TRP2_{180-188}$ with or without 7-acyl lipid A

NPs of PLGA containing TRP2 peptide with or without 7-acyl lipid A were prepared by water/oil/water (w/o/w) double emulsion/solvent evaporation method. Briefly, TRP2 peptide was dissolved in 75% acetonitrile in water to make 10 mg/mL solution. From this solution 100 µL was emulsified with PLGA solution in chloroform (300 µL, 50% w/v) using a microtip sonicator (Heat systems Inc., Farmingdale, NY, USA). For the preparation of NPs containing 7-acyl lipid A, 200 µg of 7-acyl lipid A in 100 µL of 1:4 methanol-chloroform mixture was added to the polymer-chloroform solution. The resulting primary emulsion (water/oil) was further emulsified in 2 mL of PVA solution (9% w/v PVA in PBS) by sonication for 45 sec at level 4. The secondary emulsion was added drop-wise into 8 mL of stirring PVA solution. NPs were collected and washed as

previously described in chapter 2. The particle size of the NPs was determined by dynamic light scattering technique using a Zetasizer 3000 (Malvern, UK). Quantification of 7-acyl lipid A content in PLGA-NPs was done by LC-MS as reported previously in chapter 2 [5].

4.2.3 Quantification of encapsulated $TRP2_{180-188}$ in NPs by LC-MS

Establishment of an LC-MS method for the quantification of $TRP2_{180-188}$

LC-MS analysis were performed using a Waters Micromass ZQ 4000 spectrometer, coupled to a Waters 2795 separations module with an autosampler (Milford, MA, USA). The mass spectrometer was operated in positive ionization mode with SIR acquisition. The nebulizer gas was obtained from an in house high purity nitrogen source. The temperature of source was set at 150 °C, and the voltages of the capillary and cone were 3.10 KV and 9 V, respectively. The gas flow of desolvation and the cone were set at 550 and 90 L/h, respectively. Chromatographic separation was achieved using a Waters (Milford, MA, USA) XT_{erra}MSC18 3.5 µm column (2.1×50 mm) as the stationary phase. The mobile phase consisted of 2 solutions; Solution A (acetonitrile) and Solution B (0.05% trifloro acetic acid (TFA)/Water). The mobile phase was delivered at a constant flow rate of 0.2 mL/min. The gradient conditions are shown in Table 4-1. Lansoprazole was used as the I.S. SIR at m/z 1175.2 and 369.9, related to M+H were selected for quantification of TRP2 peptide and the internal standard, respectively (Figure 4-1A). Figure 4-1B shows the SIR chromatograms of internal standard and $TRP2_{180-188}$. The Peak of $TRP2_{180-188}$ was well separated from that of the internal standard in the established chromatographic condition. The retention times of the internal standard and

$TRP2_{180-188}$ were approximately 7 and 8 min, respectively. The analytical run time was 15 mins. The regression analysis was constructed by plotting the peak-area ratio of $TRP2_{180-188}$ to I.S (response factor) versus $TRP2_{180-188}$ concentration (μg/mL). The calibration curve was linear within the range of 1.5 μg-50 μg/mL. The correlation coefficient (r^2) was always greater than 0.99 (Figure 4-1C), indicating a good linearity.

Extraction and quantification of $TRP2_{180-188}$ in PLGA-NPs

Extraction of $TRP2_{180-188}$ from PLGA-NPs was done by dispersing 5 mg of NPs in 300 μL of 85% acetonitrile in H_2O, followed by centrifugation at 15000 × *g* for 15 min. The PVA was precipitated and the supernatant (PLGA + peptide) was transferred into eppendorf tube. The solvent (acetonitrile and H_2O) was evaporated using Thermosavant SpeedVac System. Since the peptide is soluble in methanol (unlike PLGA), the residue was dissolved in 500 μL methanol, followed by centrifugation at 15000 x *g* for 15 mins. The supernatant was then assayed for $TRP2_{180-188}$ by LC-MS. The lowest panel of Figure 4-1A shows the mass spectrum of $TRP2_{180-188}$ after extraction from PLGA-NPs, which implies that intact peptide was successfully incorporated into the NP formulation.

In vitro release of $TRP2_{180-188}$ from PLGA-NPs

Five milligrams of $TRP2_{180-188}$ containing PLGA-NPs were suspended in 1 ml of water in different eppendruf tubes and incubated in a water bath at 37°C under gentle shaking. At each designated time point, three tubes were removed and centrifuged at 15000 x *g* for 10 mins. Extraction and quantification of the remaining amounts of $TRP2_{180-188}$ in the precipitated PLGA-NPs was done by LC-MS (as described above). Percentage of

released $TRP2_{180-188}$ was calculated using the following formula: [(Total amount of $TRP2_{180-188}$ –Remaining amount of $TRP2_{180-188}$ in the)/Total amount of $TRP2_{180-188}$] x100.

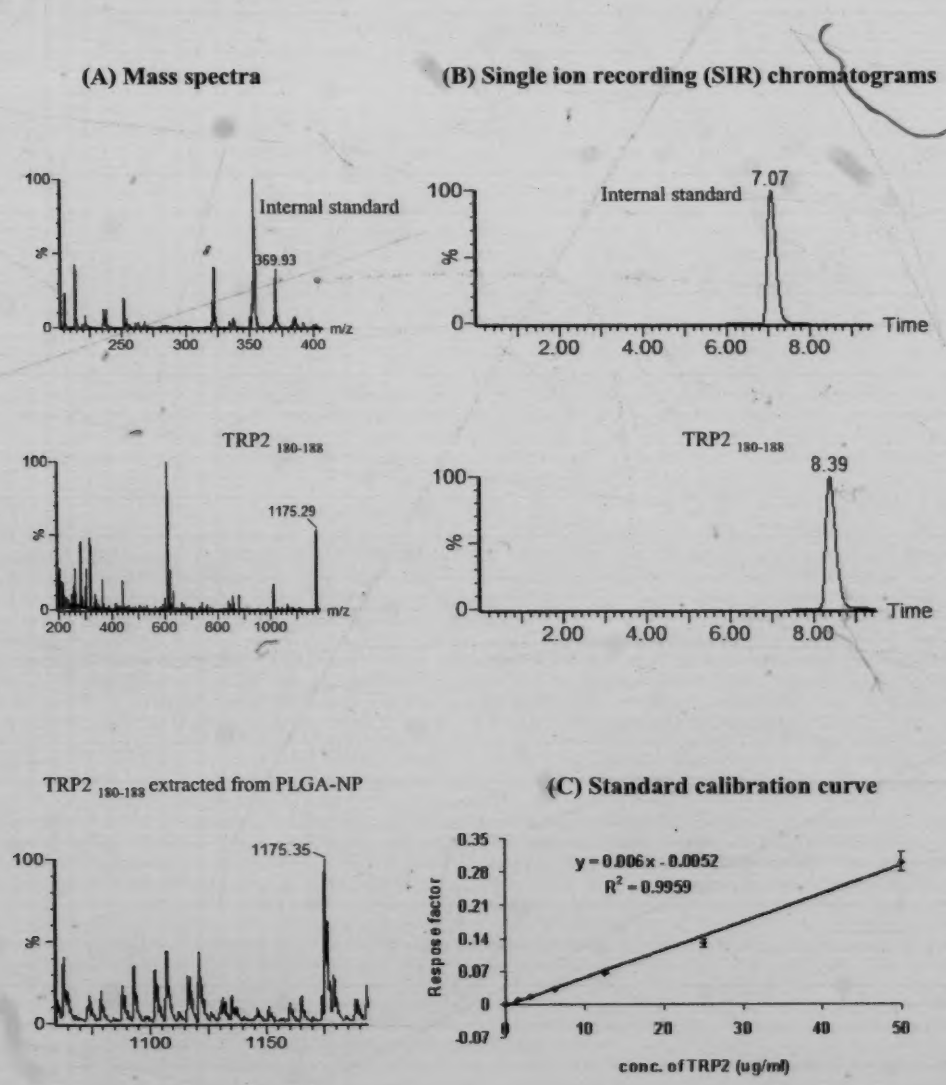

Figure 4-1. LC/MS method for $TRP2_{180-188}$ quantification- (A) Mass spectra of lansoprazole, the internal standard, $TRP2_{180-188}$ solution and $TRP2_{180-188}$ peptide extracted from PLGA-NPs. (B) SIR chromatograms of the I.S and $TRP2_{180-188}$. Gradient conditions are summarized in Table 1. (C) A representative standard curve for $TRP2_{180-188}$ extending from 1.5-50 µg/mL. The calibration curves were constructed by plotting average peak-area ratio of $TRP2_{180-188}$ to the I.S (response factor ± SD) on Y-axis versus $TRP2_{180-188}$ concentration (µg/mL) on X-axis.

Table 4-1. Chromatographic gradient program over LC-MS analysis time (15 min)

Time (mins)	Mobile phase A* %	Mobile phase B** %	Flow rate mL/min	Gradient curve
0	0	100	0.2	1
10	70	30	0.2	5
11	0	100	0.2	1

*Mobile phase A is acetonitrile.
**Mobile phase B is 0.05% TFA/Water.

Standard and stock solutions

The stock solutions were prepared by dissolving 10 mg of $TRP2_{180-188}$ in 1 mL of 75% acetonitrile in water. The stock solution was stored at -20 °C between experiments. The working solution of $TRP2_{180-188}$ was prepared fresh each day by making a 100-fold dilution of the stock solution in methanol. The calibration standards were then prepared by serial dilution of the working solution. The stock solution of the internal standard was prepared by dissolving 10 mg of lansoprazole A in 1 mL methanol, followed by the preparation of a working solution of 100 μg/mL by a further 100-fold dilution of the stock solution. The stock solution of the internal standard was stored at -20 °C between experiments, and the working solution was prepared fresh at each experiment.

4.2.4 Animal studies

Mice

Mice (C57Bl/6) were purchased from the Jackson Laboratory (Bar Harbor, ME, USA). All experiments were performed in accordance to the University of Alberta guidelines for the care and use of laboratory animals. All experiments were performed using 10 to 16 week old male mice.

Normal mice vaccination experiment

The efficacy of our vaccine formulations were first tested on normal C57Bl/6 mice (with no tumor). Animals (5 mice/group) were s.c. vaccinated in right flank region with approximately 10 μg $TRP2_{180-188}$ encapsulated in PLGA-NPs with or without ~17 μg 7-acyl lipid A (abbreviated as TRP2/7-acyl lipid A-NPs and TRP2-NPs, respectively). Control group mice received 10 mg plain PLGA-NPs (Empty-NPs). Eleven days later all mice received similar booster immunization. Seven days after the second immunization, draining lymph nodes and spleens were isolated and the ELISPOT assay was performed (see details below).

Tumor therapy experiment

B16-F10 cells were grown in DMEM supplemented with 10% FCS, 2 mM L-glutamine and 100 IU/mL penicillin/streptomycin in 5% CO_2 atmosphere. At day 0, C57Bl/6 mice were injected s.c. at their upper right flank with 0.1x 10^6 B16-F10 melanoma cells obtained from exponentially growing 90-95% confluent cultures. Three days later (Day 3), animals were randomly assigned to 3 treatment groups (8-10 mice per group). Similar to normal mice vaccination study, the three groups were s.c. vaccinated (in the lower right flank region) with either Empty-NPs, TRP2-NPs or TRP2/7-acyl lipid A-NPs. Animals were given booster immunization with the same formulations at Day 7 and 13. Palpable tumors start to appear between Day 7 and 10. Tumor size was measured with vernier caliper, starting at Day 7 and then every 2-3 days until Day 21. The longest length and the length perpendicular to the longest length were multiplied to obtain the tumor size (area) in mm^2 [6]. Animals were observed every day, and were euthanized when

tumor area exceeded 300 mm^2 or when ulceration of the tumors was observed. On Day 21 all the animals were scarified and draining lymph nodes, spleens and tumors were isolated for further analysis. Weights of individual tumors were reported and used as a tool to calculate the percentage of mice (for each treatment group) that had controlled tumor growth throughout the study, using the following formula: number of the mice that have tumor weight less than 0.3 gram (gm) at Day 21/total number of mice in that group x 100.

Assessment of vaccine-induced immune stimulation

1. ELISPOT assay

For the ELISPOT assay, spleens and draining lymph nodes (from either normal or tumor-bearing mice) were isolated and washed three times in PBS. Lymphocytes (from lymph nodes) were suspended at 1×10^7 cells/mL in complete RPMI media with 1% penicillin–streptomycin, 1% L-glutamine, and 5% FCS. On the other hand, spleenocyte cell suspensions were divided into two portions; first portion was treated by ACK lysis buffer (156 mM NH4Cl, 10 mM KHCO3, 100 μm EDTA) for removal of red blood cells (RBCs). Briefly, 5 mL of ACK lysis buffer was added (per spleen), followed by 1 min incubation at room temperature. Spleenocytes were then washed twice in cold plain RPMI media and re-suspended at 1×10^7 spleenocytes/mL in complete RPMI. Second part of spleenocyte cell suspension underwent $CD8^+$ T cell isolation, using EasySep® mouse CD8 isolation kit according to the manufacturer's instructions. Isolated $CD8^+$ T cells were washed twice in PBS and resuspended at 1×10^7 cells/mL in complete RPMI. Lymph

nodes, spleenocytes and isolated $CD8^+$ T cells were then plated in the pre-coated ELISPOT plates, as described below.

Ninety-six-well MultiScreen™ filter plates were coated overnight at 4°C with 100 µL/well of IFN-γ-specific capture antibody diluted in sterile PBS according to the manufacturer's instructions. After the overnight incubation, the coating antibody solution was decanted from the plates. The plates were washed twice with 200 µL/well PBS and then blocked for 1 hour at room temperature with 200 µL/well of complete RPMI-1640. Plates were then decanted and cells (lymph nodes, spleenocytes or isolated $CD8^+$ T cells) were added into individual wells (in triplicates) in complete RPMI medium at $1x\ 10^6$ cells/well. In addition, using lymphocytes isolated from normal mice (vaccinated from TRP2/7-acyl lipid A-NPs), two additional cell numbers were plated; $0.5x10^6$ and $2x10^6$ cells/well.

Cells were then stimulated by 20 µM of either CD8 irrelevant epitope (SIINFEKL) or positive epitope ($TRP2_{180-188}$). In negative control wells 100 µL/well of complete RPMI media was added (Non-stimulated). The cells were incubated at 37 °C for 18 hour in the presence of 5% CO_2 and then washed three times with 0.05% Tween in PBS (PBS-Tween). The anti-mouse IFN-γ detection antibody was diluted in 1% BSA in PBS according to the manufacturer's instructions. Diluted solution was added at a volume of 100 µL per well. After two hours incubation at room temperature, plates were washed four times with PBS-Tween and incubated for 45 min at room temperature with Streptavidin-HRP. Plates were then washed three times with PBS-Tween followed by

two times wash with PBS. Spots were developed by adding 100 μL/well of freshly prepared AEC substrate solution. Stopping the substrate reaction was done after 20-30 min by washing the plates three times with distilled water. Plates were then dried and spots were counted in a BioReader 3000 (BioSys, Karben, Germany).

2. ELISA

Vaccine-induced alteration in the level of pro-inflammatory cytokines and immuno-suppressive factors in tumor microenvironment was assessed by ELISA. Briefly, isolated tumors were crushed between two slides to form uniform cell suspensions, which were filtered through 70 μm cell strainers and then counted. Tumor supernatants obtained after centrifugation of approximately 20 million tumor cells were analyzed for the level of TNF-α, IL-12, IFN-γ, IL-2, IL-6 and VEGF by ELISA using the commercially available ELISA kits in a 96 well microplate using a microplate reader (Powerwave with KC Junior software; Bio-Tek, Winooski, VT) at OD of 450 nm according to the manufacturer's directions. The minimum detection levels of the cytokines were: 7, 62, 15, 2, 10 and 7.8 pg/mL for TNF-α, IL-12, IFN-γ, IL-2, IL-6 and VEGF, respectively.

Statistical analysis

The significance of differences among groups was analyzed by NOVA followed by the Student-Newman-Keuls post hoc test for multiple comparisons. *P* value of ≤ 0.05 was set for the significance of difference among groups. The statistical analysis was performed with SigmaStat software (Systat Software Inc. San Jose, California, USA).

4.3 Results

4.3.1 Characterization of PLGA-NPs

The mean diameter of NPs ranged between 350-410 nm with a polydispersity below 0.2. The efficiency of the method of $TRP2_{180-188}$ extraction from PLGA-NPs was 87.6%. Based on LC-MS analysis the encapsulation efficiency for $TRP2_{180-188}$ was 5.2±0.6% and the loading was 0.94± 0.11 µg $TRP2_{180-188}$ entrapped per 1 mg dry weight of NPs. The encapsulation efficiency for 7-acyl lipid A was 67.3 ± 6.9 % and the loading was 1.79 ± 0.18 µg 7- acyl lipid A entrapped per 1 mg dry weight of NPs.

As shown in Figure 4-2, the release of $TRP2_{180-188}$ from PLGA-NPs was biphasic. During the first 24 h, an initial burst release phase was observed where approximately 17± 5.7 % of the $TRP2_{180-188}$ was released. After 24 h, a gradual increase in the release was observed until day 30 where a total of 62.5± 3.5 % of the $TRP2_{180-188}$ was liberated into the medium.

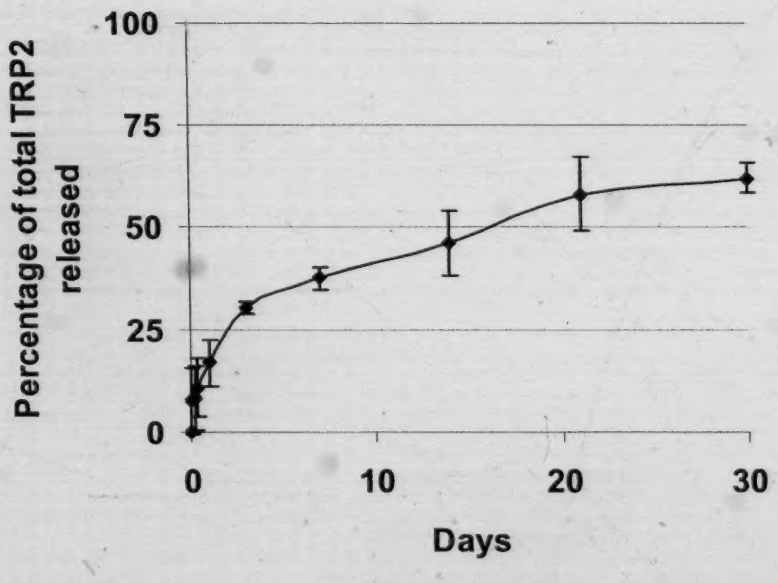

Figure 4-2. In vitro release of $TRP2_{180-188}$ from PLGA-NPs- Five milligrams of $TRP2_{180-188}$ containing PLGA-NPs were suspended in 1 ml of water in different eppendruf tubes and incubated in a water bath at 37°C under gentle shaking. At each designated time point, three tubes were removed and centrifuged at 15000 x *g* for 10 mins. Extraction and quantification of the remaining amounts of $TRP2_{180-188}$ in the precipitated PLGA-NPs was done by LC-MS (as described above). Percentage of released $TRP2_{180-188}$ was calculated using the following formula: [(Total amount of $TRP2_{180-188}$ –Remaining amount of $TRP2_{180-188}$ in the)/Total amount of $TRP2_{180-188}$] x100. All samples were performed in triplicates and the error bars represent the standard deviation.

4.3.2 Co-delivery of $TRP2_{180-188}$ and 7-acyl lipid A in PLGA-NPs induces IFN-γ secretion by TRP2-specific $CD8^+$ T cells in lymph nodes and spleens of the vaccinated mice

Despite the low encapsulated levels of $TRP2_{180-188}$ in PLGA-NPs, we were interested to see whether vaccination with such low amount of the peptide (~10 μg) will induce antigen specific $CD8^+$ T cell activation in healthy C57BL/6 mice. In this experiment, wild-type C57Bl/6 mice were vaccinated twice (11 days apart) and the induction of IFN-γ producing $CD8^+$ T cells was investigated by a single-cell, *ex vivo* ELISPOT assay. In the beginning, we performed a titration study using lymphocytes from the test group (TRP2/7-acyl lipid A-NPs immunized mice) to optimize cell number per well, that gives the highest number of antigen specific T cells and lowest background in wells stimulated with medium or irrelevant peptide. The result of this titration study is shown in Figure 4-3A. Actual number of spots/well ± SD is presented in the bar graph in the right panel of Figure 4-3A. Number of IFN-γ secreting antigen specific T cells increased as the number of lymphocyte/well increased. When we used $0.5x10^6$ lymphocytes/well, the number of antigen specific T cells was relatively low. With $1x10^6$ lymphocytes/well, there was a clear increase in the number of IFN-γ secreting cells with acceptable background. However, the background was very high when we used $2x10^6$ lymphocytes/well. Based on these observations, we concluded that the optimum cell number per well is $1x10^6$ lymphocytes.

Figure 4-3B, shows the number of IFN-γ secreting cells per million lymphocytes for the three groups tested. The actual number of spots per well± SD is presented in the bar

graph in the lower panel. Immunization with Empty-NPs did not induce any measurable amount of IFN-γ. Immunization with both TRP2-NPs and TRP2/7-acyl lipid A-NPs induced comparable numbers of INF-γ secreting T cells (113.5± 5 and 145.6± 10, respectively). However, TRP2/7-acyl lipid A-NPs immunized group induced higher levels of IFN-γ secretion as evidenced by the higher density of the spots (Figure 4-3B).

The isolated spleens were treated using either ACK lysis buffer that only removes RBCs or negative selection of only $CD8^+$ T cells. Relatively high background was observed in the negative control wells of ACK-lysed spleens of TRP2/7-acyl lipid A-NPs immunized mice (Figure 4-3C). However, when only $CD8^+$ T cells were plated, the background level dropped almost to zero (Figure 4-3D). The actual number of spots/well± SD is presented in the bar graph in the lower panels in Figure 4-3C and 4-3D. Mice immunized with TRP2/7-acyl lipid A-NPs had significantly high numbers of IFN-γ producing TRP2 specific $CD8^+$ T cells, compared to Empty-NPs immunized mice (60-fold and 65-fold in Figure 4-3C and 4-3D, respectively). Unlike lymph nodes, where immunization with either TRP2-NPs or TRP2/7-acyl lipid A-NPs gave comparable number of TRP2 specific IFN-γ secreting $CD8^+$ T cells, in spleens co-delivery of 7-acyl lipid A along with TRP2 in the same NP formulation led to 3 and 12 fold increase in the number of TRP2 specific IFN-γ secreting $CD8^+$ T cells (compared to TRP2-NPs) using either ACK lysed spleens (Figure 4-3C) or isolated $CD8^+$ T cells (Figure 4-3D), respectively.

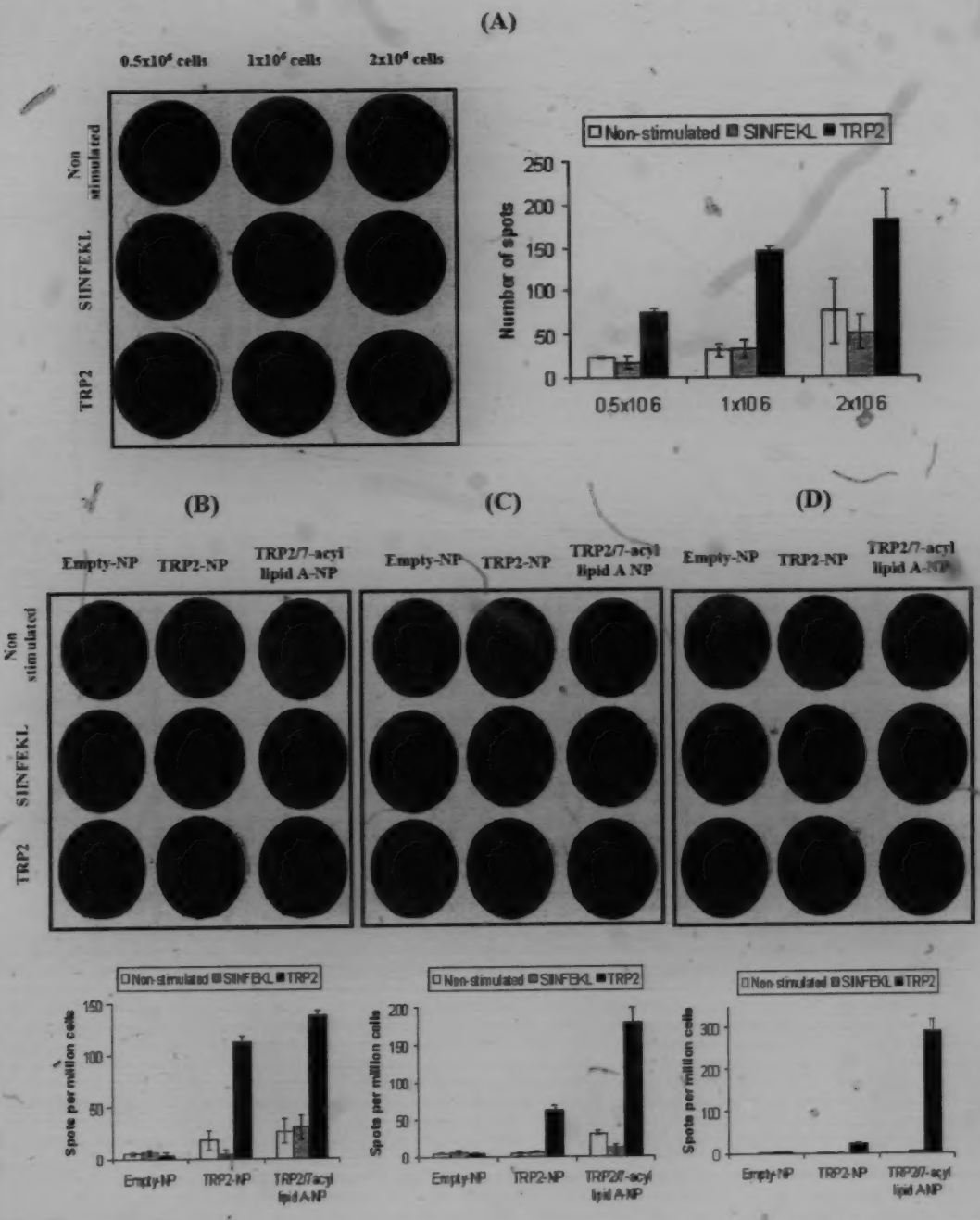
(A)
0.5x10⁶ cells
1x10⁶ cells
2x10⁶ cells
Non stimulated
SINFEKL
TRP2
Non-stimulated SINFEKL TRP2
Number of spots
250
200
150
100
50
0
0.5x106
1x106
2x106
(B)
(C)
(D)
Empty-NP
TRP2-NP
TRP2/7-acyl lipid A-NP
Non stimulated
SINFEKL
TRP2
Non-stimulated SINFEKL TRP2
Spots per million cells
150
100
50
0
200
150
100
50
0
300
200
100
0
Empty-NP
TRP2-NP
TRP2/7-acyl lipid A-NP

Figure 4-3. Vaccination of healthy mice with $TRP2_{180-188}$ containing NPs induces IFN-γ secretion by TRP2-specific $CD8^+$ T cells in lymph nodes and spleens of the vaccinated mice- C57Bl/6 mice were s.c. vaccinated in right flank region with approximately 10 μg $TRP2_{180-188}$ peptide encapsulated in PLGA-NPs with or without ~17 μg 7-acyl lipid A (TRP2/7-acyl lipid A-NPs and TRP2-NPs, respectively). Control group mice received Empty-NPs. Eleven days later all mice received similar booster immunization. Seven days after the second immunization, draining lymph nodes and spleens were isolated and the ELISPOT assay was performed (as described in text). IFN-γ secretion was measured in the vaccinated groups as evidenced by the number of spots/ million cells after overnight stimulation with either media alone (Non-stimulated) or 20 μM of either CD8 irrelevant peptide (SIINFEKL) or test peptide ($TRP2_{180-188}$). (A) Lymphocytes isolated from TRP2/7-acyl lipid A-NPs immunized group were used for optimization of cell numbers/well. Numbers of spots per different cell numbers/well are shown in the bar graph to the right side. Using one million cells/well, IFN-γ secretion was assessed in (B) lymph nodes (C-D) and spleens of the vaccinated mice. Isolated spleenocytes were either treated with ACK lysis buffer to lyse red blood cells (C). Alternatively, $CD8^+$ T cells were isolated from spleens using $CD8^+$ negative isolation kit (D). Numbers of spots/million cells for different treatment groups are shown in the bar graphs below. The values in those graphs are averages of triplicate wells± S.D. Data shown are representative of three independent experiments that gave similar results.

4.3.3 Co-delivery of $TRP2_{180-188}$ and 7-acyl lipid A in PLGA-NPs induced potent therapeutic anti-tumor immunity

Tumor growth and size measurements

Three s.c. injections of TRP2-NPs appeared to slow down the growth of the tumors compared to what observed in the Empty-NPs immunized group (Figure 4-4A), although the difference between average tumor sizes of the two groups was not statistically different. Co-delivery of 7-acyl lipid A together with $TRP2_{180-188}$ in the same NP formulation also slowed down tumor development compared to Empty-NPs group ($p< 0.05$ in Day 17 and 20). Although there was no statistical difference between TRP2-NP and TRP2/7-acyl lipid A-NP immunized groups, the average tumor size of animals immunized with TRP2/7-acyl lipid A-NPs were almost half the average size obtained in TRP2-NPs immunized animals at all times tested. Large intra-group variability might have impaired the significance of difference for results obtained from these two groups. Conducting the experiment with higher number of mice is needed to clarify the difference between the treatment groups further.

Number of mice per vaccination group ranged from 8-10, with 8, 9 and 10 mice immunized with Empty-NPs, TRP2-NPs and TRP2/7-acyl lipid A-NPs, respectively. Whereas all the 10 mice immunized with TRP2/7-acyl lipid A-NPs have survived until the end point of the study (Day 21), one animal from both Empty-NPs and TRP2-NPs groups had to be euthanized due to large tumor growth.

Tumor weight measurements

After 21 days from tumor cell injections, the mice were sacrificed, tumors were isolated from each mouse and weighted separately. Results are presented in Figure 4-4B as individual tumor weights (in gm) for all the mice that survived until the endpoint of the study (7, 8 and 10 mice for Empty-NPs, TRP2-NPs and TRP2/7-acyl lipid A-NPs immunized groups, respectively). In the group immunized with Empty-NPs, all the animals developed large tumors (>0.3 gm), with the exception of only one mouse that had a smaller tumor (~0.1 gm). On the other hand, among the 8 mice in the TRP2-NPs immunized group, only 3 mice developed tumors >0.3 gm. Co-delivery of 7-acyl lipid A with $TRP2_{180-188}$ in PLGA-NPs decreased the number of mice that develop >0.3 gm tumors to only one (out of 10 mice). Figure 4-4C illustrates the percentage of mice that had tumor weights <0.3 gm for each treatment group averaged from two independent studies showing similar results. Controlled tumor growth was observed in 16, 36 and 85% of animals immunized with Empty-NPs, TRP2-NPs and TRP2/7-acyl lipid A-NPs, respectively. Pictures of 3 mice representative from each treatment group are shown in Figure 4-4D.

(A)

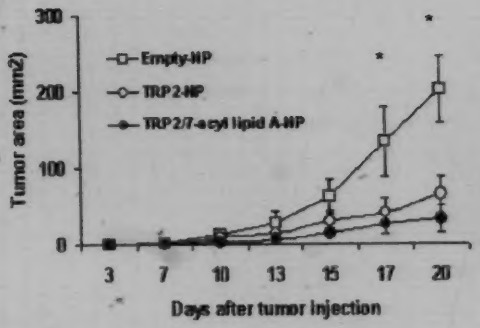
Empty-NP
TRP2-NP
TRP2/7-acyl lipid A-NP
Tumor area (mm2)
300
200
100
0
3
7
10
13
15
17
20
Days after tumor injection
*
*

(B)

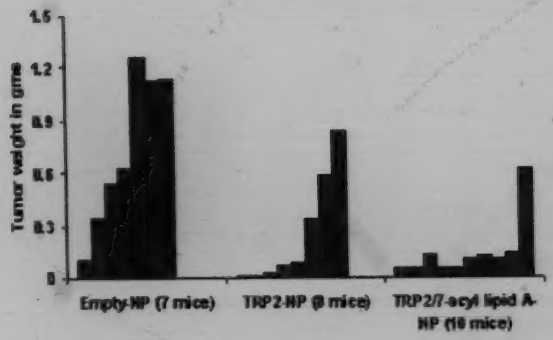
Tumor weight in gms
1.5
1.2
0.9
0.6
0.3
0
Empty-NP (7 mice)
TRP2-NP (8 mice)
TRP2/7-acyl lipid A-NP (10 mice)

(C)

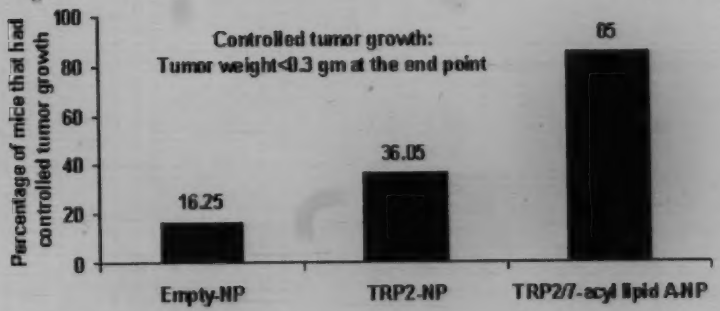
Percentage of mice that had controlled tumor growth
100
80
60
40
20
0
Controlled tumor growth:
Tumor weight<0.3 gm at the end point
16.25
36.05
85
Empty-NP
TRP2-NP
TRP2/7-acyl lipid A-NP

(D)

Empty-NP
TRP2-NP
TRP2/7-acyl lipid A-NP

Figure 4-4. Therapeutic anti-tumor immunity in mice vaccinated with $TRP2_{180-188}$ containing NPs- C57Bl/6 mice were injected s.c. at their upper right flank with 0.1×10^6 B16-F10 melanoma cells (Day 0). Three days later, animals were randomly assigned to 3 treatment groups (8-10 mice per group). Similar to normal mice vaccination study (Figure 4-3), the three groups were s.c. vaccinated (in the lower right flank region) with either Empty-NPs, TRP2-NPs or TRP2/7-acyl lipid A-NPs. Animals were given booster immunization with the same formulations at Day 7 and 13. Tumor size was measured with vernier caliper every 2-3 days. The longest length and the length perpendicular to it were multiplied to obtain the tumor area in mm^2. The mean tumor area ± standard error (S.E) for each group was plotted versus time (A). * indicates significant differences ($p<0.05$) in tumor area for mice immunized with TRP2/7-acyl lipid A-NPs, compared with Empty-NPs immunized mice. On Day 21 animals were scarified and tumors were isolated and weighted separately. Tumor weights of individual mice for each vaccination group are shown in (B). The experiment was repeated one more time, and similar results were obtained. For each treatment group, the average percentage of mice that had tumor weights less than 0.3 gm at the endpoint of the study (Day 21) is shown in (C). Pictures of representative mice in each group at the endpoint of the study are shown in (D). Arrows indicate the position of tumors.

Ex-vivo detection of TRP2-specific $CD8^+$ T cells

To examine the underlying mechanism behind controlled tumor development in TRP2/7-acyl lipid A-NP immunized mice, we have isolated lymph nodes and spleens of all the mice and used ELISPOT assay to check the ability of TRP2 specific $CD8^+$ T cells to secrete of INF-γ following *in vitro* stimulation. Immunization with Empty-NPs did not induce any measurable amount of IFN-γ either in draining lymph nodes (Figure 4-5A) or spleens (Figure 4-5B and 4-5C). On the other hand, among different treatments, mice immunized with TRP2-NPs develop strong antigen specific response in the draining lymph nodes, as evidenced by higher number of INF-γ secreting cells compared to TRP2/7-acyl lipid A-NPs immunized group (141.5± 10.8 *vs* 107.25± 8.5) ($p<0.05$, ANOVA). In contrast, analysis of spleens either by ACK lysis (Figure 4-5B) or by $CD8^+$ T cell isolation (Figure 4-5C) revealed superior TRP2 specific responses in the mice immunized with TRP2/7-acyl lipid A-NPs compared to TRP2-NPs. Consistent with our observation in the normal mice studies, immunization with TRP2/7-acyl lipid A-NPs induced high level of non-specific IFN-γ secretion both in draining lymph nodes (Figure 4-5A) or in spleenocytes treated with ACK lysis buffer (Figure 4-5B). Plating pure $CD8^+$ T cell population had eliminated any non-specific INF-γ secretion (Figure 4-5C). Average number of spots ± SD (n=3) are presented in the bar graphs on the right panel of Figure 4-5A (for draining lymph node) and in the lower panels of Figure 4-5B and 4-5C (for spleens).

(A)

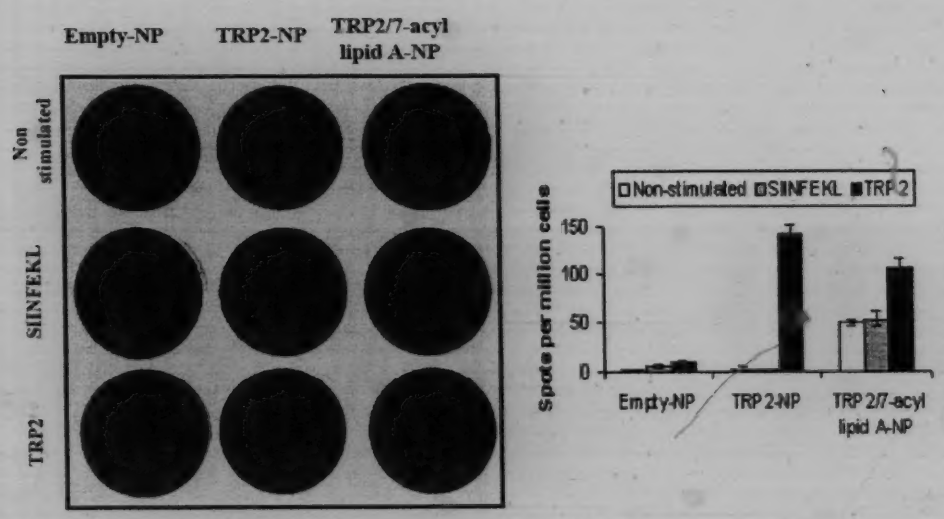
Empty-NP
TRP2-NP
TRP2/7-acyl lipid A-NP
Non stimulated
SIINFEKL
TRP2
Non-stimulated SIINFEKL TRP2
Spots per million cells
150
100
50
0
Empty-NP
TRP2-NP
TRP2/7-acyl lipid A-NP

(B)

(C)

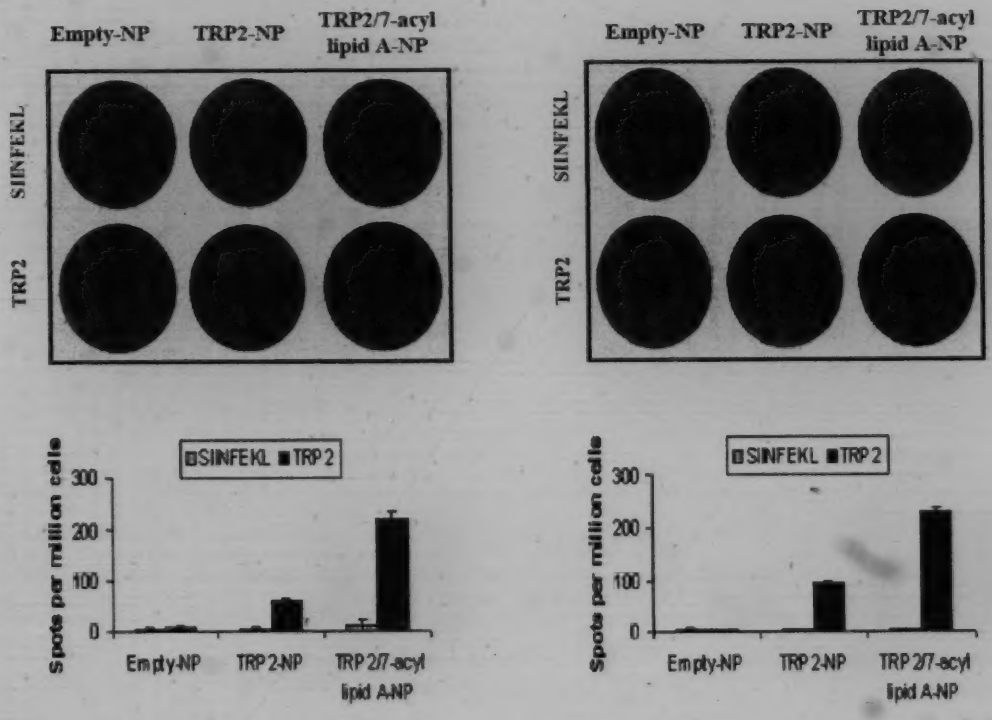
Empty-NP
TRP2-NP
TRP2/7-acyl lipid A-NP
SIINFEKL
TRP2
SIINFEKL TRP2
Spots per million cells
300
200
100
0
Empty-NP
TRP2-NP
TRP2/7-acyl lipid A-NP

Figure 4-5. *Ex-vivo* detection of IFN-γ secretion by $TRP2_{180-188}$ specific $CD8^+$ T cells in lymph nodes and spleen of the tumor-bearing vaccinated mice- C57Bl/6 mice were challenged with melanoma cells and vaccinated as described in the text and in Figure 4-4. At Day 21, animals were scarified and ELISPOT assay was performed (as described in text and in Figure 4-3) to assess IFN-γ secretion in the (A) draining lymph nodes, and (B and C) and spleen. Similar to Figure 4-3, spleens were handled by two different ways; spleenocytes were either treated with ACK lysis buffer to lyse red blood cells (B). Alternatively, $CD8^+$ T cells were isolated from spleens using $CD8^+$ negative isolation kit (C). Numbers of spots per million cells are presented in bar graphs. The values in those graphs are averages of triplicate wells ± S.D. Data shown are representative of two independent experiments that gave similar results.

Vaccine-induced alteration in the level of pro-inflammatory cytokines and immuno-suppressive factors in tumor microenvironment

Activation of antigen specific $CD8^+$ T cells within lymph nodes and/or spleens may not be enough for complete tumor immunity, as the tumor suppressive microenvironment may hinder migration of antigen specific activated T cells into the tumor site or interfere with their anti-tumor activity. So in order to carefully evaluate the effect of our vaccine formulations, it was crucial to detect the level of various immuno-stimulatory versus immuno-suppressive cytokines in the tumor microenvironmentl. Our results showed that immunization with TRP2-NPs slightly increased the level of IFN-γ, TNF-α, IL-6 and IL-2 ($p< 0.05$ compared to Empty-NPs). Co-delivery 7-acyl lipid A along with $TRP2_{180-188}$ in the same NP formulation resulted in significantly higher levels of all pro-inflammatory, Th1-related cytokines tested, including IFN-γ, TNF-α, IL-2, IL-6, and IL-12. More importantly, immunization with TRP2/7-acyl lipid A-NPs decreased the level of VEGF.

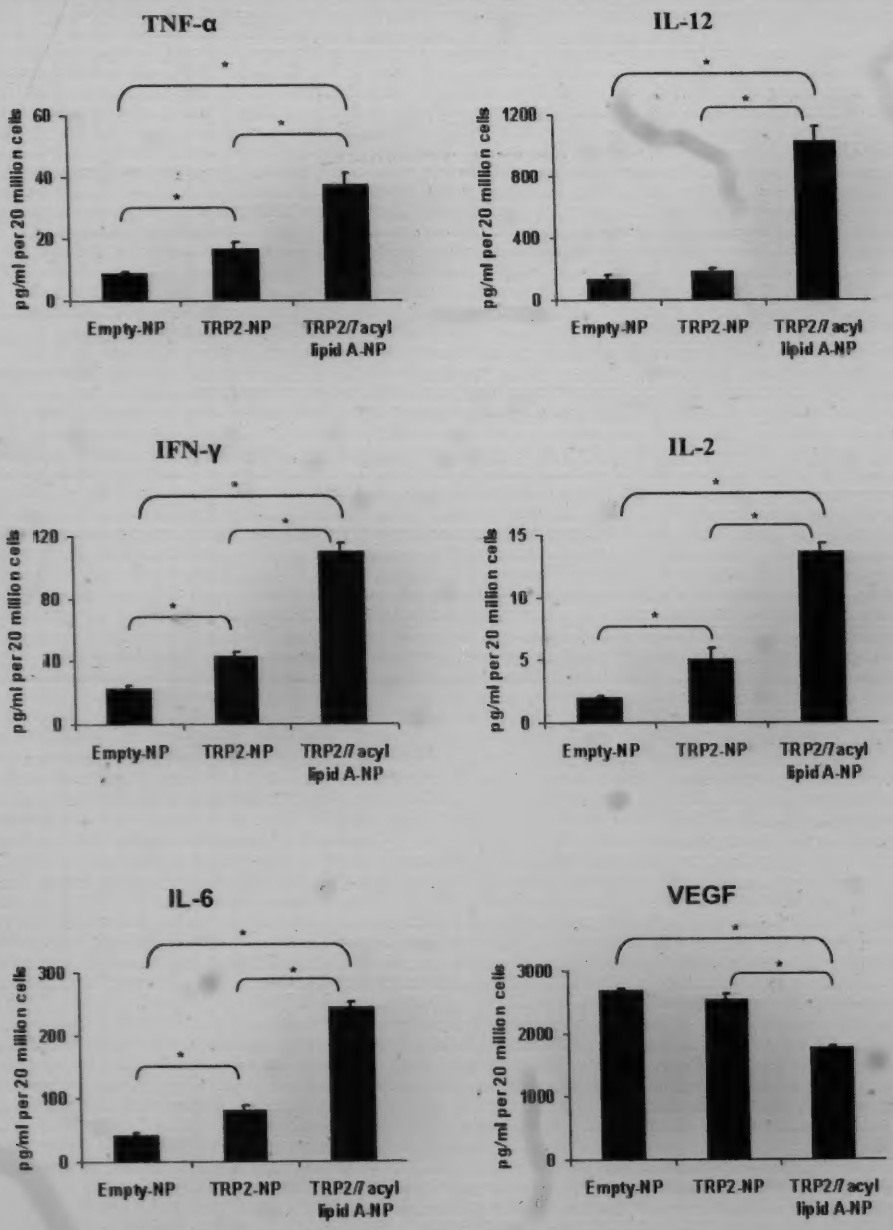

Figure 4-6. Assessment of the level of pro-inflammatory cytokines and immuno-suppressive factors in tumor microenvironment- C57Bl/6 mice were challenged with melanoma cells and vaccinated as described in the text and in Figure 3. At Day 21, animals were scarified; tumors were isolated and crushed between two slides to form uniform cell suspension, which were counted and filtered through 70 μm cell strainers. Tumor supernatants were analyzed for the level of TNF-α, IL-12, IFN-γ, IL-2, IL-6 and VEGF by ELISA. Results are presented as amount of cytokine (pg/mL) per 20 million tumor cells. Each bar represents the mean of triplicate wells± S.D. * indicates significant difference between group *($p<0.05$)*.

4.4 Discussion

Induction of potent, specific and lasting T cell responses as well as reversal of immunosuppressive network in the tumor microenvironment are two major challenges in the development of efficacious cancer vaccine strategies. Our objective was to evaluate the potential of PLGA-based cancer vaccine formulations for meeting those challenges in a reliable and realistic tumor model. Murine melanoma B16 is a very aggressive and rapidly growing tumor. These B16 cells possess extensive defects in their MHC class I antigen-processing pathway. As a result, they express very low amounts of MHC I molecules on their surface [7]. Because of their poor immunogenicity and aggressiveness, B16 melanoma represents a challenging tumor model for developing T cell-based immunotherapeutic responses. Despite its poor immunogenicity, B16 contains antigens capable of activating a specific CTL response. Some of melanoma differentiation antigens include MART-1, gp100, tyrosinase, TRP1, and TRP2 [8]. Among those antigens, one epitope of TRP2 ($TRP2_{180\text{-}188}$) is of special interest. Several research groups have shown strong correlation between the presence of $TRP2_{180\text{-}188}$ specific T cells and tumor regression [9-13]. For example, a combination therapy of anti–cytotoxic T lymphocyte antigen (CTLA)-4 monoclonal antibody and GM-CSF producing B16 melanoma vaccine revealed that successfully treated mice had elevated level (1.7%) of $TRP2_{180\text{-}188}$ specific T cells circulating in blood [14]. Other studies showed that adoptive transfer of TRP-$2_{180\text{–}188}$-specific T cells into C57BL/6 mice reduced the number of experimentally-induced B16 lung metastases [15]. Interestingly, $TRP2_{180\text{-}188}$ can bind both human HLA-A*0201 and murine MHC class I molecule H2-K^b making it an attractive model antigen that is very relevant to human use.

$TRP2_{180-188}$ was combined with TLR ligands in a wide variety of melanoma immunotherapeutic strategies [16-19]. Development of efficient methods for quantitative analysis of $TRP2_{180-188}$ and TLR ligands in a given vaccine is an essential requirement for better characterization and optimization of different aspects of the vaccine formulation e.g. encapsulation efficiency, loading and release pattern. We have recently developed a quick, sensitive and reliable LC-MS-based method for the quantification of lipid A analogues in PLGA-NPs (chapter 2). Such method had overcome all the problems associated with HPLC analysis of lipid A compounds (e.g, poor UV absorption and the need for pre-column derivatization) [5]. In the current study, we described another LC-MS-based method for the quantification of $TRP2_{180-188}$ encapsulated in PLGA-NPs (Figure 4-1 and Table 4-1). Conventional HPLC analysis of $TRP2_{180-188}$ is feasible and not as problematic as that of lipid A compounds. However, LC-MS is preferred due to quick analysis time and high sensitivity.

Our results showed that immunization of normal mice with PLGA-NPs encapsulating 10 μg of $TRP2_{180-188}$ with or without 7-acyl lipid A (TRP2/7-acyl lipid A-NPs and TRP2-NPs, respectively) activated robust TRP2 specific $CD8^+$ T cell responses in the draining lymph nodes and spleen of immunized mice and break self tolerance to TRP2 peptide. Our next challenge was to evaluate the efficacy of our vaccination strategy in tumor-bearing mice. As described in the Methods section, therapeutic immunization started three days after s.c. inoculation of 10^5 B16 melanoma cells. Although the tumors were not palpable at this stage (Day 3), previous studies have shown that 24 hours after s.c. tumor implantation, B16 cells were clearly visible at the site of injection and already

started to proliferate (several mitosis) [20]. Our data showed a remarkable reduction in the growth of tumor in the mice immunized with either TRP2-NPs or TRP2/7-acyl lipid A-NPs as evidenced by decreased tumor area (Figure 4-4A) and weight (Figure 4-4B), compared to the control group (Empty-NPs immunized mice). Due to large intra-group variability, we couldn't observe significant differences in tumor size/weights between the two test groups (TRP2-NPs and TRP2/7-acyl lipid A-NPs). However, there were several clues demonstrating the superior therapeutic effect of TRP2/7-acyl lipid A-NPs over TRP2-NPs; 1. The average tumor size of animals immunized with TRP2/7-acyl lipid A-NPs were almost half of the average tumor size obtained in TRP2-NPs immunized animals at all times tested (Figure 4-4A). 2. None of the mice in the TRP2/7-acyl lipid A NPs immunized group had reached the morbid state, where 11 % of the TRP2-NPs group had to be euthanized before the end of the study. 3. More importantly, 85% of animals immunized with TRP2/7-acyl lipid A-NPs had controlled tumor growth compared to 36% in the TRP2-NPs immunized group (Figure 4-4C).

Data obtained from *ex vivo* analysis of antigen specific $CD8^+$ T cell activation in lymph nodes and spleens of the tumor bearing mice (Figure 4-5) was consistent to what we previously observed in healthy mice study (Figure 4-3). For instance, immunization with either TRP2-NPs or TRP2/7-acyl lipid A-NPs overcame self-tolerance mechanisms and activated robust TRP2-specific $CD8^+$ T cell responses. In the TRP2-NPs immunized group, higher number of the activated $CD8^+$ T cells were found in the draining lymph nodes (Figure 4-5A), compared to spleens (Figure 4-5B and 4-5C). The opposite pattern was observed in the TRP2/7-acyl lipid A-NP immunized group, where activated $CD8^+$ T

cells were found in higher numbers in the spleens (Figure 4-5B and 4-5C), compared to lymph node (Figure 4-5A). This observation may imply that activated $CD8^+$ T cells in the TRP2/7-acyl lipid A-NPs immunized group have acquired better migratory capacity and were able to leave the lymph node and enter the spleen through the blood stream. Such T cells may also have better accessibility to the tumor site. Finally, we have noticed that s.c immunization with PLGA-NPs co-encapsulating antigens and 7-acyl lipid A always induced strong inflammatory response at the site of injection and in the draining lymph nodes (unpublished observation). In the ELISPOT assay, this inflammation could cause relatively high background readings in the wells that have no stimulation or well stimulated with the irrelevant CD8 peptide (Figure 4-3C and 4-5B), probably due to the non-specific IFN-γ secretion by innate immune cells in those wells. This background was eliminated when pure $CD8^+$ T cells were plated (Figure 4-3D & 4-5C).

B16 melanoma exhibit severe impairment in multiple components of MHC class I antigen processing machinery, including TAP, the proteasome subunits LMP2, LMP7, and LMP10, PA28α and -β, and the chaperone tapasin [7]. Down regulations or loss of expression and/or functions of those components result in the reduction or loss of MHC class I surface expression, which often leads to immune escape of the tumor cells. Interestingly, earlier studies have shown that all these defects could be corrected by the administration of IFN-γ, which induces the expression of multiple components of the MHC class I antigen processing machinery, and ultimately enhances the surface expression of MHC class I [7]. In the present study, the induction of IFN-γ secretion by host immune cells may have great impact on the success of our vaccination strategy. The

elevated level of IFN-γ secretion (either by antigen specific $CD8^+$ T cells or innate cells) could up-regulate MHC class I surface expression on B16 tumor cells, resulting in immune recognition and increased lysis of tumor cells by CTLs.

The immunosuppressive environment around the tumor is one of the major elements of compromised anti-tumor immune responses (reviewed in [21-23]). Several lines of evidence indicate that dominant immunosuppressive cytokines in the tumor microenvironment e.g IL-10, TGF-β, and VEGF, significantly inhibit DC maturation/activation, leading to preferential activation of Treg cells on the expense of anti-tumor effector T cells [24-26]. One of the most remarkable finding of our current study is the ability of our vaccine formulation (TRP2/7-acyl lipid A-NPs) to shift the balance at the tumor microenvironment towards immune stimulation, as evidenced by the increase in the level of pro-inflammatory/Th1-biased cytokines (IL-2, IL-6, IL-12, TNF-α and IFN-γ) and the decrease in the level of the immunosuppressant VEGF (Figure 4-6). These results imply that our vaccine is able to provide immune stimulation and rescue impaired DCs from tumor-induced immune suppression.

In conclusion, our results validated the potential of PLGA-based cancer vaccines to break self-tolerance against caner antigen, induce potent and specific anti-tumor T cell responses with no concomitant autoimmunity, activate IFN-γ secretion by antigen specific $CD8^+$ T cells as well as innate immune cells and finally, reverse the immunosuppressive network in the tumor microenvironment. It also highlights the immuostimulatory properties of 7-acyl lipid A as a novel adjuvant can potentially serve

as a powerful companion to antigens in vaccine formulation. To our knowledge, this is the first report showing that co-delivery of a real cancer antigen along with TLR ligand in PLGA-NPs could induce such effects.

4.5 References

[1] P. Elamanchili, C.M. Lutsiak, S. Hamdy, M. Diwan, J. Samuel, "Pathogen-mimicking" nanoparticles for vaccine delivery to dendritic cells, J Immunother (1997) 30 (2007) 378-95.

[2] S. Hamdy, P. Elamanchili, A. Alshamsan, O. Molavi, T. Satou, J. Samuel, Enhanced antigen-specific primary CD4+ and CD8+ responses by codelivery of ovalbumin and toll-like receptor ligand monophosphoryl lipid A in poly(D,L-lactic-co-glycolic acid) nanoparticles, J Biomed Mater Res A 81 (2007) 652-62.

[3] A. Heit, F. Schmitz, T. Haas, D.H. Busch, H. Wagner, Antigen co-encapsulated with adjuvants efficiently drive protective T cell immunity, Eur J Immunol 37 (2007) 2063-74.

[4] M. Bellone, D. Cantarella, P. Castiglioni, M.C. Crosti, A. Ronchetti, M. Moro, M.P. Garancini, G. Casorati, P. Dellabona, Relevance of the tumor antigen in the validation of three vaccination strategies for melanoma, J Immunol 165 (2000) 2651-6.

[5] S. Hamdy, A. Haddadi, V. Somayaji, D. Ruan, J. Samuel, Pharmaceutical analysis of synthetic lipid A-based vaccine adjuvants in poly (D,L-lactic-co-glycolic acid) nanoparticle formulations, J Pharm Biomed Anal 44 (2007) 914-23.

[6] K. Zaks, M. Jordan, A. Guth, K. Sellins, R. Kedl, A. Izzo, C. Bosio, S. Dow, Efficient immunization and cross-priming by vaccine adjuvants containing TLR3 or TLR9 agonists complexed to cationic liposomes, J Immunol 176 (2006) 7335-45.

[7] B. Seliger, U. Wollscheid, F. Momburg, T. Blankenstein, C. Huber, Characterization of the major histocompatibility complex class I deficiencies in B16 melanoma cells, Cancer Res 61 (2001) 1095-9.

[8] A.F. Kirkin, K. Dzhandzhugazyan, J. Zeuthen, Melanoma-associated antigens recognized by cytotoxic T lymphocytes, Apmis 106 (1998) 665-79.

[9] H.T. Khong, S.A. Rosenberg, Pre-existing immunity to tyrosinase-related protein (TRP)-2, a new TRP-2 isoform, and the NY-ESO-1 melanoma antigen in a patient with a dramatic response to immunotherapy, J Immunol 168 (2002) 951-6.

[10] G. Liu, H.T. Khong, C.J. Wheeler, J.S. Yu, K.L. Black, H. Ying, Molecular and functional analysis of tyrosinase-related protein (TRP)-2 as a cytotoxic T lymphocyte target in patients with malignant glioma, J Immunother 26 (2003) 301-12.

[11] S.A. Rosenberg, J.C. Yang, D.J. Schwartzentruber, P. Hwu, F.M. Marincola, S.L. Topalian, N.P. Restifo, M.E. Dudley, S.L. Schwarz, P.J. Spiess, J.R. Wunderlich, M.R. Parkhurst, Y. Kawakami, C.A. Seipp, J.H. Einhorn, D.E. White, Immunologic and therapeutic evaluation of a synthetic peptide vaccine for the treatment of patients with metastatic melanoma, Nat Med 4 (1998) 321-7.

[12] J. Wang, S. Saffold, X. Cao, J. Krauss, W. Chen, Eliciting T cell immunity against poorly immunogenic tumors by immunization with dendritic cell-tumor fusion vaccines, J Immunol 161 (1998) 5516-24.

[13] R.F. Wang, S.L. Johnston, S. Southwood, A. Sette, S.A. Rosenberg, Recognition of an antigenic peptide derived from tyrosinase-related protein-2 by CTL in the context of HLA-A31 and -A33, J Immunol 160 (1998) 890-7.

[14] A. van Elsas, R.P. Sutmuller, A.A. Hurwitz, J. Ziskin, J. Villasenor, J.P. Medema, W.W. Overwijk, N.P. Restifo, C.J. Melief, R. Offringa, J.P. Allison, Elucidating the autoimmune and antitumor effector mechanisms of a treatment based on cytotoxic T

lymphocyte antigen-4 blockade in combination with a B16 melanoma vaccine: comparison of prophylaxis and therapy, J Exp Med 194 (2001) 481-9.

[15] R.F. Wang, E. Appella, Y. Kawakami, X. Kang, S.A. Rosenberg, Identification of TRP-2 as a human tumor antigen recognized by cytotoxic T lymphocytes, J Exp Med 184 (1996) 2207-16.

[16] J.N. Kochenderfer, C.D. Chien, J.L. Simpson, R.E. Gress, Synergism between CpG-containing oligodeoxynucleotides and IL-2 causes dramatic enhancement of vaccine-elicited CD8+ T cell responses, J Immunol 177 (2006) 8860-73.

[17] M. Mansour, B. Pohajdak, W.M. Kast, A. Fuentes-Ortega, E. Korets-Smith, G.M. Weir, R.G. Brown, P. Daftarian, Therapy of established B16-F10 melanoma tumors by a single vaccination of CTL/T helper peptides in VacciMax, J Transl Med 5 (2007) 20.

[18] K. Mahnke, Y. Qian, S. Fondel, J. Brueck, C. Becker, A.H. Enk, Targeting of antigens to activated dendritic cells in vivo cures metastatic melanoma in mice, Cancer Res 65 (2005) 7007-12.

[19] E. Davila, R. Kennedy, E. Celis, Generation of antitumor immunity by cytotoxic T lymphocyte epitope peptide vaccination, CpG-oligodeoxynucleotide adjuvant, and CTLA-4 blockade, Cancer Res 63 (2003) 3281-8.

[20] M. Bellone, G. Iezzi, A. Martin-Fontecha, L. Rivolta, A.A. Manfredi, M.P. Protti, M. Freschi, P. Dellabona, G. Casorati, C. Rugarli, Rejection of a nonimmunogenic melanoma by vaccination with natural melanoma peptides on engineered antigen-presenting cells, J Immunol 158 (1997) 783-9.

[21] G.A. Rabinovich, D. Gabrilovich, E.M. Sotomayor, Immunosuppressive strategies that are mediated by tumor cells, Annu Rev Immunol 25 (2007) 267-96.

[22] T.F. Gajewski, Y. Meng, C. Blank, I. Brown, A. Kacha, J. Kline, H. Harlin, Immune resistance orchestrated by the tumor microenvironment, Immunol Rev 213 (2006) 131-45.

[23] T.F. Gajewski, Failure at the effector phase: immune barriers at the level of the melanoma tumor microenvironment, Clin Cancer Res 13 (2007) 5256-61.

[24] D. Gabrilovich, T. Ishida, T. Oyama, S. Ran, V. Kravtsov, S. Nadaf, D.P. Carbone, Vascular endothelial growth factor inhibits the development of dendritic cells and dramatically affects the differentiation of multiple hematopoietic lineages in vivo, Blood 92 (1998) 4150-66.

[25] C. Mesa, L.E. Fernandez, Challenges facing adjuvants for cancer immunotherapy, Immunol Cell Biol 82 (2004) 644-50.

[26] H. Jonuleit, E. Schmitt, G. Schuler, J. Knop, A.H. Enk, Induction of interleukin 10-producing, nonproliferating CD4(+) T cells with regulatory properties by repetitive stimulation with allogeneic immature human dendritic cells, J Exp Med 192 (2000) 1213-22.

Chapter Five

General Discussion and Conclusions

5.1 General discussion

The overall objective response rate to current cancer vaccine formulations is only 3.3% [1]. Among the various reasons for this failure in immune response, two important issues stand out: 1. Current cancer vaccines can only induce "weak" qualitative and quantitative T cell responses. 2. The immunosuppressive tumor microenvironment inhibits anti-tumor T cell activity at the effector phase [2,3]. The major goal for the improvement of response to cancer vaccines is to develop immunotherapy strategies that can activate robust and lasting immune responses against cancer antigens and, at the same time, be able to reverse the 'immunosuppressive milieu' of the tumor microenvironment. The goal of this research was to evaluate PLGA-NPs as delivery vehicles for targeting vaccine components to DCs for meeting those challenges. Formulating antigens in PLGA-NPs offers distinct advantages over soluble formulation [4]. PLGA-NPs can protect the antigen from proteolytic degradation and deliver it to the phagocytic cells (mainly DCs) in a targeted and prolonged manner while restricting the entry of encapsulated antigen to the systemic circulation. Besides, particulate antigens are more efficiently cross-presented than soluble antigens. Furthermore, PLGA-NPs facilitate co-delivery of various immunomodulators (such as TLR ligands) to DCs. Co-delivery of antigens along with TLR ligands to the same DC result in concomitant antigen processing and presentation in addition to triggering of TLR signaling leading to the generation of mature DCs capable of activating cellular immune responses [5].

Lipid A anchor of bacterial LPS is a well characterized TLR4 ligand that is responsible for both immunostimulatory properties and toxicity of LPS [6]. Previous studies have shown that the toxicity of LPS can be largely reduced by selective hydrolysis of the anomeric phosphate group of lipid A molecule [7]. In fact, MPLA is now extensively studied in various vaccine formulations in clinic [8-10] with an excellent record of safety [11]. However, being extracted and purified from bacterial culture, the process of MPLA manufacture is laborious, inconsistent and often leads to batch to batch difference in terms of activity and structure of MPLA. With this in mind, several lipid A analogues have been designed and chemically synthesized. Synthetic lipid A analogues are very promising adjuvants for future cancer vaccine formulations. In addition to their potent immunostimulatory activity, lower toxicity (compared to LPS), the process of their manufacture is consistent and often leads to highly pure and stable molecules of single structure [12].

We believed that the initial step towards the development of lipid A-based vaccine is the establishment of a satisfactory analytical method for their quantification. In fact, previous attempts to analyze lipid A have been hampered by its extremely low sensitivity to UV detection. This problem had been circumvented by pre-column derivatization of lipid A (in a 3 h chemical reaction) [13]. In the present study (chapter 2), we have developed and validated an LC-MS method for the quantitative analysis of lipid A analogues inside PLGA-NPs. The LC-MS method proved to be quick, easy, reliable, reproducible, accurate and more sensitive than the previously reported methods for lipid A quantification. Remarkably, this method enables simultaneous quantification of several

lipid A analogues without the need for any pre-column derivatization or radiolabeling. As a preliminary application, this method has been used in the quantification of two synthetic lipid A analogues in PLGA-NPs: 7-acyl lipid A and PET lipid A. Both analogues (in soluble form) exert similar immunostimulatory effects on BMDCs, as measured by up-regulation of co-stimulatory molecules (CD40 and CD86) and secretion of cytokines (IL-6, IL12 and TNF-α). However, the encapsulation efficiency of 7-acyl lipid A in PLGA-NPs was almost 3 fold higher than that of PET lipid A. The presence of an extra lipid chain in 7-acyl lipid A may account for its higher lipophilicity and hence better encapsulation in PLGA-NP. Different formulation parameters could be further optimized to increase the encapsulation efficiency of PET lipid A in PLGA-NPs. The optimization studies were not performed in the current series of investigations. Owing to a better encapsulated, 7-acyl lipid A was the adjuvant of choice in all our subsequent studies.

Our next goal was to formulate a model antigen (OVA) along with 7-acyl lipid A in PLGA-NPs and to evaluate the potential of this formulation to stimulate OVA specific T cell responses (chapter 3). PLGA-based vaccines are designed to target DCs both *in vitro* and *in vivo*. DCs exhibit several features which are required for the generation of efficient T cell mediated immune responses including wide distribution in the body, high efficiency in taking up antigens and transferring them to secondary lymphoid organs; intrinsic migratory capacity, ability to cross-present exogenous antigens to $CD8^+$ T cells through multiple pathways (described in chapter 1); constitutive expression of MHC class I and class II molecules as well as co-stimulatory molecules; ability to secrete high

amount of IL-12 that derives Th1-biased immune response and unique ability to stimulate immunological naive T cells. Our results showed that PLGA-NPs can deliver the encapsulated protein (OVA) to DCs both *in vitro* and *in vivo*. Released OVA could be further processed to give CD4 (OVA323-339) and CD8 epitope (SIINFEKL), resulting in simultaneous activation of $CD4^+$ and $CD8^+$ T cells. The presence of 7-acyl lipid A along with OVA in the same nanoparticle formulation further increased the extent of T cell activation, as measured by proliferative response, up-regulation of activation markers and ability to secrete IFN-γ. These results are in agreement with recent studies that reported enhanced and prolonged antigen presentation when antigen is co-delivered with TLR9 ligand in PLGA-NPs [5].

Particulate antigens are more efficiently taken up and cross-presented by DCs compared to soluble antigens [14]. Similarly, particulate delivery of TLR ligands offers several advantages over their administration in a soluble form. Interestingly, persistent signaling through TLR was required for overcoming tumor-induced immunosuppression mediated by Treg cells [15]. Particulate delivery systems could facilitate a sustained TLR signaling in DCs. Consequently, avoid the need of repeated administration or high dosages of TLR ligands. In fact, most of TLR ligands may show serious side effects when administered in high dose. For example, repeated daily injections of 60 μg of CpG in mice caused severe damages to lymphoid tissues and hepatic toxicity after 14 days of treatment [16]. Delivery of TLR ligands in PLGA-NPs would permit the use of very small doses and limit the non-specific immune activation and/or toxicity that may result upon systemic administration of those compounds. A previous study in our lab had shown that the

effective dose of TLR9 ligands (CpG) needed for *in vivo* priming of antigen-specific T cell response can be reduced by 10-100 fold when it was delivered in PLGA-NPs [17]. This dose sparing effect is probably not restricted to CpG, but can also be extended to other TLR ligands and/or immunomodulatory molecules. Particulate delivery can also facilitate simultaneous delivery of more than one TLR ligand in the same formulation. Warger *et al* [18] have recently shown a synergistic effect of combined-TLR triggering (TLR3 and TLR7) on BMDCs, as evidenced by a faster and more sustained secretion of pro-inflammatory cytokines (IL-6 and IL-12). More importantly, $CD4^+$ and $CD8^+$ T cells activated by DCs treated with a combination of both TLR3 and TLR7 ligands were completely resistant to Treg-mediated immune suppression. Untreated DCs or DCs treated with a single TLR ligand were unable to reverse Treg mediated suppression of $CD4^+$ and $CD8^+$ T cell responses.

Given the demonstrated effectiveness of 7-acyl lipid A as a vaccine adjuvant, and the ability of DCs pulsed with OVA along with 7-acyl lipid A in PLGA-NPs to dramatically enhance *in vitro* and *in vivo* OVA specific $CD4^+$ and $CD8^+$ primary T cell responses (chapter 3), we hypothesized that particulate delivery of cancer antigen (TRP2) and 7-acyl lipid A would be very effective at eliciting *in vivo* potent cellular responses that could mediate therapeutic anti-tumor response in the poorly immunogenic murine B16 melanoma model. The capability of TRP2/7-acyl lipid A-NPs vaccine strategy to break self-tolerance and to induce superior anti-tumor effect (chapter 4) could be explained through numerous mechanisms. Co-delivery of 7-acyl lipid A along with $TRP2_{180\text{-}188}$ to the same DC poulation provides the three signals required for optimum CTL activation.

DCs stimulated with TLR ligand increase the expression of peptide/MHC I complex on the cell surface (signal 1), upregulate costimulatory molecules e.g CD40, CD80 and CD86 (signal 2), and secrete various cytokines e.g. IL-12 (signal 3). The three signals combined lead to enhanced activation and proliferation of TRP2 specific $CD8^+$ T cell. Another avenue for breaking self-tolerance is through the ability of TLR activated DCs to reverse the Treg suppressive effects. In fact, it has been recently shown that IL-6 secreted by TLR4-activated DCs renders antigen specific T cells refractory to Treg-mediated immune suppression [19]. Other studies have shown that stimulation of DCs with TLR ligands enhances the proliferation of antigen specific T cells, making it more difficult for Treg cells to inhibit them [20,21]. Recent studies from our lab have shown that particulate delivery of 7-acyl lipid A leads to 1000-fold increase in the amount of IL-6 secreted by DCs (relative to soluble form) [22]. Furthermore, co-delivery of OVA and 7-acyl lipid A in PLGA-NPs to DCs have dramatically enhanced the extent of *in vitro* primary $CD4^+$ T cell activation by 1000 fold (compared to soluble formulation) [22]. Vaccine delivery system capable of inducing IL-6 production by DCs, and activation of primary T cell responses to this extent, may assure overcoming Treg-mediated immunosuppression through the involvement of such activated effector T cells.

5.2 Conclusions

In conclusion, we have developed and validated LC-MS analytical method for quantitative analysis of lipid A analogues in PLGA-NP formulations. This method proved to be rapid, sensitive, reliable and accurate. Using OVA as a model antigen, we have shown that PLGA-NPs can efficiently deliver encapsulated antigens to both MHC class I and MHC class II processing pathways, resulting in simultaneous activation of $CD8^+$ and $CD4^+$ T cell responses, respectively. Presence of 7-acyl lipid A in the same NP formulation dramatically enhances the extent of T cell clonal expansion as well as IFN-γ secretion by activated $CD4^+$ and $CD8^+$ T cells. Our studies using the poorly immunogenic melanoma antigen (TRP2) have shown that PLGA-based cancer vaccine is capable of enhancing ***magnitude*** and ***quality*** of T cell immune responses in both normal and tumor-bearing mice. Remarkably, delivery of cancer antigen along with 7-acyl lipid A in PLGA-NPs was successful in ***breaking self-tolerance*** against cancer self-antigen and ***reversing the immunosuppressive network*** in the tumor microenvironment. All these effects lead to the induction of ***therapeutic anti-tumor immunity*** in the murine B16 melanoma model. These results support the potential use of PLGA-NPs as competent vaccine delivery system, and introduce 7-acyl lipid as a very promising immunostimulatory djuvant for future cancer vaccine formulations.

5.3 Future directions

The promising results that we obtained from B16 melanoma tumor model (chapter 4) is a real driving force for us to rigorously evaluate the efficacy of our vaccination strategy in a more challenging and realistic tumor model. Unfortunately, transplanted tumor models harbor several drawbacks that limit their applicability to human disease and make them poor predictors of vaccine efficacy in patients. First, transplanted tumors don't grow in the anatomically appropriate site; as they are usually inoculated s.c. or i.v. As a result, they don't mimic the organ-specific physiology characteristic of the naturally occurring tumor. Moreover, transplantable tumors progress very rapidly following inoculation, and the immune system is suddenly exposed to them, whereas spontaneous tumors develop much more slowly. This slow development provides sufficient time for the battle between host immunity and cancer, with two possible outcomes; tumor elimination or most probably, tumor escape. Finally, most transplantable mouse tumors are not spontaneously metastatic, so immunotherapeutic studies using these models are not particularly relevant for most types of human cancer, where the metastatic spread of the disease is the major cause of death [23]. Assessing whether PLGA-based cancer vaccine is capable of eliminating metastatic tumors that have comparable onset, progression, staging and pathology to the human cancer, for which the vaccine is designed, will be a great challenge and will truly demonstrate the effectiveness of PLGA-based vaccine.

Among various spontaneous tumor models (reviewed in [23]), MUC1-expressing mammary tumor (MMT) appear to be an ideal model for our future investigations. MMT mice express human MUC1 as a self antigen, and spontaneously develop MUC1

expressing mammary gland tumor at 10-16 weeks after birth [24]. Development of MMT transgenic mice is schematically illustrated in Figure 5-1 (adopted from [25]). Advantages of MMT model over other spontaneous tumor models are summarized below.

1. The expression of MUC1 in MTT mice provides a useful target for immunotherapy as well as a marker for detecting ongoing immune responses. Similar to MUC1.Tg mice, MMT mice show immune tolerance against MUC1 and; therefore is suitable for evaluation of vaccination strategies to break self-tolerance against MUC1 antigens and evaluation of any potential autoimmunity. In addition to the MMT model, MET [26] and MUC1/MIN [27] double transgenic mouse models also develop spontaneous MUC1 expressing tumors in the pancreas and intestine, respectively. However, mammary tumors in particular, are superior to the other tumors, as it can be followed by palpation and are very useful for the assessment of therapeutic vaccines, as the location of the tumor alleviates the need to sacrifice the animal to follow the clinical outcome. Mammary tumors are also ideal for prophylactic vaccine studies, as the tumors develop after birth, allowing enough time for the immunizations to be performed prior to tumor development [28]. This is in contrast to MET model, where the mice exhibit acinar dysplasia "pre-cancerous lesion" at birth, which very rapidly progresses to invasive cancer by week 10, resulting in losing 90% of the mice by week 16 [29].

2. Whereas the incidence of spontaneous tumors in many of genetically modified mouse models can be very low (less than 10%), and tumor development can take up to several months [30], 100% of the female MMT mice get develop spontaneous tumors within reasonable time frame (10-16 weeks). Thus it is very useful in experimental settings.

3. Immunohistochemistry and western blot studies have shown that spontaneous mammary gland tumors in MTT mice expressed MUC1 protein in a similar pattern to what is observed in human [31]. In addition, tumors pathology in MTT mice closely mimics human breast cancer situation "highly fibrotic with dense connective tissue separating individual nests of tumor" [24].

4. More importantly, MMT tumors are spontaneously metastatic. Lung and bone metastasis were detected in the MTT mice by the age of 17-24 weeks (Figure 5-1). Thus it is an excellent model to investigate the efficacy of prophylactic and therapeutic immunotherapies against metastatic spread of the disease. It is worth mentioning that the mortality among breast cancer patients is mainly related to lung and bone metastasis. MMT model is then more useful than MUC/MIN model, in which no visible metastasis was observed [27].

For all the aforementioned reasons, we believe that MMT mouse is very reliable and appropriate model that closely mimics human cancer and will be an excellent tool for future investigations on the effects of PLGA-based vaccine on self-tolerance, immune activation and autoimmunity to MUC1 antigens.

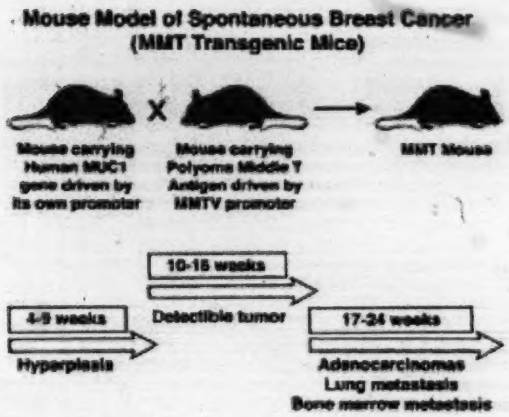

Figure 5-1. Schematic representation of the MTT bitransgenic mouse model and the approximate time line of the tumor progression (adopted from [25])- MMT mice were developed by mating mice that carry the human MUC1 transgene driven by its own promoter (MUC1.Tg mice) with mice that carry the polyomavirus middle T oncogene under the transcriptional control of the mouse mammary tumor virus promoter. Middle T antigen specifically associate with and activates the tyrosine kinase activity of a number of signal transduction proteins such as the c-Src family, phosphatidylinositol 3'-kinase, Ras, and c-Myc. Activation of these proteins leads to the promotion of cell growth and/or survival and result in widespread transformation of the mammary epithelia resulting in rapid production of multifocal mammary adenocarcinomas. Tumors are usually detected at 10-16 weeks after birth, whereas lung and bone metastasis occur after 17-24 weeks

The relative contribution of $CD4^+$ and $CD8^+$ T cells to the efficacy and success of cancer vaccines differs from one vaccination strategy to another [32-35]. It also depends on whether the vaccine is employed in prophylactic or therapeutic setting [35]. One of the future goals of this research is to investigate the ability of PLGA-based cancer vaccine formulations to stimulate both $CD4^+$ and $CD8^+$ T cell responses in MTT spontaneous tumor model, and to assess the relative contribution of vaccine-induced $CD4^+$ and $CD8^+$ T cell responses in mediating anti-tumor immunity. Using this model, the effect of PLGA-based vaccine on long-term survival and the induction of memory T cell responses in both prophylactic and therapeutic settings can be examined.

Modification of physical properties of PLGA to shift the delivery of encapsulated antigens to either cytoplasm (for MHC I presentation and $CD8^+$ T cell activation), to the endosome (for MHC II presentation and $CD4^+$ T cell activation), or to both MHC I and II pathways can also be investigated. Previous studies in our lab [36] have shown that, cytoplasmic delivery of PLGA content is affected by difference in molecular weight of PLGA. Small molecular weight PLGA (6000 gm/mol) delivered its content faster than larger molecular weight polymer (60,000 gm/mol). Further studies may be needed to define additional physical properties that can be adjusted to tailor cytoplasmic delivery of PLGA (such as; hydrophobicity, lactic/glycolic ratio, particle size, surface charge), and the effect of these parameters on the ability of PLGA-NPs to induce either $CD4^+$ and/or $CD8^+$ T cell responses in the MTT model.

The magnitude of the anti-tumor immune responses has been demonstrated to be a significant factor in tumor eradication [37]. Augmentation of anti-tumor immune responses could be achieved by adoptive transfer of *ex vivo* expanded effector T cells [38]. Previous animal studies have shown that a frequency of tumor specific T cells of at least 1–10% of $CD8^+$ T cells is needed for successful eradication of established tumors [38] . In human, this corresponds to an approximate dose of 2 to 20 × 10^9 $CD8^+$ T cells. Many methods have been employed to expand effector T cells *in vitro* (such as treatment with cytokines or non-specific triggering of TCR/co-stimulatory molecules). These methods could successfully expand effector cells to more than 10^{10} cells *in vitro* within 14-28 days [39,40]. However, such methods are laborious, expensive and time consuming. The robust expansion of T cells by DCs loaded with particulate antigen (chapter 3) can be employed in adoptive transfer therapy. Interestingly, recent studies have demonstrated that a combination of *in vivo* vaccination and adoptive T-cell transfer results in more robust anti-tumor activity than the use of each strategy individually [41]. Particulate delivery of antigen plus 7-acyl lipid A to DCs *in vitro* could be an optimum strategy to generate a population of T cells of desired magnitude with defined phenotypic and functional properties in a very short time. Those expanded T cells could be optimized to be used in adoptive transfer studies along with *in vivo* vaccination protocol.

Natural killer T (NKT) cells are a specialized subset of T cells that share some properties of NK cells and conventional T cells [42]. Whereas conventional $CD8^+$ and $CD4^+$ T cells recognize peptide antigens in association with MHC class I and MHC class II, respectively, NKT cells respond to glycolipids in the context of CD1d molecule [43]. a-galactosyl-ceramide (a-GalCer) is a synthetic ligand that is efficiently presented on CD1d molecules to NKT cells [44]. a-GalCer–stimulated NKT cells don't kill tumor directly, but instead they stimulate down stream innate and adoptive anti-tumor immune responses through secretion of large amount of cytokines needed for recruitment and activation of various immune cells (such as DCs, NK cells and CTLs).

Previous studies have shown that i.v. injection of *ex vivo* a-GalCer-loaded DCs resulted in up to 100 fold expansion of several subsets of NKT cells in a group of patients with advanced cancer. Expanded NKT cells could be detected for up to 6 months after vaccination. NKT activation was associated with an elevated serum level of IL-12 and IFN-γ inducible protein-10 (IP-10) [45]. These observations can open a new avenue for targeted delivery of a-GalCer to DCs *in vivo* using PLGA-NPs. Particulate delivery of a-GalCer to DCs will lead to sustained expansion of NKT cells *in vivo* resulting in downstream activation of both innate and adoptive anti-tumor immune responses.

The involvement of NK cells in mediating anti-tumor responses has been well described in different experimental systems [46]. Furthermore, a cross-talk between NK cells and DCs has been found to orchestrate both innate and adoptive anti-tumor immune responses. NK cells can facilitate adaptive anti-tumor immunity by producing IFN-γ and other cytokines that lead to the recruitment and activation/maturation of DCs [47]. Lysis of tumor targets by NK cells could further provide DCs with increased access to tumor antigens (to be cross-presented to CTLs) [47]. On the other hand, activated DCs constitute a source of numerous cytokines that in turn induce NK cell activation. In particular, DCs-derived IL-15, IL-12/IL-18 and IFNα/β could induce NK cell proliferation, IFN-γ secretion and cytotoxic function, respectively [48-50]. In the light of these findings, systemic administration of IL-15, IL-12/IL-18 and IFNα/β was employed for harnessing NK cells to reject established tumors. However, the systemic administration of these cytokines (particularly IL-2 and IFN-α) often leads to non-specifically activation of a broad range of immune cells, resulting in serious undesirable side effects. Co-delivery of tumor antigens and 7-acyl lipid A in PLGA-NPs can selectively stimulate DCs to produce NK cell-activating cytokines. This strategy might provide a precise route for triggering NK-cell activation and circumvent the need for systemic cytokine administration. One of our next research goals is to directly monitor the relative contribution of NK cells to the anti-tumor effects of our vaccination strategy. NK cell activation induced by PLGA-based vaccination will be assessed, with respect to increase in number, cytokine and functional activity.

In summary, we believe that PLGA-NPs are competent carriers for future cancer vaccine formulations. The aforementioned proposed investigations will clearly define the way to refine PLGA formulations for optimum cellular immunity. Results obtained could help in designing a single vaccination strategy capable of activating robust $CD4^+$, $CD8^+$ T cells, NK cells and NKT cells that could mediate full-scale anti-tumor immune responses. Such vaccine could act as double-edged sword, capable of targeting and killing both MHC class I positive and negative tumor cells, with the added advantage of help provided by activated Th and NKT cells.

5.4 References

[1] S.A. Rosenberg, J.C. Yang, N.P. Restifo, Cancer immunotherapy: moving beyond current vaccines, Nat Med 10 (2004) 909-15.

[2] W. Zou, Immunosuppressive networks in the tumour environment and their therapeutic relevance, Nat Rev Cancer 5 (2005) 263-74.

[3] H.L. Kaufman, M.L. Disis, Immune system versus tumor: shifting the balance in favor of DCs and effective immunity, J Clin Invest 113 (2004) 664-7.

[4] R. Audran, K. Peter, J. Dannull, Y. Men, E. Scandella, M. Groettrup, B. Gander, G. Corradin, Encapsulation of peptides in biodegradable microspheres prolongs their MHC class-I presentation by dendritic cells and macrophages in vitro, Vaccine 21 (2003) 1250-5.

[5] S.K. Datta, V. Redecke, K.R. Prilliman, K. Takabayashi, M. Corr, T. Tallant, J. DiDonato, R. Dziarski, S. Akira, S.P. Schoenberger, E. Raz, A subset of Toll-like receptor ligands induces cross-presentation by bone marrow-derived dendritic cells, J Immunol 170 (2003) 4102-10.

[6] H. Takada, S. Kotani, Structural requirements of lipid A for endotoxicity and other biological activities, Crit Rev Microbiol 16 (1989) 477-523.

[7] N. Qureshi, K. Takayama, E. Ribi, Purification and structural determination of nontoxic lipid A obtained from the lipopolysaccharide of Salmonella typhimurium, J Biol Chem 257 (1982) 11808-15.

[8] J.T. Evans, C.W. Cluff, D.A. Johnson, M.J. Lacy, D.H. Persing, J.R. Baldridge, Enhancement of antigen-specific immunity via the TLR4 ligands MPL adjuvant and Ribi.529, Expert Rev Vaccines 2 (2003) 219-29.

[9] J.T. Ulrich, K.R. Myers, Monophosphoryl lipid A as an adjuvant. Past experiences and new directions, Pharm Biotechnol 6 (1995) 495-524.

[10] J.R. Baldridge, P. McGowan, J.T. Evans, C. Cluff, S. Mossman, D. Johnson, D. Persing, Taking a Toll on human disease: Toll-like receptor 4 agonists as vaccine adjuvants and monotherapeutic agents, Expert Opin Biol Ther 4 (2004) 1129-38.

[11] P. Baldrick, D. Richardson, G. Elliott, A.W. Wheeler, Safety evaluation of monophosphoryl lipid A (MPL): an immunostimulatory adjuvant, Regul Toxicol Pharmacol 35 (2002) 398-413.

[12] Z.H. Jiang, W.A. Budzynski, D. Qiu, D. Yalamati, R.R. Koganty, Monophosphoryl lipid A analogues with varying 3-O-substitution: synthesis and potent adjuvant activity, Carbohydr Res 342 (2007) 784-96.

[13] S.R. Hagen, J.D. Thompson, D.S. Snyder, K.R. Myers, Analysis of a monophosphoryl lipid A immunostimulant preparation from Salmonella minnesota R595 by high-performance liquid chromatography, J Chromatogr A 767 (1997) 53-61.

[14] H. Shen, A.L. Ackerman, V. Cody, A. Giodini, E.R. Hinson, P. Cresswell, R.L. Edelson, W.M. Saltzman, D.J. Hanlon, Enhanced and prolonged cross-presentation following endosomal escape of exogenous antigens encapsulated in biodegradable nanoparticles, Immunology 117 (2006) 78-88.

[15] Y. Yang, C.T. Huang, X. Huang, D.M. Pardoll, Persistent Toll-like receptor signals are required for reversal of regulatory T cell-mediated CD8 tolerance, Nat Immunol 5 (2004) 508-15.

[16] M. Heikenwalder, M. Polymenidou, T. Junt, C. Sigurdson, H. Wagner, S. Akira, R. Zinkernagel, A. Aguzzi, Lymphoid follicle destruction and immunosuppression after repeated CpG oligodeoxynucleotide administration, Nat Med 10 (2004) 187-92.

[17] M. Diwan, P. Elamanchili, M. Cao, J. Samuel, Dose sparing of CpG oligodeoxynucleotide vaccine adjuvants by nanoparticle delivery, Curr Drug Deliv 1 (2004) 405-12.

[18] T. Warger, P. Osterloh, G. Rechtsteiner, M. Fassbender, V. Heib, B. Schmid, E. Schmitt, H. Schild, M.P. Radsak, Synergistic activation of dendritic cells by combined Toll-like receptor ligation induces superior CTL responses in vivo, Blood 108 (2006) 544-50.

[19] C. Pasare, R. Medzhitov, Toll pathway-dependent blockade of CD4+CD25+ T cell-mediated suppression by dendritic cells, Science 299 (2003) 1033-6.

[20] Z. Fehervari, S. Sakaguchi, Control of Foxp3+ CD25+CD4+ regulatory cell activation and function by dendritic cells, Int Immunol 16 (2004) 1769-80.

[21] T. Kubo, R.D. Hatton, J. Oliver, X. Liu, C.O. Elson, C.T. Weaver, Regulatory T cell suppression and anergy are differentially regulated by proinflammatory cytokines produced by TLR-activated dendritic cells, J Immunol 173 (2004) 7249-58.

[22] P. Elamanchili, C.M. Lutsiak, S. Hamdy, M. Diwan, J. Samuel, "Pathogen-mimicking" nanoparticles for vaccine delivery to dendritic cells, J Immunother 30 (2007) 378-95.

[23] S. Ostrand-Rosenberg, Animal models of tumor immunity, immunotherapy and cancer vaccines, Curr Opin Immunol 16 (2004) 143-50.

[24] P. Mukherjee, C.S. Madsen, A.R. Ginardi, T.L. Tinder, F. Jacobs, J. Parker, B. Agrawal, B.M. Longenecker, S.J. Gendler, Mucin 1-specific immunotherapy in a mouse model of spontaneous breast cancer, J Immunother 26 (2003) 47-62.

[25] P. Mukherjee, T.L. Tinder, G.D. Basu, L.B. Pathangey, L. Chen, S.J. Gendler, Therapeutic efficacy of MUC1-specific cytotoxic T lymphocytes and CD137 co-stimulation in a spontaneous breast cancer model, Breast Dis 20 (2004) 53-63.

[26] P. Mukherjee, A.R. Ginardi, C.S. Madsen, C.J. Sterner, M.C. Adriance, M.J. Tevethia, S.J. Gendler, Mice with spontaneous pancreatic cancer naturally develop MUC-1-specific CTLs that eradicate tumors when adoptively transferred, J Immunol 165 (2000) 3451-60.

[27] E.T. Akporiaye, D. Bradley-Dunlop, S.J. Gendler, P. Mukherjee, C.S. Madsen, T. Hahn, D.G. Besselsen, S.M. Dial, H. Cui, K. Trevor, Characterization of the MUC1.Tg/MIN transgenic mouse as a model for studying antigen-specific immunotherapy of adenomas, Vaccine 25 (2007) 6965-74.

[28] S.J. Gendler, P. Mukherjee, Spontaneous adenocarcinoma mouse models for immunotherapy, Trends Mol Med 7 (2001) 471-5.

[29] E.J. McConnell, L.B. Pathangey, C.S. Madsen, S.J. Gendler, P. Mukherjee, Dendritic cell-tumor cell fusion and staphylococcal enterotoxin B treatment in a pancreatic tumor model, J Surg Res 107 (2002) 196-202.

[30] G.J. Walker, N.K. Hayward, Pathways to melanoma development: lessons from the mouse, J Invest Dermatol 119 (2002) 783-92.

[31] J. Xia, Y. Tanaka, S. Koido, C. Liu, P. Mukherjee, S.J. Gendler, J. Gong, Prevention of spontaneous breast carcinoma by prophylactic vaccination with dendritic/tumor fusion cells, J Immunol 170 (2003) 1980-6.

[32] T. Kikuchi, S. Uehara, H. Ariga, T. Tokunaga, A. Kariyone, T. Tamura, K. Takatsu, Augmented induction of CD8+ cytotoxic T-cell response and antitumour resistance by T helper type 1-inducing peptide, Immunology 117 (2006) 47-58.

[33] A. van Elsas, R.P. Sutmuller, A.A. Hurwitz, J. Ziskin, J. Villasenor, J.P. Medema, W.W. Overwijk, N.P. Restifo, C.J. Melief, R. Offringa, J.P. Allison, Elucidating the autoimmune and antitumor effector mechanisms of a treatment based on cytotoxic T lymphocyte antigen-4 blockade in combination with a B16 melanoma vaccine: comparison of prophylaxis and therapy, J Exp Med 194 (2001) 481-9.

[34] J. Steitz, J. Bruck, J. Knop, T. Tuting, Adenovirus-transduced dendritic cells stimulate cellular immunity to melanoma via a CD4(+) T cell-dependent mechanism, Gene Ther 8 (2001) 1255-63.

[35] R.S. Goldszmid, J. Idoyaga, A.I. Bravo, R. Steinman, J. Mordoh, R. Wainstok, Dendritic cells charged with apoptotic tumor cells induce long-lived protective CD4+ and CD8+ T cell immunity against B16 melanoma, J Immunol 171 (2003) 5940-7.

[36] K.D. Newman, G.S. Kwon, G.G. Miller, V. Chlumecky, J. Samuel, Cytoplasmic delivery of a macromolecular fluorescent probe by poly(d, l-lactic-co-glycolic acid) microspheres, J Biomed Mater Res 50 (2000) 591-7.

[37] P.D. Greenberg, Adoptive T cell therapy of tumors: mechanisms operative in the recognition and elimination of tumor cells, Adv Immunol 49 (1991) 281-355.

[38] C. Yee, Adoptive T cell therapy: Addressing challenges in cancer immunotherapy, J Transl Med 3 (2005) 17.

[39] G.G. Laport, B.L. Levine, E.A. Stadtmauer, S.J. Schuster, S.M. Luger, S. Grupp, N. Bunin, F.J. Strobl, J. Cotte, Z. Zheng, B. Gregson, P. Rivers, R.H. Vonderheide, D.N. Liebowitz, D.L. Porter, C.H. June, Adoptive transfer of costimulated T cells induces lymphocytosis in patients with relapsed/refractory non-Hodgkin lymphoma following CD34+-selected hematopoietic cell transplantation, Blood 102 (2003) 2004-13.

[40] M.V. Maus, A.K. Thomas, D.G. Leonard, D. Allman, K. Addya, K. Schlienger, J.L. Riley, C.H. June, Ex vivo expansion of polyclonal and antigen-specific cytotoxic T lymphocytes by artificial APCs expressing ligands for the T-cell receptor, CD28 and 4-1BB, Nat Biotechnol 20 (2002) 143-8.

[41] Y. Lou, G. Wang, G. Lizee, G.J. Kim, S.E. Finkelstein, C. Feng, N.P. Restifo, P. Hwu, Dendritic cells strongly boost the antitumor activity of adoptively transferred T cells in vivo, Cancer Res 64 (2004) 6783-90.

[42] J.C. Mercer, M.J. Ragin, A. August, Natural killer T cells: rapid responders controlling immunity and disease, Int J Biochem Cell Biol 37 (2005) 1337-43.

[43] M. Brigl, M.B. Brenner, CD1: antigen presentation and T cell function, Annu Rev Immunol 22 (2004) 817-90.

[44] T. Kawano, J. Cui, Y. Koezuka, I. Toura, Y. Kaneko, K. Motoki, H. Ueno, R. Nakagawa, H. Sato, E. Kondo, H. Koseki, M. Taniguchi, CD1d-restricted and TCR-mediated activation of valpha14 NKT cells by glycosylceramides, Science 278 (1997) 1626-9.

[45] D.H. Chang, K. Osman, J. Connolly, A. Kukreja, J. Krasovsky, M. Pack, A. Hutchinson, M. Geller, N. Liu, R. Annable, J. Shay, K. Kirchhoff, N. Nishi, Y. Ando, K. Hayashi, H. Hassoun, R.M. Steinman, M.V. Dhodapkar, Sustained expansion of NKT cells and antigen-specific T cells after injection of alpha-galactosyl-ceramide loaded mature dendritic cells in cancer patients, J Exp Med 201 (2005) 1503-17.

[46] M.J. Smyth, Y. Hayakawa, K. Takeda, H. Yagita, New aspects of natural-killer-cell surveillance and therapy of cancer, Nat Rev Cancer 2 (2002) 850-61.

[47] M.A. Degli-Esposti, M.J. Smyth, Close encounters of different kinds: dendritic cells and NK cells take centre stage, Nat Rev Immunol 5 (2005) 112-24.

[48] I. Zanoni, M. Foti, P. Ricciardi-Castagnoli, F. Granucci, TLR-dependent activation stimuli associated with Th1 responses confer NK cell stimulatory capacity to mouse dendritic cells, J Immunol 175 (2005) 286-92.

[49] T. Walzer, M. Dalod, S.H. Robbins, L. Zitvogel, E. Vivier, Natural-killer cells and dendritic cells: "l'union fait la force", Blood 106 (2005) 2252-8.

[50] A.T. Kamath, C.E. Sheasby, D.F. Tough, Dendritic cells and NK cells stimulate bystander T cell activation in response to TLR agonists through secretion of IFN-alpha beta and IFN-gamma, J Immunol 174 (2005) 767-76.